Asymmetric Synthesis of β-Lactams through Copper-Catalyzed Alkyne-Nitrone Coupling

Yurie Takayama

2017

Contents

Chapter 1

General Introduction

Introduction

Terminal alkynes are essential building blocks in organic synthesis, which utilized as carbon–carbon triple bond components and other carbon sources.[1] Since the alkynes have a relatively acidic C–H bond at the terminus, the deprotonation and subsequent metallation form alkynylmetal species, that is, metal acetylide. Metal acetylide is typically prepared in advance by organometallic reagents or inorganic strong bases. However the highly reactive alkynylmetals are difficult to handle and do not tolerate functional groups. Therefore, catalytic *in situ* generation of metal acetylide is the perfect strategy for facile and atom-economical synthesis.

Transition metal acetylide acts as carbon nucleophile in nucleophilic addition and substitution, and dipolarophile in 1,3-dipolor cycloaddition. Therefore its stereoselective reaction with prochiral compounds is a powerful method for direct asymmetric alkynylation and other C–C bond formations. The development of catalytic enantioselective functionalizations of terminal alkynes provides practical accesses to pharmaceuticals and bioactive molecules.

In particular, the catalytic stereoselecetive coupling reaction between alkynes and nitrones is one of the efficient routes to enantiomerically pure β-lactams that construct many antibiotics and drugs. The chiral β-lactam synthetic methodologies will be focused in the latter section.

1. Stereoselective Alkynylation of Prochiral Compounds with Terminal Alkynes

Enantioselective addition of terminal alkynes to polar unsaturated compounds affords the alkynylated stereogenic carbon bearing a functional group at α position. Stereocontrolled nucleophilic substitution with terminal alkynes also furnishes important chiral structures in bioactive compounds and natural products. Moreover, further transformations of C–C triple bond lead to more complex molecules.

1.1. Aldehydes

The asymmetric 1,2-addition of terminal alkynes to aldehydes is important for

preparation of optically active propargylic alcohols that are a key structure in synthetic chemistry.[2–6]

1.1.1. Zinc catalysis

A monoalkylzinc reacts slowly and chemoselectively with carbonyl group and shows a high functional group tolerance. Carreira pioneered the enantioselective addition of terminal alkynes to aldehydes using a catalytic ammount of $Zn(OTf)_2$ and (+)-*N*-methylephedrine (Scheme 1a).[2a,2b] Although aromatic aldehydes cannot be used owing to consumption by Cannizzaro reaction, the alkyl-substituted propargylic alcohols were obtained in high yields with excellent enantioselectivities. The terminal C–H stretch of phenylacetylene monitored by IR spectroscopy suggested that zinc acetylide was generated via the formation of a π complex and deprotonation of the alkyne (Scheme 1b).[2c]

Scheme 1. Zinc-catalyzed alkynylation of aliphatic aldehydes.

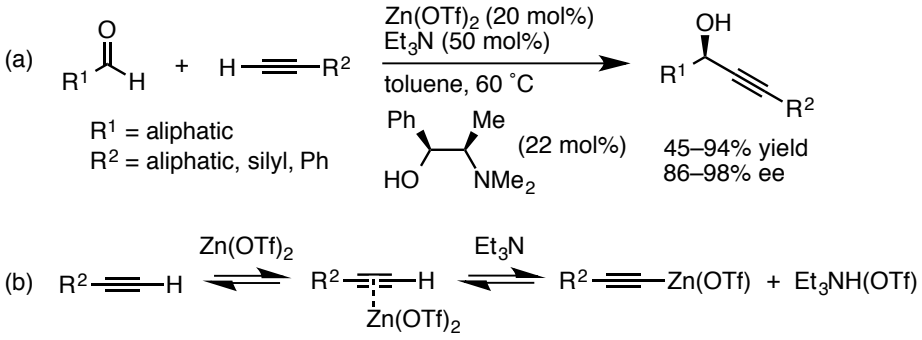

1.1.2. Indium catalysis

Shibasaki reported a bifunctional strategy for direct alkynylation of aldehyde and ketone catalyzed a indium(III) salt, which serves as both a soft transition metal and a hard Lewis acid (Scheme 2a).[3a] A chiral indium(III)/BINOL-complex accomplished the enantioselective version, which underwent with various aldehydes (Schems 2b).[3b]

Scheme 2. Indium/BINOL-catalyzed asymmetric alkynylation.

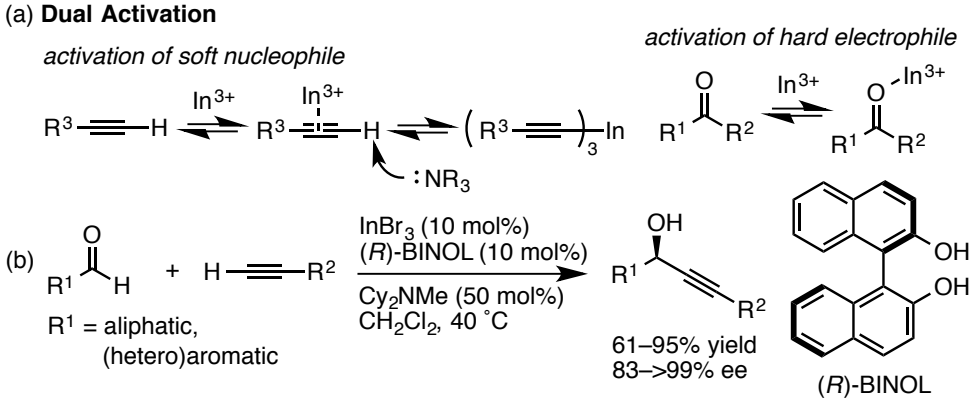

1.1.3. Copper catalysis

The copper-catalyzed direct alkynylation reactions of aldehydes were demonstrated by Sawamura, using chiral bisphosphine TRAP or chiral hydroxy amino phosphine (P,N,OH) ligand (Scheme 3).[4a,4b] The Cu-TRAP complex generates active monomeric alkynyl species due to the large P–Cu–P bite angle. Alcoholic solvents participate in the activation of substrates to accelerate the reaction and improve the enantioselectivity, as shown in Scheme 3a. This assumption inspired them to design a cooperative catalysis, in which an alcoholic Brønsted acid site was incorporated into a proline-based phosphine ligand (Scheme 3b).[4c] The ligand-substrate hydrogen bonding interaction achieved excellent selectivity and broad functional group tolerance.

Scheme 3. Copper-catalyzed enantioselective direct alkynylation of aldehydes.

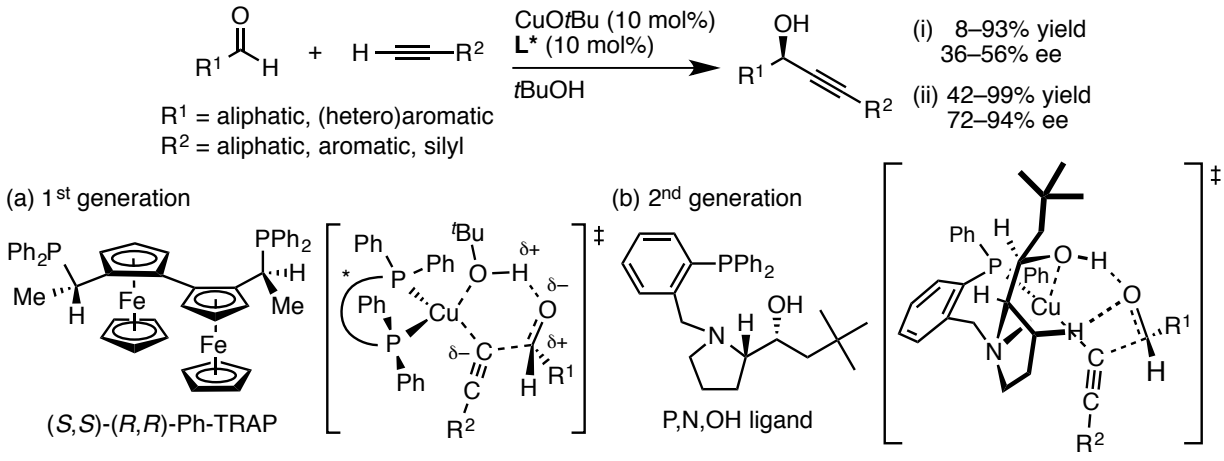

The catalytic enantioselective alkynylation of benzopyranyl acetals was reported to give chiral alkynylated isochromans and chromene (Scheme 4a and 4b).[5] The C–C bond formation occurs via π-complexation of the oxocarbenium to Cu (Scheme 4c).

Scheme 4. Copper-catalyzed enantioselective addition to oxocarbenium ions.

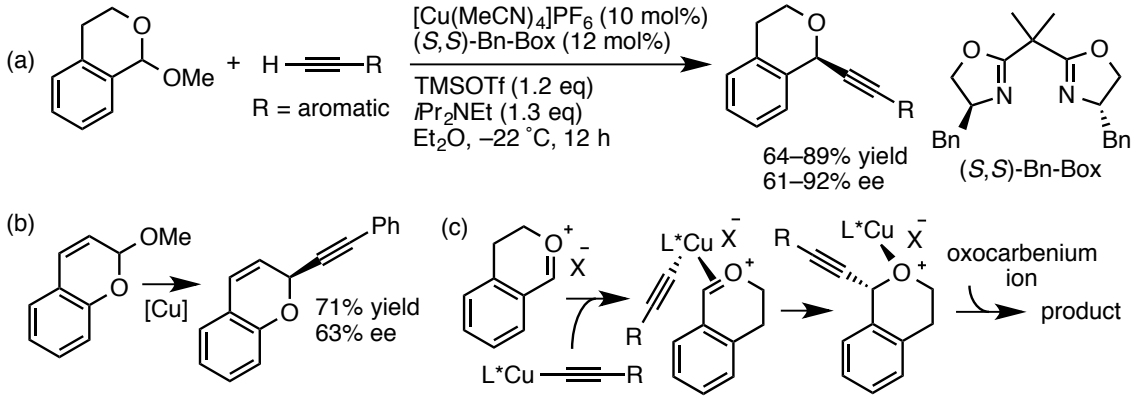

1.2. Ketones

Asymmetric alkynylation of ketones enables to afford chiral propargyl alcohols with a quaternary stereogenic carbon center. Although the addition reactions of metal acetylide to aldehydes were widely explored, few studies on the enantioselective alkynylation of ketones were reported, and scope was limited to activated ketones and α-ketoesters.[7,8]

1.2.1. Trifluoromethyl ketones

Shibasaki demonstrated an enantioselective alkynylation of activated trifluoromethyl ketones using a catalytic copper salt and chiral bidentate phosphine ligand, albeit with moderate enantioselectivity (Scheme 5).[7] This protocol can be a platform for the synthesis of Efavirenz (Merck's anti-HIV drug) and its derivatives.

Scheme 5. Copper-catalyzed enantioselective alkynylation of trifluoromethyl ketones.

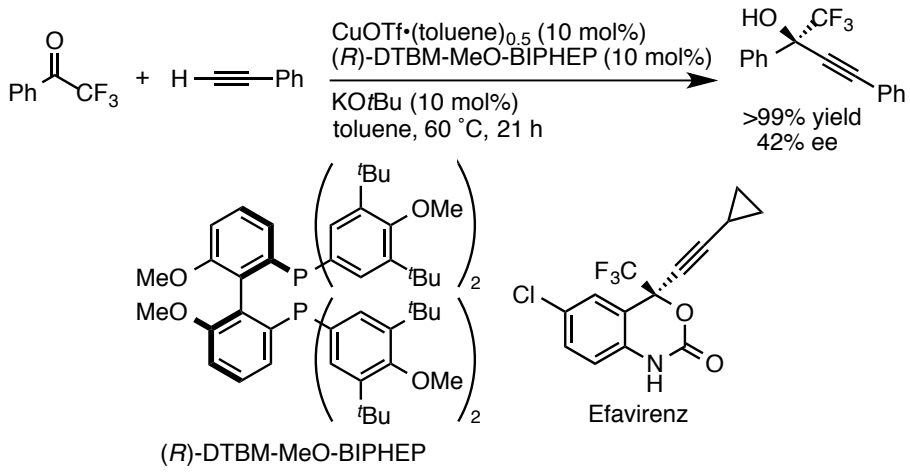

1.2.2. α-Ketoesters

Ohshima and Mashima developed a catalytic asymmetric alkynylation of trifluoromethyl-substituted α-ketoesters (Scheme 6).[8b] The Rh center acts as a π acid and Lewis acid to activate the substrates, and the acetate group on the Rh acts as a Brønsted base in the deprotonation step of the alkyne. The reaction of α-diketone in the presense of a rhodium catalyst was performed with low reactivity and enantioselectivity.

Scheme 6. Rhodium-catalyzed alkynylation of trifluoromethyl-substituted α-ketoesters.

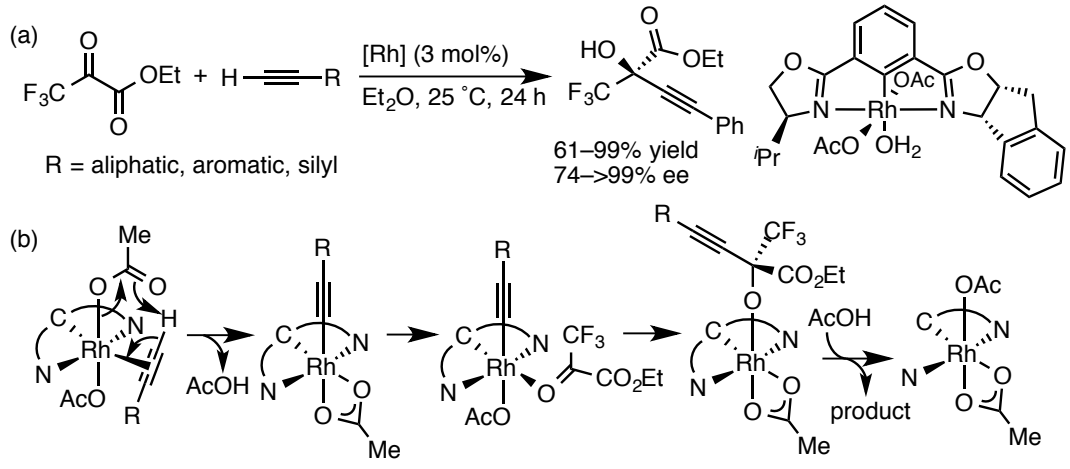

1-3. Imine derivatives

The asymmetric alkynylation of imines have established the general methods for

the synthesis of chiral propargyl amines.[9–15] In addition, the enantioselective reaction of α-iminoesters produces α-amino acid derivatives with high optical purity. Among many efforts on catalytic enantioselective alkynylation of imines, some examples are shown here, in which a transition metal and a chiral ligand participate in the activation of substrates.

1.3.1. Aldimines

In the early report on enantioselective alkynylation of imines, the imines were *in situ* generated prior to the addition of copper phenylacetylide. Although the substrate scope was quite limited to only aryl amines, the corresponding propargyl amines were isolated in excellent yields with enantioselectivities (Scheme 7).[12d] A Cu(I) salt and Pybox ligand can form a pentacoordinated complex, and the *N* atom of the imine chelates with the Cu complex by involving three π-interactions; two C–H···π and one π···π as suggested by the corresponding distances between the aryl groups of the imine and the ligand (~3.5 Å).

Scheme 7. Copper-catalyzed aldehyde-amine-alkyne coupling reaction.

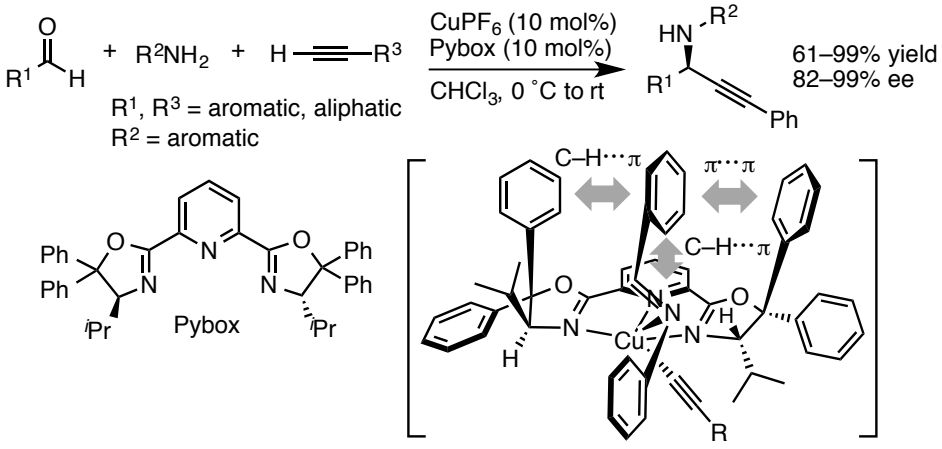

Cooperative catalytic model involving α-amino acid as catalysts was reported by Arndtsen (Scheme 8).[13] The combination of Cu(I) with α-amino acid, which forms chiral hydrogen bonding complex with the imine substrate, induced high

enantioselection. Another advantage of this catalysis is the modularity that enables to tune the chiral activity by combining commercially available amino acids and phosphines.

Scheme 8. α-Amino acid-controlled alkynylation of aromatic imines.

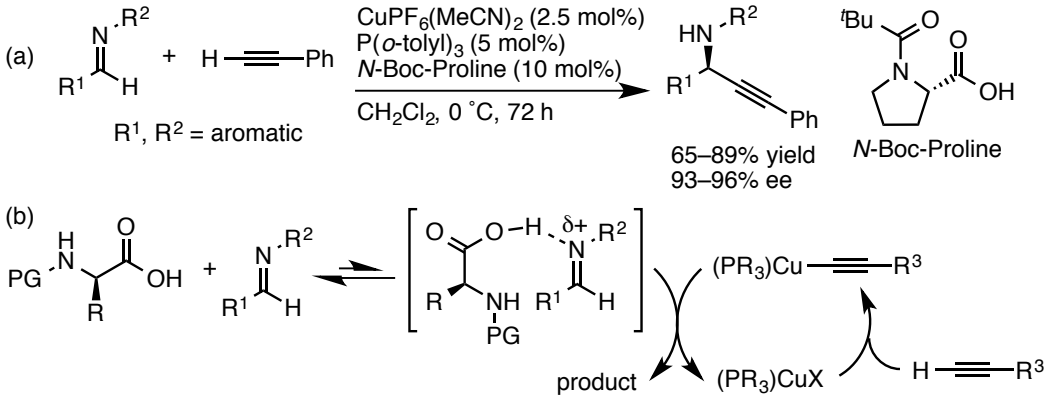

For other examples, cyclic imines and iminium ions can reacted with terminal alkynes, affording the chiral propargyl amine derivatives.[14] Furthermore, the use of *C*,*N*-cyclic azomethine imine gave the chiral alkynylated tetrahydroisoquinoline, in contrast to *N*,*N*'-cyclic type that underwent 1,3-dipolar cycloaddition (Scheme 9).[15] The addition of an axially chiral dicarboxylic acid as a Brønsted acid improved the enantioselectivity to construct a quaternary carbon center at the α position of C–N double bond.

Scheme 9. Copper-catalyzed asymmetric alkynylation of *C*,*N*-cyclic azomethine imines.

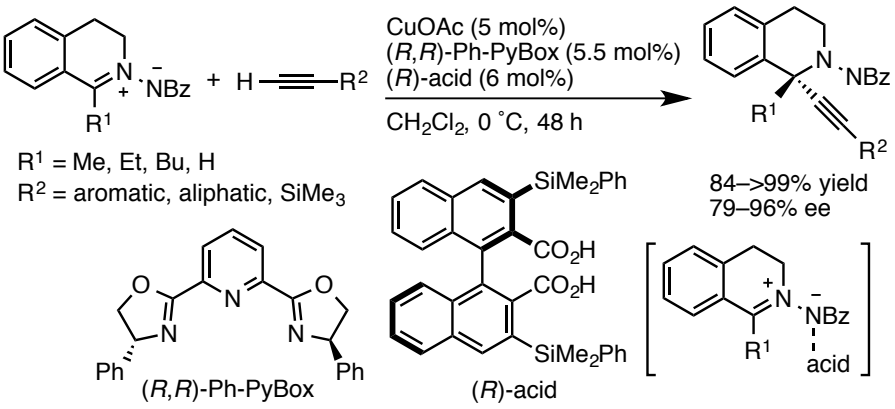

1.3.2. Ketimines

Shibasaki reported the direct catalytic alkynylation of thiophosphinyl ketimines using a chiral bisphosphine ligand, albeit with moderate enantioselectivity (Scheme 10).[16a] In the initial step, a soft Lewis acidic Cu(I) activates both soft Lewis basic C–C triple bond and *S* moiety of the substrates to form the intermediate Cu-amido complex, which acts as a soft Lewis acid/hard Brønsted base cooperative catalyst to drive the following reaction.

Scheme 10. Copper-catalyzed asymmetric alkynylation of thiophosphinyl ketimines.

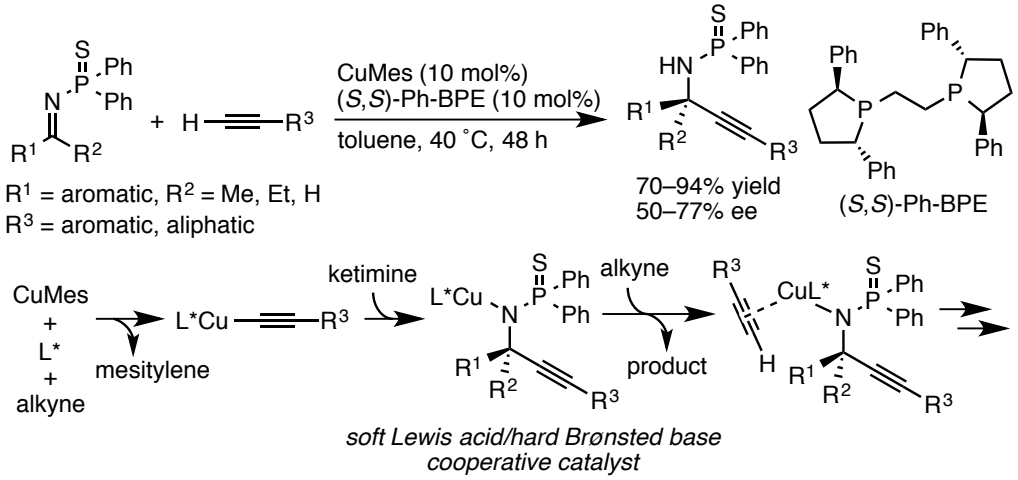

1.3.3. α-Iminoesters

The enantioselecetive alkynylation of α-iminoesters is a facile synthetic route to α-alkynylated amino acids. A chiral BINOL hydrogen phosphate served as a Brønsted acid catalyst for the activation of the α-iminoester (Scheme 11).[17b]

Scheme 11. Silver-catalyzed enantioselective alkynylation of α-iminoesters.

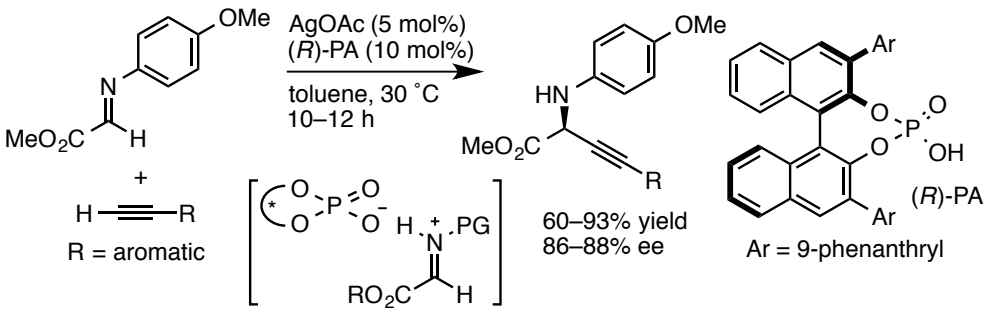

Ohshima and co-workers developed a direct enantioselective alkynylation of trifluoromethyl-substituted α-ketiminoesters using Phebox-Rh(III) acetate complex to give α-amino acid derivatives (Scheme 12).[18a] Further investigation disclosed that the monoalkynyl rhodium complex enhanced the catalytic activity and the expansion of substrate scope on α-ketiminoesters was achieved.[18b]

Scheme 12. Rh(III)/PheBox complex-catalyzed alkynylation of α-ketiminoesters.

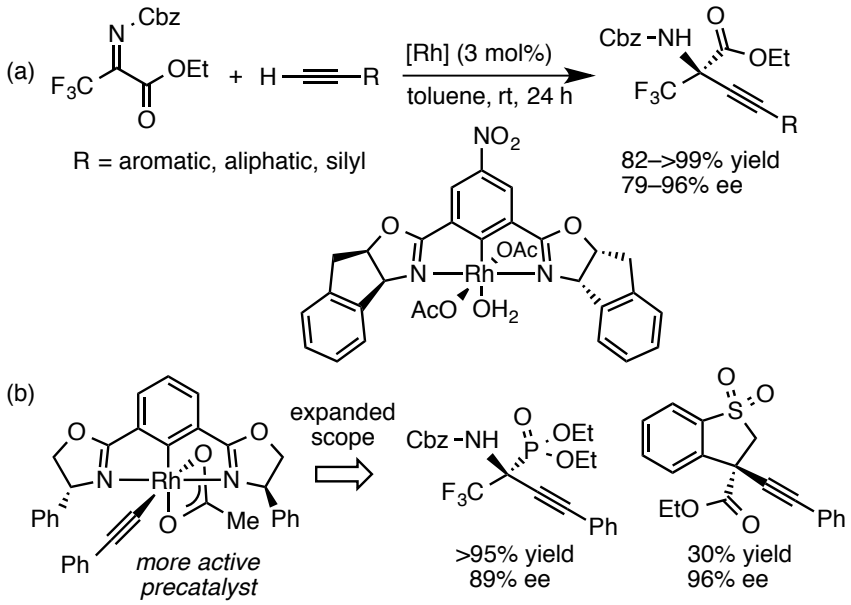

1.4. Conjugate addition to unsaturated compounds

Catalytic enantioselective conjugate addition of carbon nucleophiles is an atom-economical approach to construct the all-carbon stereogenic center. In particular,

the direct use of terminal alkynes can introduce a chiral building block both regio- and stereoselectively.[19–23]

1.4.1. Copper-catalyzed 1,4-addition

The enantioselective conjugate alkynylation of α,β-unsaturated thioamides was developed by Kumagai and Shibasaki (Scheme 13).[20] Soft Lewis acid/hard Brønsted base cooperative catalysis is critical for simultaneous activation of alkynes and thioamides, affording the β-alkynylated product. Although the reaction with aliphatic acetylenes showed small loss of enantioselectivity, a chiral phosphoric acid instead of phosphine oxide as a hard Brønsted base improved enantioselectivity. The last interaction in the C–C bond formation is caused by a Brønsted basicity of the reaction intermediate involving a pendant on Cu.

Scheme 13. Copper-catalyzed conjugate alkynylation of α,β-unsaturated thioamides.

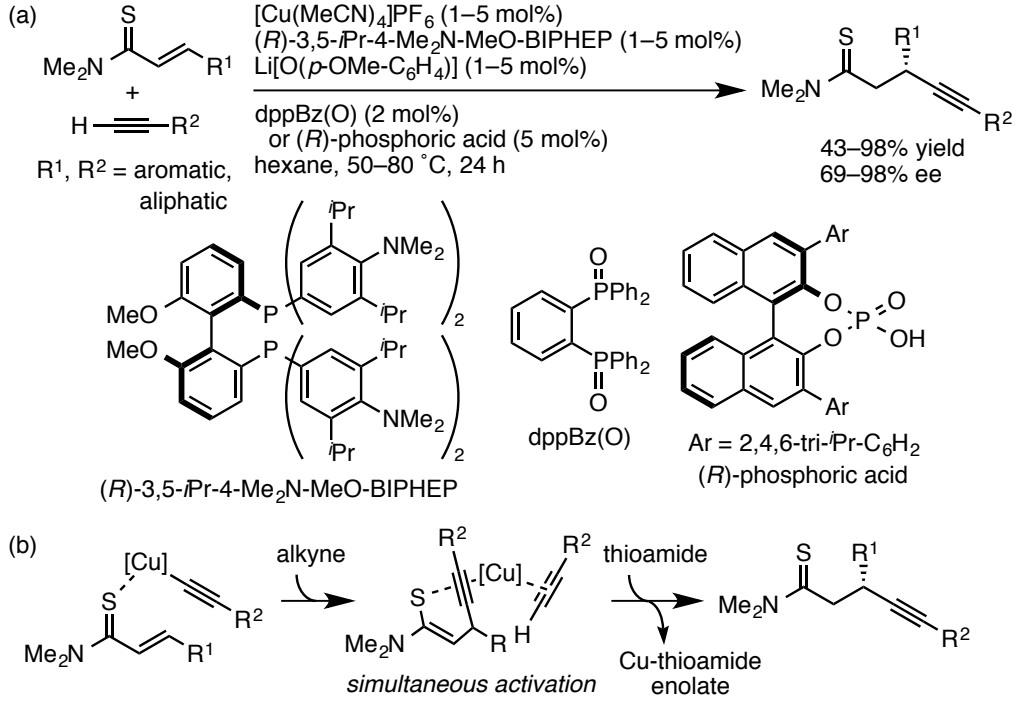

1.4.2. Cobalt-catalyzed 1,6-conjugate addition

Asymmetric 1,6-addition of triisopropylsilylacetylene to α,β,γ,δ-unsaturated esters

and amides in the presense of a cobalt/Duphos catalyst to give δ-alkynylated products in high yields with high regio- and enantioselectivity (Scheme 14).[23] Coordination of the dienoate to cobalt(I) acetylide forms a (η^4-diene)-cobalt complex. The insertion of the diene moiety into the alkynylcobalt occurs to afford π-allyl cobalt species, followed by protonation at γ-position giving the corresponding product.

Scheme 14. Cobalt-catalyzed 1,6-conjugate alkynylation of unsaturated compounds.

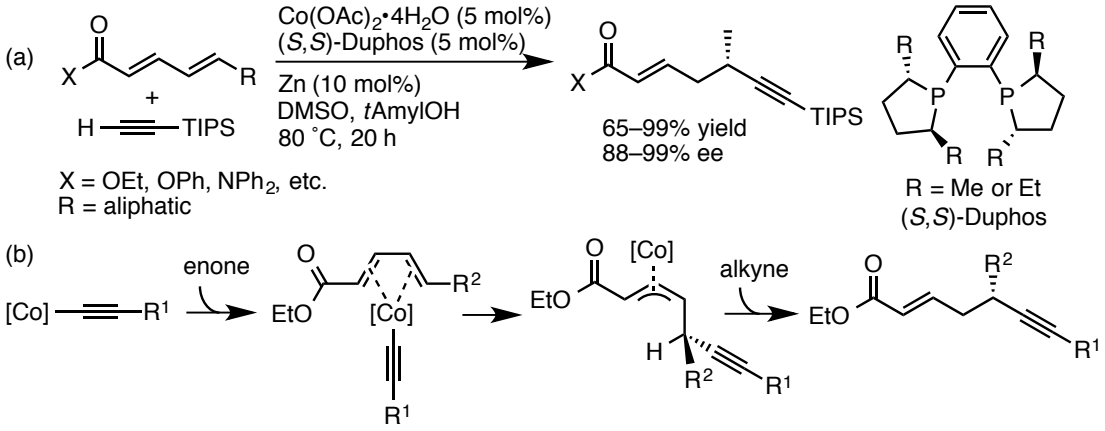

1.5. Allylic alkylation of terminal alkynes

The auther previously reported a copper-catalyzed regioselective and stereospecific direct allylic alkynylation of terminal alkynes. The reaction of optically active secondary allylic phosphates proceeded with 1,3-anti chemistry to furnish chiral 1,4-enynes bearing a stereogenic center at the allylic and propargylic position. The synthetic application was also demonstrated to accomplish a formal total synthesis of GnRH (Gonadotropin Releasing Hormone) antagonist (Scheme 15a).[24a]

Sawamura developed its enantioselective version using primary allylic phosphates in the presence of a chiral NHC ligand bearing a phenolic hydroxy group (Scheme 15b).[24b]

Scheme 15. Copper-catalyzed enantioselective allylic alkylation of terminal alkynes.

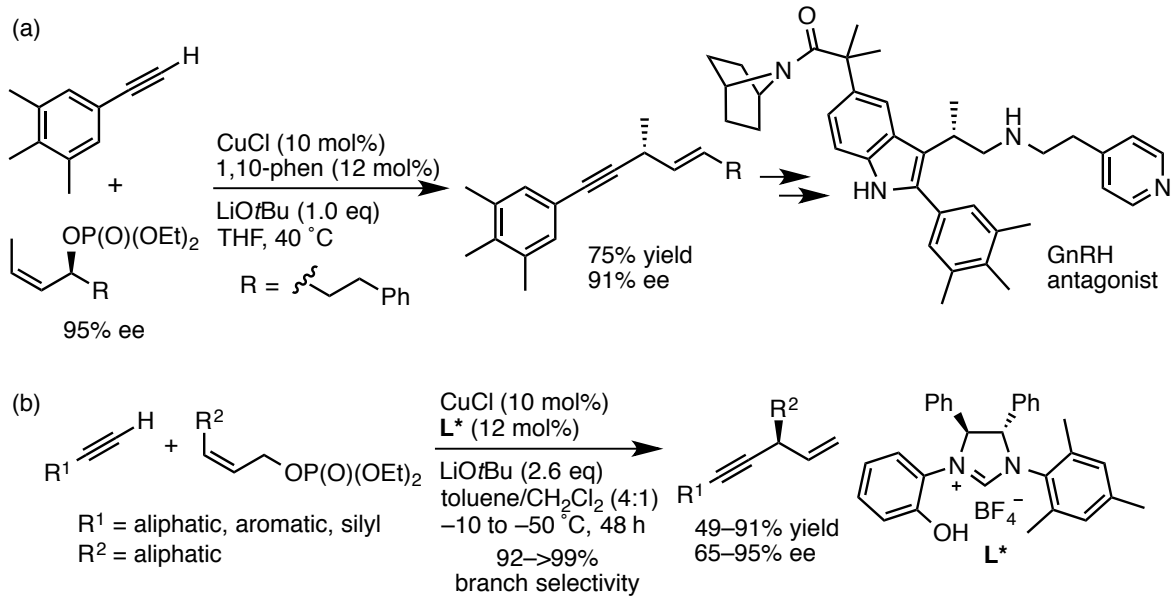

2. Other Transformations via Metal Acetylide Generation

2.1. Ruthenium or copper-catalyzed asymmetric propargylic substitution

Several groups reported ruthenium or copper-catalyzed enantioselective propargylic substitution reactions of propargylic alcohols or esters with a variety of heteroatom- and carbon-centered nucleophiles (Scheme 16).[26] The *in situ* generated metal allenylidene complex is electrophilic and undergoes addition at the γ-carbon to form a new asymmetric C–C bond over the inherent substituent, in contrast to the direct use of terminal alkynes as nucleophiles.

Scheme 16. Catalytic enantioselective propargylic substitution.

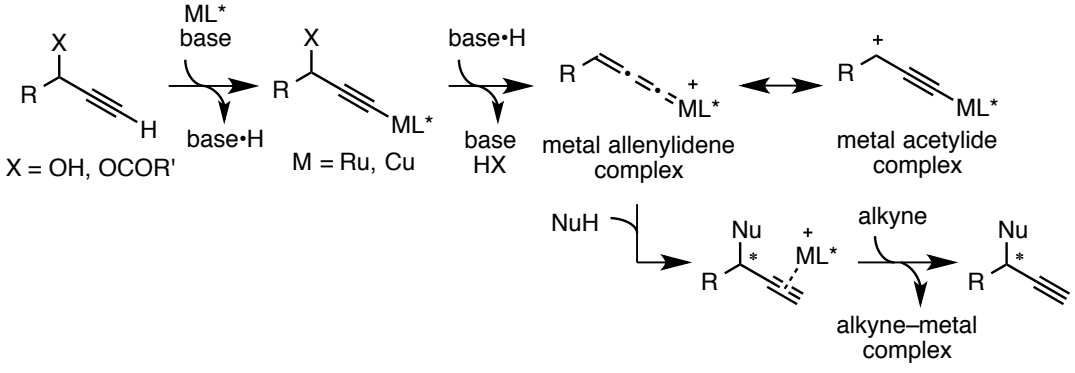

2.2. Copper-catalyzed 1,3-dipolar cycloaddition of nitrones (Kinugasa reaction)

Copper acetylide species can react with 1,3-dipoles through [3+2] cycloaddition to give sophisticated heterocyclic compounds, as shown in Scheme 17.[27] A nitrone is known as the coupling partner with a terminal alkyne and forms a β-lactam, which was discovered by Kinugasa in 1972.[28] Few methods of the catalytic enantioselective Kinugasa reaction for the synthesis of chiral β-lactams has been developed, even though it has two advantages in terms of high atom economy, and accessibility and stability of starting materials.

Scheme 17. Copper-catalyzed alkyne-nitrone coupling for the synthesis of β-lactam.

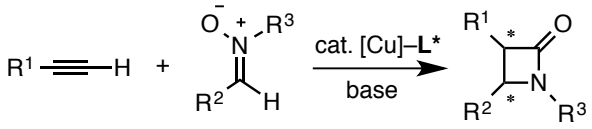

3. Chiral β-Lactam Synthesis

Chiral β-lactams play an essential role due to their biological activity. From the discovery of penicillins, they have caught wide attentions in antibiotics, as well as drugs that reveal such properties as anticancer, antiviral, antifungal and cholesterol-lowering. In addition, β-lactams show their utility as building blocks. For example, β-lactam was employed for preparation of paclitaxel (taxol) to install a β-amino acid derived side chain. As a result of the significance of β-lactams in medicinal and synthetic chemistry, many methodologies for efficient construction of the four-membered β-lactam ring were investigated. In most classical approaches, stereocontrol of chiral substituents at C-3 and 4 positions depends on chiral auxiliaries or enantiomerically pure starting materials. On the other hand, direct catalytic enantioselective routes to β-lactams are rare; only four strategies including Kinugasa reaction have been reported (Figure 1).

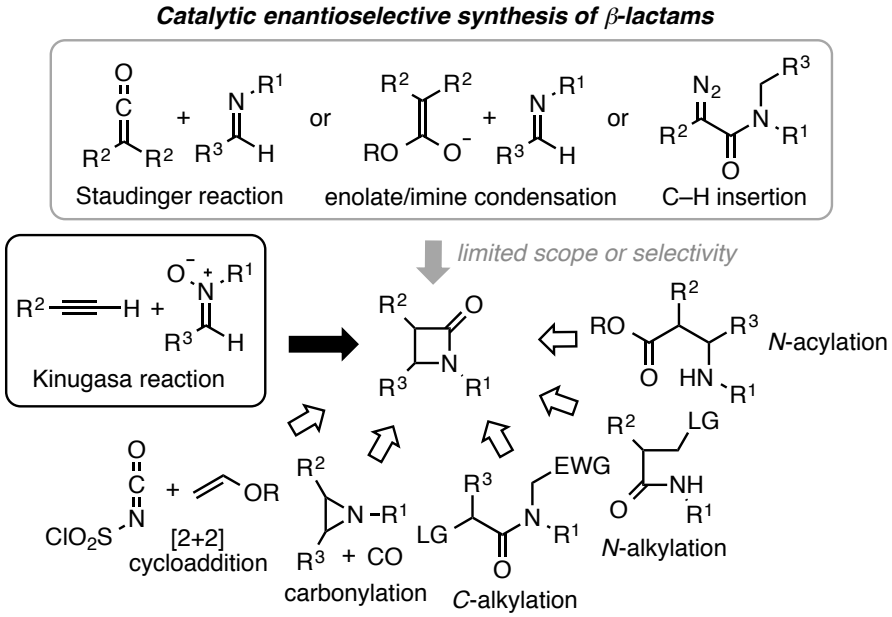

Figure 1. General strategies for β-lactam synthesis.

3.1. Rhodium-catalyzed intramolecular C–H insertion of α-diazoamide

A chiral Rh(II) carboxylate was used to decompose α-diazocarbonyl, affording *trans*-β-lactam with moderate enantioselectivity (Scheme 18).[29]

Scheme 18. Rhodium-catalyzed intramolecular C–H insertion of α-diazoamide.

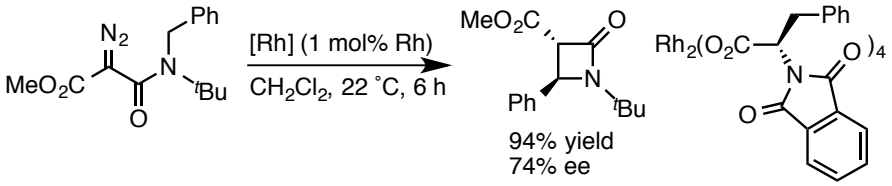

3.2. Asymmetric reaction of lithium ester enolates with imines

The reaction between lithium ester enolates and imines proceeded enantioselectively in the presence of a chiral ether to give the corresponding 3-dialkylated β-lactams (Scheme 19).[30]

Scheme 19. Asymmetric condensation of lithium ester enolates and imines

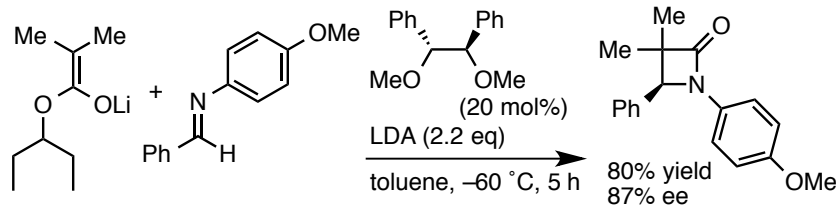

3.3. Alkaloid-catalyzed ketene-imine cycloaddition

A catalytic enantioselective formal [2+2] cycloaddition was accomplished with the use of optically active cinchona alkaloid derivatives as a catalyst (Scheme 20).[31] The reaction initiated by the nucleophilic deprotonation furnished highly enantioenriched β-lactams.

Scheme 20. Catalytic enantioselective Staudinger reaction.

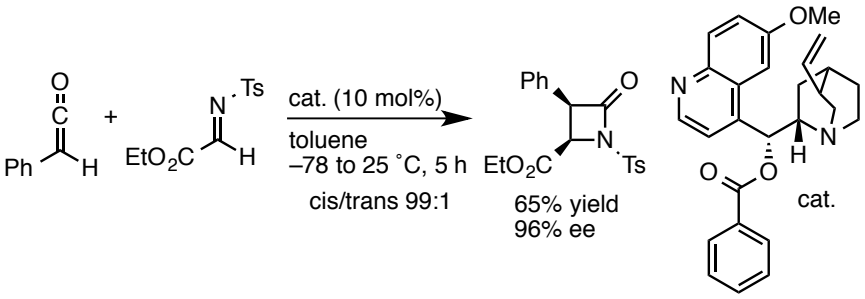

Overview of this thesis

The author focused on a transition metal catalyzed asymmetric C–C bond formation reaction via catalytic metalation of terminal alkynes in order to provide efficient approaches for the synthesis of useful compounds. A new general method of catalytic enantioselective Kinugasa reaction was developed using the copper/hydroxy amino phosphine ligand catalyst (Scheme 21). This reaction proceeded in the presense of stoichiometric secondary amine to furnish highly stereocontrolled β-lactams with broad functional group compatibility. It is noteworthy that some products bearing enantioenriched alkyl side chains are β-lactam drug analogues. The system was driven by cooperative catalysis, which activated the nitrone substrate and led to stereoselective construction of chiral β-lactams. DFT calculations also indicated the ligand-substrate hydrogen-bonding interactions, and provided a new suggestion concerning its mechanistic details.

Scheme 21. Copper-catalyzed enantioselective Kinugasa reaction with a silyl-induced hydroxy amino phosphine ligand.

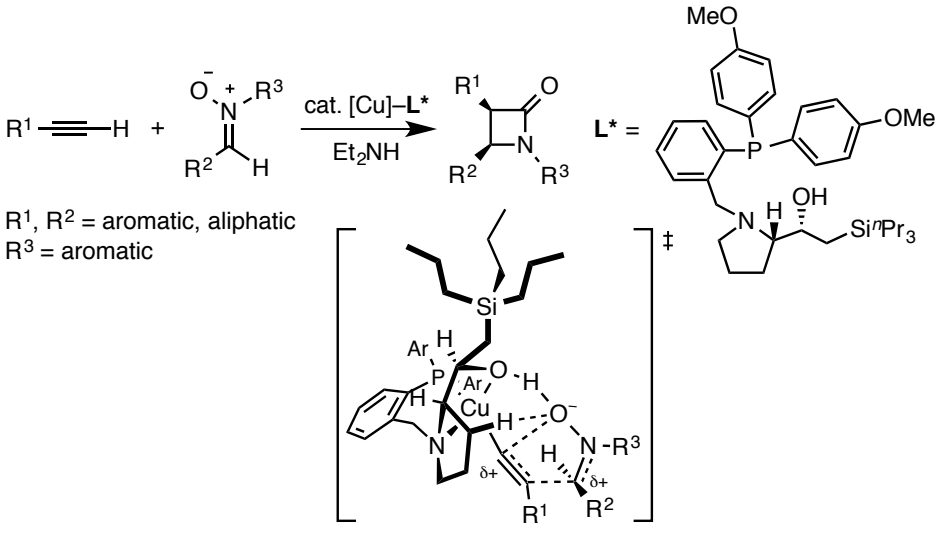

References and Notes

(1) For reviews, see: (a) Trost, B. M.; Weiss, A. H. *Adv. Synth. Catal.* **2009**, *351*, 963–983. (b) Bisai, V.; Singh, V. K. *Tetrahedron Lett.* **2016**, *57*, 4771–4784.

(2) (a) Anand, N. K.; Carreira, E. M. *J. Am. Chem. Soc.* **2001**, *123*, 9687–9688. (b) Frantz, D. E.; Fässler, R.; Carreira, E. M. *J. Am. Chem. Soc.* **2000**, *122*, 1806–1807. (c) Fässler, R.; Tomooka, C. S.; Frantz, D. E.; Carreira, E. M. *Proc. Natl. Acad. Sci. USA.* **2004**, *101*, 5843–5845.

(3) (a) Takita, R.; Yakura, K.; Ohshima, T.; Shibasaki, M. *J. Am. Chem. Soc.* **2005**, *127*, 13760–13761. (b) Takita, R.; Fukuta, Y.; Tsuji, R.; Ohshima, T.; Shibasaki, M. *Org. Lett.* **2005**, *7*, 1363–1366.

(4) (a) Asano, Y.; Hara, K.; Ito, H.; Sawamura, M. *Org. Lett.* **2007**, *9*, 3901–3904. (b) Asano, Y.; Ito, H.; Hara, K.; Sawamura, M. *Organometallics* **2008**, *27*, 5984–5996. (c) Ishii, T.; Watanabe, R.; Moriya, T.; Ohmiya, H.; Mori, S.; Sawamura, M. *Chem. Eur. J.* **2013**, *19*, 13547–13553.

(5) Maity, P.; Srinivas, H. D.; Watson, M. P. *J. Am. Chem. Soc.* **2011**, *133*, 17142–17145.

(6) Ito, J.; Asai, R.; Nishiyama, H. *Org. Lett.* **2010**, *12*, 3860–3862.

(7) Motoki, R.; Kanai, M.; Shibasaki, M. *Org. Lett.* **2007**, *9*, 2997–3000.

(8) (a) Jiang, B.; Chen, Z.; Tang, X. *Org. Lett.* **2002**, *4*, 3451–3453. (b) Ohshima, T.; Kawabata, T.; Takeuchi, Y.; Kakinuma, T.; Iwasaki, T.; Yonezawa, T.; Murakami, H.; Nishiyama, H.; Mashima, K. *Angew. Chem. Int. Ed.* **2011**, *50*, 6296–6300. (c) Wang, T.; Niu, J.-L.; Liu, S.-L.; Huang, J.-J.; Gong, J.-F.; Song, M.-P. *Adv. Synth. Catal.* **2013**, *355*, 927–937.

(9) Wei, C.; Li, Z.; Li, C.-J. *Synlett* **2004**, *9*, 1472–1483.

(10) Wei, C.; Li, C.-J. *J. Am. Chem. Soc.* **2002**, *124*, 5638–5639.

(11) (a) Koradin, C.; Polborn, K.; Knochel, P. *Angew. Chem. Int. Ed.* **2002**, *41*, 2535–2538. (b) Gommermann, N.; Koradin, C.; Polborn, K.; Knochel, P. *Angew. Chem. Int. Ed.* **2003**, *42*, 5763–5766. (c) Koradin, C.; Gommermann, N.; Polborn, K.; Knochel, P. *Chem. Eur. J.* **2003**, *9*, 2797–2811.

(12) (a) Knöpfel, T. K.; Aschwanden, P.; Ichikawa, T.; Watanabe, T.; Carreira, E. M. *Angew. Chem. Int. Ed.* **2004**, *43*, 5971–5973. (b) Benaglia, M.; Negri, D.; Dell'Anna, G. *Tetrahedron Lett.* **2004**, *45*, 8705–8708. (c) Weissberg, A.; Halak, B.; Portnoy, M. *J. Org. Chem.* **2005**, *70*, 4556–4559. (d) Bisai, A.; Singh, V. *Org. Lett.* **2006**, *8*, 2405–2408. (e) Colombo, F.; Benaglia, M.; Orlandi, S.; Usuelli, F.; Celentano, G. *J. Org. Chem.* **2006**, *71*, 2064, 2070.

(13) Lu, Y.; Johnstone, T. C.; Arndtsen, B. A. *J. Am. Chem. Soc.* **2009**, *131*, 11284–11285.

(14) For cyclic imines: (a) Ren, Y.-Y.; Wang, Y.-Q.; Liu, S. *J. Org. Chem.* **2014**, *79*, 11759–11767. For iminium ions: (b) Taylor, A. M.; Schreiber, S. L. *Org. Lett.* **2006**, *8*, 143–146. (c) Lin, W.; Cao, T.; Fan, W.; Han, Y.; Kuang, J.; Luo, H.; Miao, B.; Tang, X.; Yu, Q.; Yuan, W.; Zhang, J.; Zhu, C.; Ma, S. *Angew. Chem. Int. Ed.* **2014**, *53*, 277–281. For acylpyridinium ions: (d) Sun, Z.; Yu, S.; Ding, Z.; Ma, D. *J. Am. Chem. Soc.* **2007**, *129*, 9300–9301. (e) Black, D. A.; Beveridge, R. E.; Arndtsen, B. A. *J. Org. Chem.* **2008**, *73*, 1906–1910.

(15) Hashimoto, T.; Omote, M.; Maruoka, K. *Angew. Chem. Int. Ed.* **2011**, *50*, 8952–8955.

(16) (a) Yin, L.; Otsuka, Y.; Takada, H.; Mouri, S.; Yazaki, R.; Kumagai, N.; Shibasaki, M. *Org. Lett.* **2013**, *15*, 698–701. (b) Takada, H.; Kumagai, N.; Shibasaki, M. *Org. Lett.* **2015**, *17*, 4762–4765.

(17) (a) Ji, J.-X.; Wu, J.; Chan, A. S. C. *Proc. Natl. Acad. Sci.* **2005**, *102*, 11196–11200. (b) Rueping, M.; Antonchick, A. P.; Brinkmann, C. *Angew. Chem. Int. Ed.* **2007**, *46*, 6903–6906. (c) Peng, F.; Shao, Z.; Chan, A. S. C. *Tetrahedron: Asymm.* **2010**, *21*, 465–468. (d) Bisai, A.; Singh, V. K. *Tetrahedron* **2012**, *68*, 3480–3486.

(18) (a) Morisaki, K.; Sawa, M.; Nomaguchi, J.; Morimoto, H.; Takeuchi, Y.; Mashima, K.; Ohshima, T. *Chem. Eur. J.* **2013**, *19*, 8417–8420. (b) Morisaki, K.; Sawa, M.; Yonesaki, R.; Morimoto, H.; Mashima, K.; Ohshima, T. *J. Am. Chem. Soc.* **2016**, *138*, 6194–6203.

(19) (a) Knöpfel, T. F.; Zarotti, P.; Ichikawa, T.; Carreira, E. M. *J. Am. Chem. Soc.*

2005, *127*, 9682–9683. (b) Fillion, E.; Zorzitto, A. K. *J. Am. Chem. Soc.* **2009**, *131*, 14608–14609.

(20) Yazaki, R.; Kumagai, N.; Shibasaki, M. *J. Am. Chem. Soc.* **2010**, *132*, 10275–10277.

(21) (a) Nishimura, T.; Guo, X.-X.; Uchiyama, N.; Katoh, T.; Hayashi, T. *J. Am. Chem. Soc.* **2008**, *130*, 1576–1577. (b) Nishimura, T.; Katoh, T.; Takatsu, K.; Shintani, R.; Hayashi, T. *J. Am. Chem. Soc.* **2007**, *129*, 14158–14159. (c) Nishimura, T.; Sawano, T.; Ou, K.; Hayashi, T. *Chem. Commun.* **2011**, *47*, 10142–10144.

(22) Ito, J.; Fujii, K.; Nishiyama, H. *Chem. Eur. J.* **2013**, *19*, 601–605.

(23) Sawano, T.; Ashouri, A.; Nishimura, T.; Hayashi, T. *J. Am. Chem. Soc.* **2012**, *134*, 18936–18939.

(24) (a) Makida, Y.; Takayama, Y.; Ohmiya, H.; Sawamura, M. *Angew. Chem. Int. Ed.* **2013**, *52*, 5350–5354. (b) Harada, A.; Makida, Y.; Sato, T.; Ohmiya, H.; Sawamura, M. *J. Am. Chem. Soc.* **2014**, *136*, 13932–13939.

(25) Nishiyama, T.; Guo, X.-X.; Hayashi, T. *Chem. Asian. J.* **2008**, *3*, 1505–1510.

(26) For a selected review: Nishibayashi, Y. *Synthesis* **2012**, *44*, 489–503.

(27) Stanley, L. M.; Sibi, M. P. *Chem. Rev.* **2008**, *108*, 2887–2902.

(28) Kinugasa, M.; Hashimoto, S. *J. Chem. Soc., Chem. Commun.* **1972**, 466–467.

(29) (a) McCarthy, N.; McKervey, A.; Ye, Tao. *Tetrahedron Lett.* **1992**, *33*, 5983–5986. (b) Watanabe, N.; Anada, M.; Hashimoto, S.; Ikegami, S. *Synlett* **1994**, 1031–1033. (c) Anada, M.; Watanabe, N.; Hashimoto, S. *Chem. Commun.* **1998**, 1517–1518.

(30) (a) Fujieda, H.; Kanai, M.; Kambara, T.; Iida, A.; Tomioka, K. *J. Am. Chem. Soc.* **1997**, *119*, 2060–2061. (b) Tomioka, K.; Fujieda, H.; Hayashi, S.; Hussein, M. A.; Kambara, T.; Nomura, Y.; Kanai, M.; Koga, K. *Chem. Commun.* **1999**, 715–716.

(31) Taggi, A. E.; Hafez, A. M.; Wack, H.; Young, B.; Drury, W. J.; Lectka, T. *J. Am. Chem. Soc.* **2000**, *122*, 7831–7832.

Chapter 2

Asymmetric Synthesis of β-Lactams through Copper-Catalyzed Alkyne-Nitrone Coupling

Introduction

Chiral β-lactams are a key heterocycle family due to their biological activity and their utility as building blocks in synthetic chemistry (Figure 1).[1–3] Among the approaches for the construction of β-lactams, Kinugasa reported a stoichiometric reaction of copper phenylacetylide with nitrone, which after hydrolysis formed the *cis*-β-lactam.[4] The first catalytic asymmetric version of alkyne-nitrone coupling reaction was achieved by Miura in 1995.[5] The reaction between phenylacetylene and *C*,*N*-biphenylnitrone in the presense of copper(I) iodide and a chiral bisoxazoline ligand catalyst afforded the *cis* and *trans* isomeric mixture of enantioenriched β-lactam with moderate stereoselectivities (Scheme 1a). Based on this pioneering work, the development of asymmetric Kinugasa reactions has been performed by other researchers.[6,7] In contrast, a scope of terminal alkyne substrates is limited to aromatic acetylenes.

Many of biologically important β-lactams have an aliphatic side chain at the carbonyl α-position (Figure 1b).[8,9] To synthesize these compounds through Kinugasa reaction, alkylacetylenes must be employed as partners of nitrones. Fu demonstrated that a copper and a chiral phosphaferrocene-oxazoline catalyst mediated an asymmetric intramolecular Kinugasa reaction to produce polycyclic β-lactams with good enantioselectivity (Scheme 1b).[6b] Recently two independent example of a stereocontrolled induction of *n*-heptyl group at 3-position of β-lactam were reported, although its enantiomeric excess was not high (Scheme 1c).[7a,10] Therefore a range of applicability to various alkylacetylenes remains unsatisfactory.

Herein, the author describes an asymmetric Kinugasa reaction between aryl- or alkyl-substituted alkynes and nitrones, using a copper and prolinol-based hydroxy amino phosphine ligand catalyst (Scheme 1d). This system serves as cooperative catalysis for constructing a chiral environment in Kinugasa reaction to give highly enantiocontrolled β-lactams.

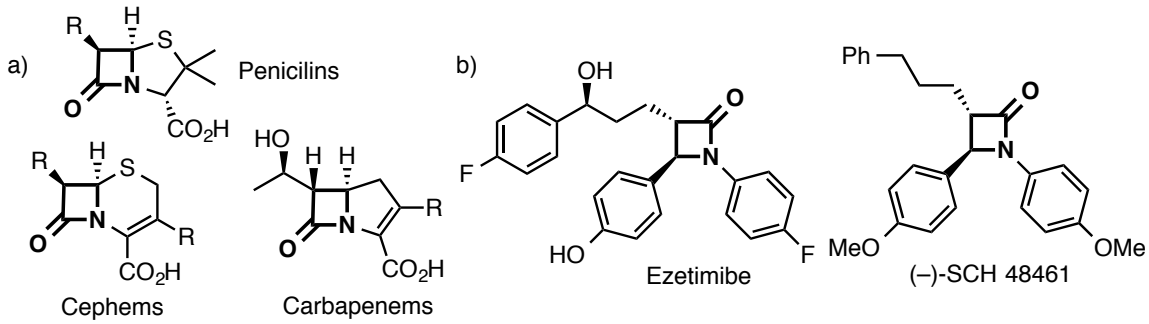

Figure 1. Major bioactive β-lactams: a) antibiotics, and b) drugs.

Scheme 1. Asymmetric Kinugasa reactions.

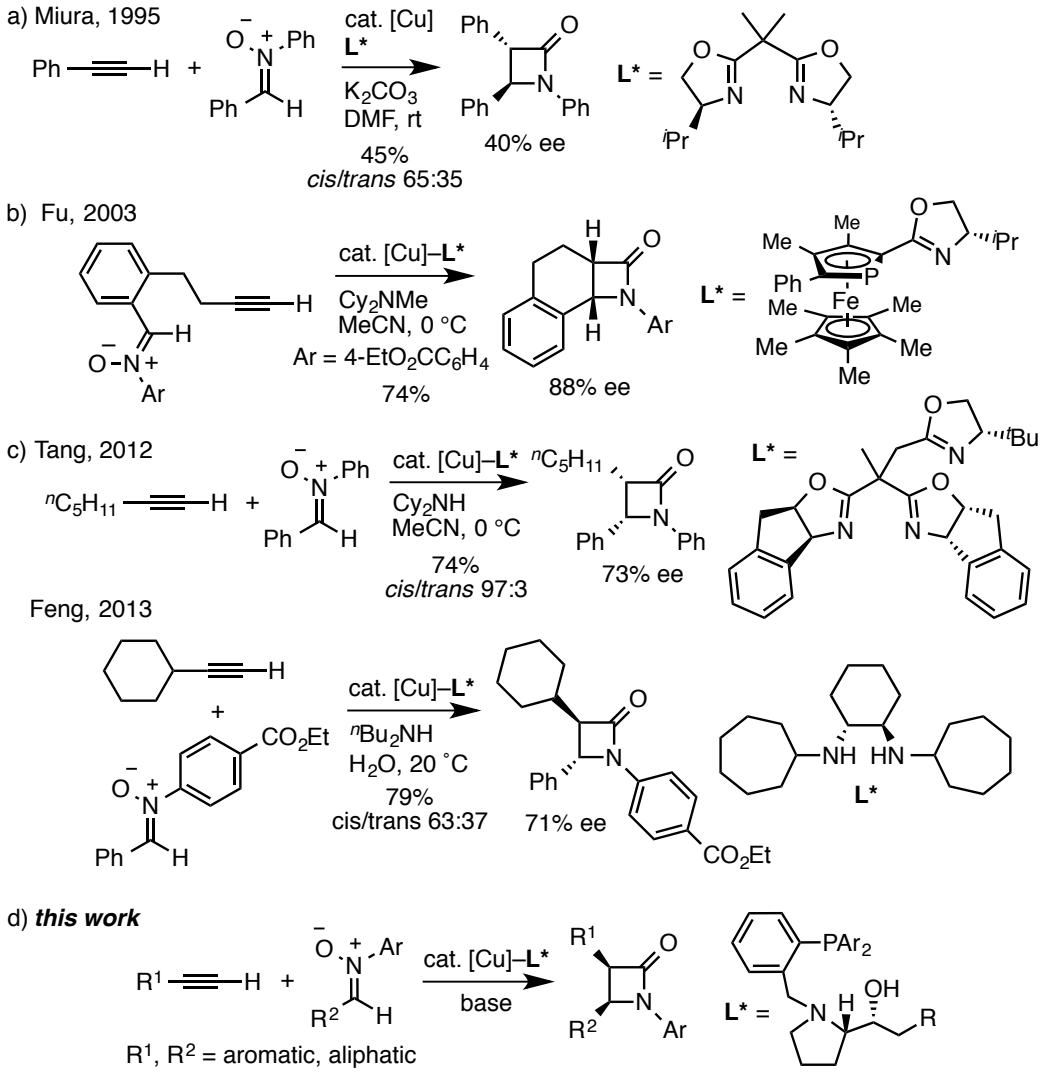

Results and Discussion

Initial studies of Kinugasa reaction by hydrogen-bonding-based catalysts

The hydroxy amino phosphine chiral ligand was developed for copper-catalyzed asymmetric direct alkynylation of aldehydes by Sawamura's group (Scheme 2a).[11] DFT calculations revealed a hydrogen-bonding interaction between the ligand and the substrate occurs to allow an enantioselective synthesis of chiral propargyl alcohols. The author expected that the hydrogen-bonding-assistance tolerate the use of nitrones instead of aldehydes to cause a coupling reaction with terminal alkynes in a stereoselective manner (Scheme 2b).

Scheme 2. Hydrogen-bonding-assisted enantioselective alkynylation reactions.

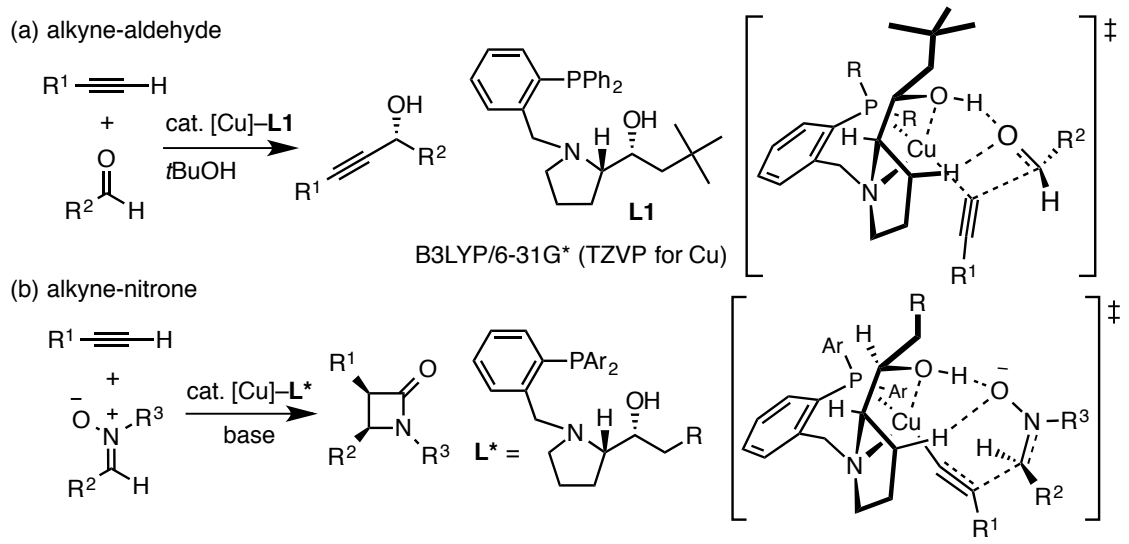

Triggered by this assumption, the utility of the hydroxy amino phosphine ligand in the coupling between phenylacetylene (**1a**) and *C*-cyclohexyl-*N*-phenylnitrone (**2a**) was examined (Scheme 3). The reactions were conducted in the presense of copper(II) triflate with a stoichiometric amount of diethylamine in toluene at 25 °C for 24 h. The use of the prototype hydroxy amino phosphine chiral ligand **L1**, which performed as the best ligand in the asymmetric alkynylation of aldehydes, afforded the corresponding β-lactam **3aa** in 67% yield with 74% diastereoselectivity and 68% enantioselectivity. In the control reaction without any ligand, drops in both yield and diastereoselectivity were

observed. To know the involvement of the hydrogen bonding, the hydroxy group of **L1** was protected with a methyl group. Although the reaction with the OMe-substituted ligand (**L1-OMe**) proceeded, the appearance of enantioselectivity was completely inhibited. This result suggests that the hydrogen bond derived from **L1** is critically important for the stereocontrol in Kinugasa reaction.

Scheme 3. Cu/**L1**-catalyzed Kinugasa reaction with phenylacetylene (**1a**).

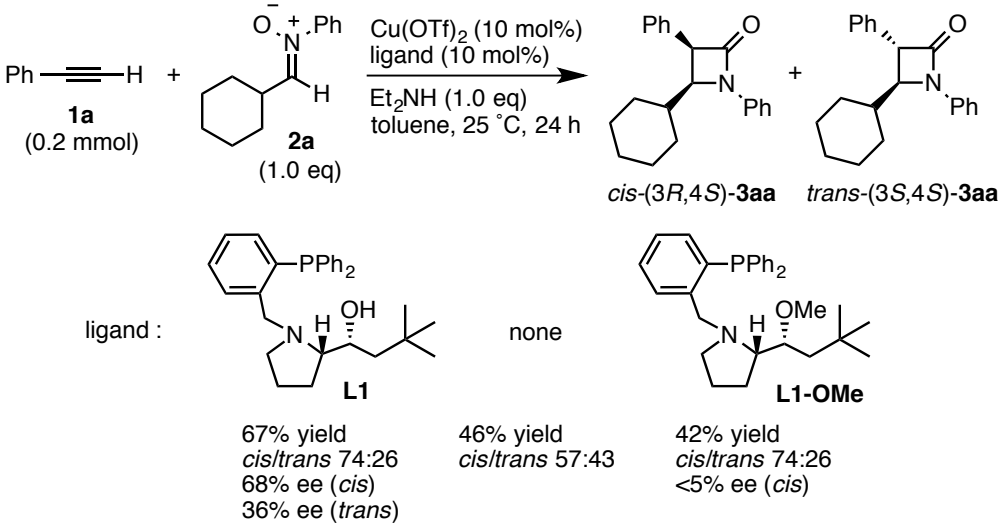

The use of an aliphatic acetylene was also tested. When the reaction with 1-hexyne (**1b**) was carried out at 0 ˚C taking more rapid consumption of copper alkylacetylide into consideration, the chiral *cis*- and *trans*-β-lactams **3ba** were furnished with excellent enantioselectivities (Scheme 4).

Scheme 4. Cu/**L1**-catalyzed Kinugasa reaction with 1-hexyne (**1b**).

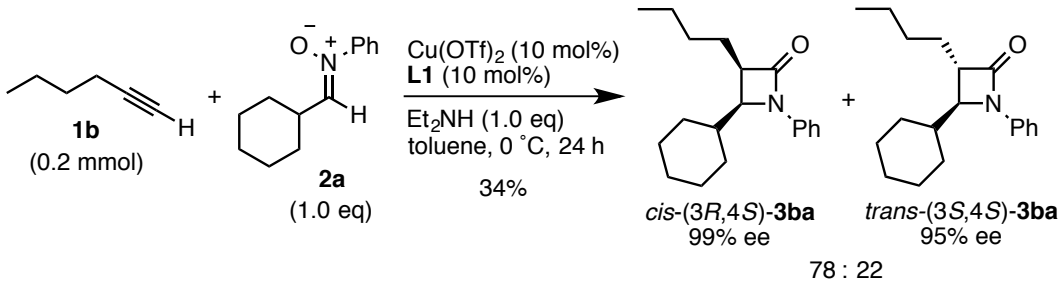

Ligand effect

Encouraged by the initial results, the conditions was optimized in Kinugasa reaction between **1a** and **2a** using **L1** were conducted. when the concentration of **1a** and **2a** was reduced from 0.5 to 0.2 M in toluene, higher yield (76%) of **3aa** was achieved (Table1, entry 1 versus entry 2). The lower reaction temperature, the more diastereo- and enantioselectivity were improved (entries 3–5).

To investigate the effect of the structure of the hydroxy amino phosphine ligand on the reactivity, diastereoselectivity, and enantioselectivity, the reaction between **1a** and **2a** was performed. **L2** bearing a primary hydroxy group was less reactive and showed slightly lower diastereoselectivity than **L1** (entry 6 versus entry 5). In addition, when a neopentyl moiety was replaced with a trimethylsilylmethyl group (**L3**), the improvement on yield (95%) and enantioselectivity (88% ee) was observed (entry 7). Elongation of alkyl chain into ethyl (**L4**) and *n*-propyl (**L5**) on *Si* atom enhanced the enantiomeric excess of *cis*-(3*R*,4*S*)-**3aa**, albeit with loss of the product yield (entries 8 and 9). On the other hand, electronic and steric effects on phosphorus substituents with the neopentyl skeleton were examined. The OMe group at *para* position of *P*-aryl groups gave high enantiomeric excess of the *cis*-product (86% ee), while the reaction with F-containing **L7** proceeded in moderate yield and stereoselectivities (entries 10 and 11). In entry 12 the use of **L8** with steric hinderance on *P* moiety resulted in the drop of yield and enantioseleectivity. The reaction with **L9** bearing dicyclohexyl phophino group proceeded moderately to give less enantioselective **3aa** (entry 13). Taking these results into consideration, the combination of tri-*n*-propylsilylmethyl group at α position of the alcohol moiety and *p*-methoxyphenyl substituent on *P* atom, **L10**, was performed to afford **3aa** in 97% yield with excellent enantioselectivity (92% ee) (entry 14). Even though the use of **L11** bearing di(4-fluorophenyl)phosphino moiety with the alkylsilyl side chain also provided a comparable result (entry 15), the best ligand was **L10** in terms of yield and diastereoselectivity.

Based on these results, a new chiral silyl-induced hydroxy amino phosphine ligand was developed for the catalytic asymmetric Kinugasa reaction that allowed highly

diastereoselective and enantioselective access to β-lactams.

Table 1. Ligand optimization in the reaction between **1a** and **2a**.[a]

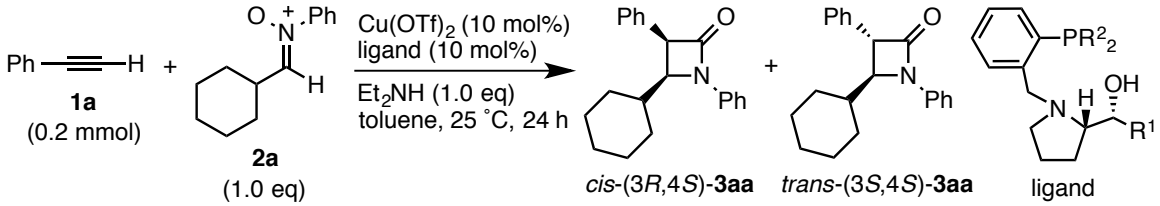

entry	ligand			temp.	yield	*cis*/*trans*[d]	ee (%)[e]	
		R^1	R^{2} [b]	(°C)	(%)[c]		*cis*	*trans*
1[f]	**L1**	$CH_2{}^t$Bu	Ph	25	67	74:26	68	36
2	**L1**	$CH_2{}^t$Bu	Ph	25	76	76:24	77	37
3	**L1**	$CH_2{}^t$Bu	Ph	0	77	82:18	76	32
4	**L1**	$CH_2{}^t$Bu	Ph	–20	71	86:14	86	21
5	**L1**	$CH_2{}^t$Bu	Ph	–40	81	87:13	84	20
6	**L2**	H	Ph	–40	68	81:19	88	41
7	**L3**	CH_2SiMe_3	Ph	–40	95	86:14	87	31
8	**L4**	CH_2SiEt_3	Ph	–40	90	87:13	89	47
9	**L5**	$CH_2Si^nPr_3$	Ph	–40	89	88:12	89	49
10	**L6**	$CH_2{}^t$Bu	Ph^{OMe}	–40	84	90:10	86	8
11	**L7**	$CH_2{}^t$Bu	Ph^{F}	–40	67	86:14	71	31
12	**L8**	$CH_2{}^t$Bu	Ph^{DTBM}	–40	52	71:29	1[g]	5
13	**L9**	$CH_2{}^t$Bu	Cy	–40	43	69:31	29	52
14	**L10**	$CH_2Si^nPr_3$	Ph^{OMe}	–40	97	90:10	92	51
15	**L11**	$CH_2Si^nPr_3$	Ph^{F}	–40	94	87:13	92	59

[a] Reaction conditions: **1a** (0.2 mmol), **2a** (0.2 mmol), $Cu(OTf)_2$ (10 mol%), ligand (10 mol%), and Et_2NH (0.2 mmol) in toluene (1.0 mL) at –40 °C for 24 h. [b] Ph^{OMe} = 4-$MeOC_6H_4$, Ph^{F} = 4-FC_6H_4, Ph^{DTBM} = 3,5-di-^{t}Bu-4-$MeOC_6H_4$, Cy = cyclohexyl. [c] Yield of isolated product as isomeric mixture. [d] The ratios were determined by ^{1}H NMR spectroscopy. [e] The ee values were determined by HPLC analysis using a chiral

stationary phase. [f] Toluene (0.4 mL) was used. [g] The product was obtained as an opposite enantiomer to the one shown above.

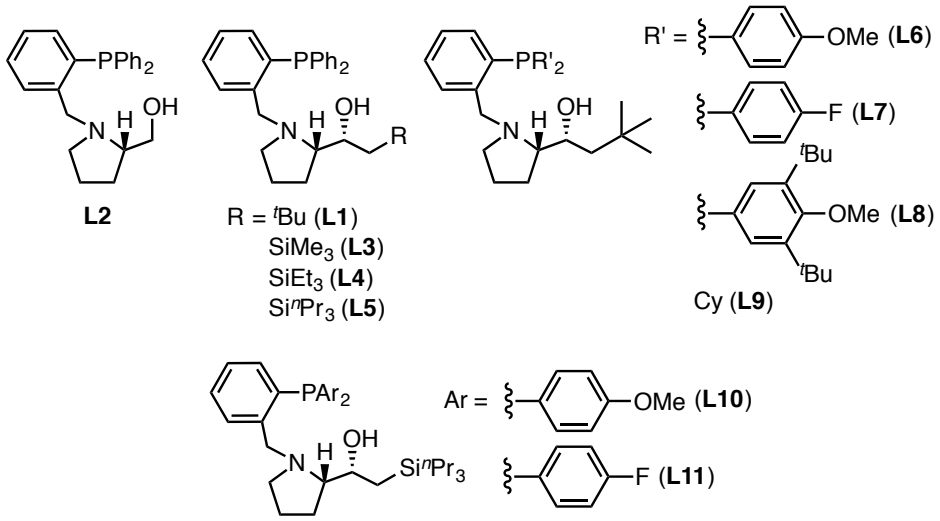

Figure 2. Ligands bearing the hydroxy amino phosphine scafford.

The comparison with other chiral ligands disclosed the effect of the hydroxy amino phosphine ligand. In the case of alkyne **1a** an oxazoline ligand **L12** did not show high reactivity and selectivities (Table 2, entry 1), unlike the catalytic systems reported by Miura nor Tang. When (*R*)-Segphos (**L13**) was employed, the reaction also proceeded moderately despite the ee value of the *trans* product is lacking (entry 2). The use of *N*-heterocyclic carbene that is C_2-symmetric (**L14**) or bearing a phenolic pendant (**L15**)[12] gave nearly racemic **3aa** (entries 3 and 4). When **1b** was used, the reaction also showed quite low enantioselelectivity (entries 5 and 6). This indicated that the hydroxy amino phosphine ligand has a remarkable catalytic activity, especially for alkylacetylenes.

Table 2. Copper-catalyzed enantioselective Kinugasa reactions with phenylacetylene (**1a**) or 1-hexyne (**1b**).[a]

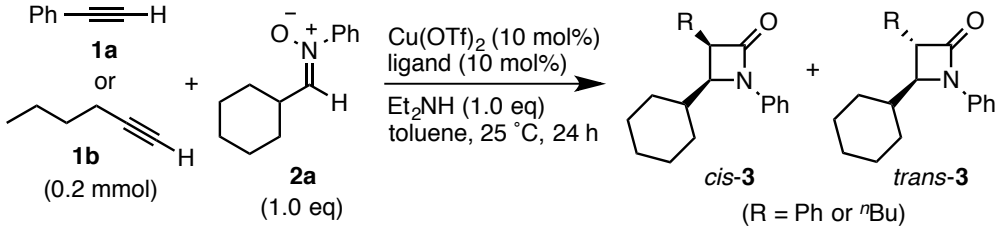

entry	alkyne	ligand	yield (%)[b]	*cis*/*trans*[c]	ee (%)[d]	
					cis	*trans*
1	**1a**	**L12**	55	54:46	40[e]	44[e]
2	**1a**	**L13**	40	62:38	10[e]	7[e]
3	**1a**	**L14**	50	65:35	10	7
4	**1a**	**L15**	45	60:40	6	5
5[f]	**1b**	**L12**	50	75:25	11[e]	8[e]
6[f]	**1b**	**L15**	45	70:30	11	15

[a] Reaction conditions: **1a** or **1b** (0.2 mmol), **2a** (0.2 mmol), $Cu(OTf)_2$ (10 mol%), ligand (10 mol%), and Et_2NH (0.2 mmol) in toluene (0.4 mL) at 25 ˚C for 24 h. [b] Yield of isolated product as isomeric mixture. [c] The ratios were determined by ^1H NMR spectroscopy. [d] The ee values were determined by HPLC analysis using a chiral stationary phase. [e] The product was obtained as an opposite enantiomer to the one shown above. [f] Run at 0 ˚C.

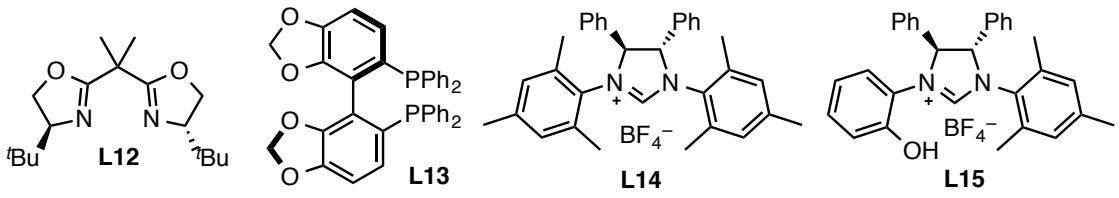

Figure 3. Typical chiral ligands.

Condition screening

The effect of copper source was summarized in Table 3. A catalytic $Cu(OTf)_2$ worked the best in high yield (67%) and enantioselectivity (68% ee) (entry 1). The

reaction with copper(I) salt such as CuI or CuCl proceeded moderately with no enantiocontroll on both isomers of **3aa** (entries 2 and 3). When cationic copper(I) complexes were used, the enantiomeric excess of *cis*-β-lactam **3aa** elevated to moderate level (entries 4 and 5). Copper(II) salts gave poor results (entries 6–8). In contrast, the presense of cationic Cu(II) salts accelerated this process. The use of $Cu(ClO_4)_2 \cdot 6H_2O$ also resulted in good enantioselectivities (entry 9 versus entry 1).

Table 3. Effect of Copper catalyst in the reaction between **1a** and **2a**.[a]

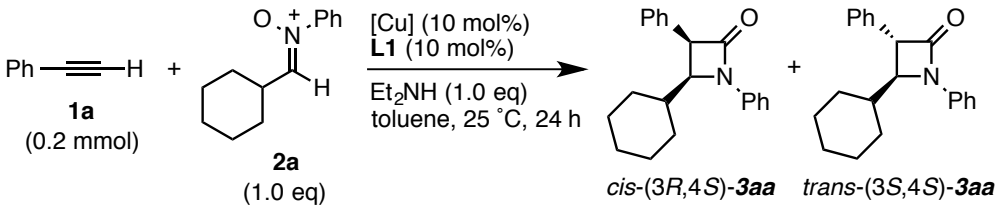

entry	[Cu]	yield (%)[b]	*cis*/*trans*[c]	ee (%)[d]	
				cis	*trans*
1	$Cu(OTf)_2$	67	74:26	68	36
2	CuI	54	83:17	0	5[e]
3	CuCl	64	79:21	0	2[e]
4	$CuOTf \cdot (toluene)_{1/2}$	70	80:20	53	19
5	$[Cu(MeCN)_4]BF_4$	55	81:19	44	16
6	$CuCl_2$	53	69:31	8[e]	31[e]
7	$Cu(OAc)_2$	45	74:26	24	12[e]
8	$Cu(acac)_2$	17	78:22	22	21[e]
9	$Cu(ClO_4)_2 \cdot 6H_2O$	49	74:26	60	52

[a] Reaction conditions: **1a** (0.2 mmol), **2a** (0.2 mmol), [Cu] (10 mol%), **L1** (10 mol%), and Et_2NH (0.2 mmol) in toluene (0.4 mL) at 25 °C for 24 h. [b] Yield of isolated product as isomeric mixture. [c] The ratios were determined by ^1H NMR spectroscopy. [d] The ee values were determined by HPLC analysis using a chiral stationary phase. [e] The product was obtained as an opposite enantiomer to the one shown above.

The best performing base is diethylamine (Table 4, entry 1). Elongation of alkyl groups of secondary amines slightly increased reactivity or enantioselectivity (entries 2 and 3); however, *n*-dibutylamine tended to show relatively poor reproducibility by causing an isomerization of β-lactam products. Furthermore, bulkier substituents on the *N* atom did not improve the yield and selectivities (entries 4–6). The reaction with primary (entries 7 and 8), or tertiary amine (entries 9–11) including dicyclohexylamine employed by Fu's protocol gave **3aa** of low enantiomeric excess. In addition, cyclic secondary amines were ineffective (entries 12–14). The use of pyridine and potassium carbonate, which was typically found in the non-asymmetric Kinugasa reaction, did not afford the product or resulted in quite low selectivities (entries 15 and 16).

Table 4. Base effect in the reaction between **1a** and **2a**.[a]

entry	base	yield (%)[b]	*cis*/*trans*[c]	ee (%)[d]	
				cis	*trans*
1	Et_2NH	67	74:26	69	36
2	$^{n}Pr_2NH$	68	77:23	67	37
3	$^{n}Bu_2NH$	71	71:29	71	47
4	$^{i}Bu_2NH$	42	75:25	33	29
5	$^{sec}Bu_2NH$	20	86:14	32	21
6	Cy_2NH	37	82:18	67	8
7	$^{t}BuNH_2$	58	81:19	5	11[e]
8	$AdNH_2$	34	71:29	1[e]	8
9	Et_3N	26	91:9	26	34
10	Et_2NMe	30	89:11	27	23

11	Cy_2NMe	25	92:8	24	21
12	piperidine	37	61:39	8[e]	14
13	TMP[f]	15	75:25	17	47
14	morpholine	32	61:39	2[e]	2
15	pyridine	n.d.[g]	–	–	–
16	K_2CO_3	12	68:32	13	19

[a] Reaction conditions: **1a** (0.2 mmol), **2a** (0.2 mmol), $Cu(OTf)_2$ (10 mol%), **L1** (10 mol%), and base (0.2 mmol) in toluene (0.4 mL) at 25 ˚C for 24 h. [b] Yield of isolated product as isomeric mixture. [c] The ratios were determined by ^1H NMR spectroscopy. [d] The ee values were determined by HPLC analysis using a chiral stationary phase. [e] The product was obtained as an opposite enantiomer to the one shown above. [f] 2,2,6,6-tetramethylpiperidine. [g] not detected.

Various solvents were screened in the presense of $Cu(OTf)_2$ and Et_2NH (Table 5). The best reaction solvent was toluene (entry 1). MeCN gave the racemic *cis*-β-lactam **3aa** (entry 2), even though it was the efficient solvent in most cases of the previously reported Kinugasa reactions. The reaction in other coordinating solvents such as THF or dioxane provided the moderate product yield and enantioselectivity (entries 3 and 4). Highly polar solvents showed a drop of enantiomeric excess of the β-lactam (entries 5–8). Surprisingly, an alcoholic solvent, which caused a great enhancement of reactivity and enantioselectivity in the alkynylation of aldehydes with **L1**, was not suitable for Kinugasa reaction (entry 9). In contrast, the reaction proceeded well in aromatic hydrogen carbon solvents as well as toluene, thus affording **3aa** in good to high yields with good enantioselectivities (entries 10–12).

Table 5. Solvent effect in the reaction between **1a** and **2a**.[a]

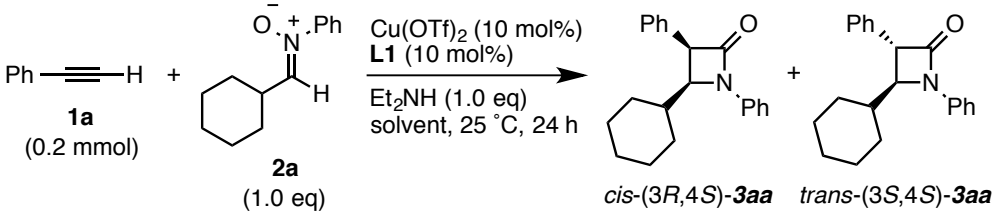

entry	solvent	yield (%)[b]	*cis*/*trans*[c]	ee (%)[d]	
				cis	*trans*
1	toluene	67	74:26	68	36
2	MeCN	47	84:16	0	21
3	THF	57	75:25	48	24
4	1,4-dioxane	52	79:21	52	17
5	TBME[e]	60	75:25	21	37
6	EtOAc	77	84:16	57	42
7	DMF	47	67:33	2	5
8	CH_2Cl_2	47	78:22	38	20
9	MeOH	40	65:35	5	13
10	benzene	52	80:20	64	55
11	*p*-xylene	47	68:32	66	37
12	mesitylene	82	75:25	67	34

[a] Reaction conditions: **1a** (0.2 mmol), **2a** (0.2 mmol), $Cu(OTf)_2$ (10 mol%), **L1** (10 mol%), and Et_2NH (0.2 mmol) in solvent (0.4 mL) at 25 °C for 24 h. [b] Yield of isolated product as isomeric mixture. [c] The ratios were determined by ^1H NMR spectroscopy. [d] The ee values were determined by HPLC analysis using a chiral stationary phase. [e] *tert*-Butyl methyl ether.

Scope and limitation on substrates

The copper/hydroxy amino phosphine ligand catalysis was applicable to various combinations of aryl- or alkyl-substituted alkynes and nitrones, affording the enantioenriched β-lactams. As summarized in Table 6, in some cases with

phenylacetylene (**1a**) loss of enantiomeric excess was observed for *trans*-β-lactam, while the use of 1-hexyne (**1b**) provided excellent enantioselectivity both isomers of products. For example **1a** reacted completely with **2a**, and the reaction of **1b** with **L10** under the optimized conditions proceeded in moderate yield (entry 1 versus entry 2). The electronic effects of the *N*-aryl moiety of nitrones on the reactivity and stereoselectivities were evaluated (entries 3–6). The nitrones possessing substituents (OMe; **2b**, or F; **2c**) also proceed with excellent enantioselectivities, even though the product yields decreased related to with **2a**. The nitrone **2d** bearing a bulky substituent at the *ortho* position was efficiently coupled with **1a** (entries 7 and 8), albeit with loss of reactivity in the case of phenylacetylene (**1a**). In addition, **2e** was perfect since both **3ae** and **3be** were obtained quantitatively with excellent selectivities (entries 9 and 10). The variation of the *C*-alkyl substituent on nitrones was also investigated. The cyclohexyl group could be replaced with isopropyl (**2f**), which led to high enantioselectivities (entries 11 and 12). In contrast, the reaction with **1a** and nitrone **2g** having *n*-butyl moiety was less enantioselective, especially with a significant drop of the ee value of *trans*-**3ag** (entry 13). The combination between **1b** and **2g** reacted as well as others to furnish **3bg** with excellent enantioselectivity (entry 14). Functionality on nitrones was tolerated such as *N*-Boc-4-piperidyl (**2h**) (entry 15). The combination between **1a** and *C*,*N*-biarylnitrones was found to be less enantioselective. Entry 16 described the reaction with **2i** derived from benzaldehyde, affording moderate enantiomeric excess of β-lactams. This combination was also influenced by the electronic property of substituents on aryl moieties. **1a** reacted with nitrone bearing phenyl with methoxy group (**2j**) or with trifluoromethyl group (**2k**) at *para* position to afford the corresponding products in 27% and 72% yields, respectively (entries 17 and 18). This fact indicated that the electronic properties of substituents on *C*,*N*-biarylnitrones are of significance in this catalytic system.

Table 6. The reactions of various nitrones with phenylacetylene (**1a**) or 1-hexyne (**1b**).[a]

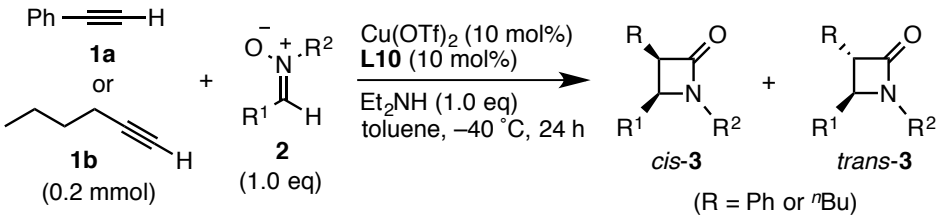

entry	alkyne	nitrone		yield(%)[b]	*cis*/*trans*[c]	ee (%)[d]	
		R^1	R^2			*cis*	*trans*
1	**1a**	Cy	Ph (**2a**)	97 (**3aa**)	90:10	92	51
2	**1b**	Cy	Ph (**2a**)	55 (**3ba**)	80:20	98	97
3	**1a**	Cy	4-MeO-C_6H_4 (**2b**)	54 (**3ab**)	87:13	80	37
4	**1b**	Cy	4-MeO-C_6H_4 (**2b**)	44 (**3bb**)	88:12	>99	99
5	**1a**	Cy	4-F-C_6H_4 (**2c**)	61 (**3ac**)	80:20	90	54
6	**1b**	Cy	4-F-C_6H_4 (**2c**)	30 (**3bc**)	79:21	98	97
7	**1a**	Cy	2-Me-C_6H_4 (**2d**)	31 (**3ad**)	92:8	92	80
8	**1b**	Cy	2-Me-C_6H_4 (**2d**)	92 (**3bd**)	71:29	>99	98
9	**1a**	Cy	1-naphthyl (**2e**)	91 (**3ae**)	90:10	99	90
10	**1b**	Cy	1-naphthyl (**2e**)	>99 (**3be**)	68:32	99	98
11	**1a**	^{i}Pr	Ph (**2f**)	79 (**3af**)	89:11	91	54
12	**1b**	^{i}Pr	Ph (**2f**)	38 (**3bf**)	79:21	99	98
13	**1a**	^{n}Pent	Ph (**2g**)	72 (**3ag**)	77:23	82	7
14	**1b**	^{n}Pent	Ph (**2g**)	50 (**3bg**)	72:28	98	96
15	**1a**	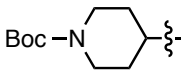	Ph (**2h**)	71 (**3ah**)	75:25	92	46
16	**1a**	Ph	4-MeO_2C-C_6H_4 (**2i**)	43 (**3ai**)	59:41	72	65
17[e,f]	**1a**	4-MeO-C_6H_4	4-MeO_2C-C_6H_4 (**2j**)	27 (**3aj**)	63:37	60	59
18[f]	**1a**	4-F_3C-C_6H_4	4-MeO_2C-C_6H_4 (**2k**)	72 (**3ak**)	57:43	73	67

[a] Reaction conditions: **1a** or **1b** (0.2 mmol), **2** (0.2 mmol), $Cu(OTf)_2$ (10 mol%), **L10** (10 mol%), and Et_2NH (0.2 mmol) in toluene (1.0 mL) at –40 °C for 24 h. [b] Yield of

isolated product as isomeric mixture. [c] The ratios were determined by ^{1}H NMR spectroscopy. [d] The ee values were determined by HPLC analysis using a chiral stationary phase. [e] THF was used as solvent. [f] Run at –20 °C.

The compatibility of various functional groups on the nitrones **2** was also investigated. The reactions of phenylacetylene derivatives with electronically diverse substituents including MeO, F, Br, and CO_2Me groups at *para* position (**1c**, **1d**, **1e** and **1f**) afforded the corresponding products in high yields with high enantioselectivities (entries 1–4). A sulfur-containing heteroaromatic alkyne, 2-ethynyl-5-methylthiophene (**1g**), was tolerated (entry 5). A conjugate enyne **1h** underwent the reaction with **2a** to provide the corresponding β-lactam **3ha** with 98% enantioselectivity (entry 6).

Table 7. The reactions of aromatic acetylenes with nitrone **2a**.[a]

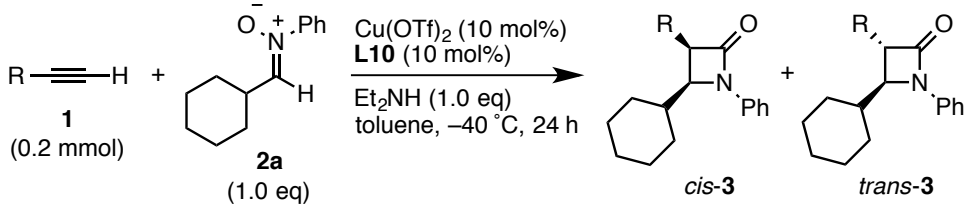

entry	alkyne R	yield (%)[b]	*cis*/*trans*[c]	ee (%)[d] *cis*	ee (%)[d] *trans*
1	4-MeO-C_6H_4 (**1c**)	95 (**3ca**)	96:4	92	36
2	4-F-C_6H_4 (**1d**)	55 (**3da**)	88:12	91	44
3	4-Br-C_6H_4 (**1e**)	67 (**3ea**)	83:17	92	41
4	4-MeO_2C-C_6H_4 (**1f**)	82 (**3fa**)	62:38	83	78
5	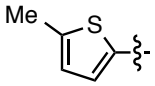 (**1g**)	71 (**3ga**)	83:17	99	98
6	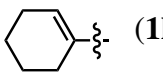 (**1h**)	73 (**3ha**)	78:22	98	73

[a] Reaction conditions: **1** (0.2 mmol), **2a** (0.2 mmol), $Cu(OTf)_2$ (10 mol%), **L10** (10 mol%), and Et_2NH (0.2 mmol) in toluene (1.0 mL) at –40 °C for 24 h. [b] Yield of isolated product as isomeric mixture. [c] The ratios were determined by ^{1}H NMR

spectroscopy. [d] The ee values were determined by HPLC analysis using a chiral stationary phase.

The applicability toward aliphatic alkynes is shown in Table 8. Steric variety of terminal alkynes has no influence on both reactivity and stereoselectivities (entry 1–3). The reaction between 6-chloro-1-hexyne (**1l**) and **2a** gave the chlorinated *cis*- and *trans*-products **3la** in 49% yield with 98% and 95% ee (entry 4). Functionalized alkylacetylenes with a pivalate ester (**1m**), phthalimide (**1n**), or silyl ether (**1o**) substituent at their chain terminus reacted with excellent enantioselectivities (entries 5–7). The alkyne containing cyclic acetal (**1p**) showed moderate yield (66%) and high enantioselectivities (entry 8). Propargylic functionalities such as dibenzylamine (**1q**) and methoxymethyl ether (**1r**) were introduced into the chiral β-lactams with more than 95% enantiomeric excesses (entries 9 and 10). In addition, free propargylic alcohol (**1s**) were also tolerated (entry 11). Other reaction combinations were demonstrated with chlorine-containing alkyne **1l** to afford **3le** or **3li** with excellent enantioselectivities, respectively (entries 12 and 13). Entry 14 between **1k** and **2j** was performed in THF at 0 ˚C due to relatively poor solubility and reactivity of the nitrone, thus resulted in small loss of enantioselectivity. It should be noted that **3kj** has the characteristic structure in β-lactam drug (–)-SCH 48461[9], and thus the protocol can be expected as a facile preparation method for β-lactam drugs.

Table 8. The reactions of aliphatic acetylenes.[a]

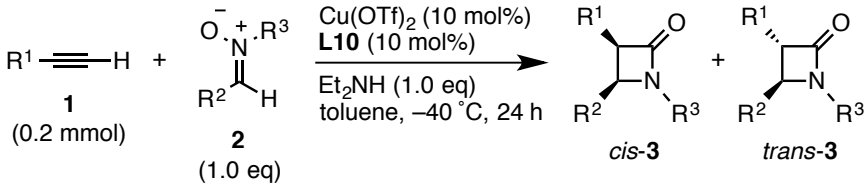

entry	alkyne	nitrone		yield (%)[b]	*cis*/*trans*[c]	ee (%)[d]	
	R^1	R^2	R^3			*cis*	*trans*
1	^{i}Bu (**1i**)	Cy	Ph (**2a**)	52 (**3ia**)	67:33	99	98
2	Cy (**1j**)	Cy	Ph (**2a**)	48 (**3ja**)	78:22	97	92
3	Ph (**1k**)	Cy	Ph (**2a**)	50 (**3ka**)	78:22	96	91
4	Cl (**1l**)	Cy	Ph (**2a**)	49 (**3la**)	82:18	98	95
5	^{t}BuO(C=O) (**1m**)	Cy	Ph (**2a**)	48 (**3ma**)	71:29	99	99
6	(**1n**)	Cy	Ph (**2a**)	28 (**3na**)	71:29	96	94
7	TBDMSO (**1o**)	Cy	Ph (**2a**)	53 (**3oa**)	84:16	98	97
8	(**1p**)	Cy	Ph (**2a**)	66 (**3pa**)	80:20	97	94
9	Bn_2N (**1q**)	Cy	Ph (**2a**)	42 (**3qa**)	68:32	99	97
10	MOMO (**1r**)	Cy	Ph (**2a**)	69 (**3ra**)	54:46	96	97
11	HO (**1s**)	Cy	Ph (**2a**)	76 (**3sa**)	87:13	98	95
12	Cl (**1l**)	Cy	1-naphthyl (**2e**)	>99 (**3le**)	75:25	99	98
13	Cl (**1l**)	Ph	4-MeO_2C-C_6H_4 (**2i**)	41 (**3li**)	89:11	94	78
14[e]	Ph (**1k**)	4-MeO-C_6H_4	4-MeO_2C-C_6H_4 (**2j**)	31 (**3kj**)	79:21	87	84

[a] Reaction conditions: **1b** (0.2 mmol), **2** (0.2 mmol), $Cu(OTf)_2$ (10 mol%), **L10** (10 mol%), and Et_2NH (0.2 mmol) in toluene (1.0 mL) at –40 °C for 24 h. [b] Yield of isolated product as isomeric mixture. [c] The ratios were determined by ^{1}H NMR spectroscopy. [d] The ee values were determined by HPLC analysis using a chiral

stationary phase. [e] The reaction was in toluene at 0 ˚C.

The use of 1-substituted propargyl alcohols and the derivatives gave 3-methylene-2-azetidinones (Figure 4a). These alkynes with copper catalyst form allenylidene copper species.[13] Thus subsequent cycloaddition with **2a** furnished β-lactams induced a methylene group. This behavior was not much observed in primary propargyl alcohols, such as **1r** and **1s**. Furthermore, Figure 4b shows unreactive nitrone substrates. The reaction with conjugate nitrone did not occur. This protocol did not tolerate cyclic nitrone, even though it has the substituent manner similar to the standard one, **2a**. In addition, a nitrone bearing the reverse substituent such as *C*-aryl and *N*-alkyl afforded no product.

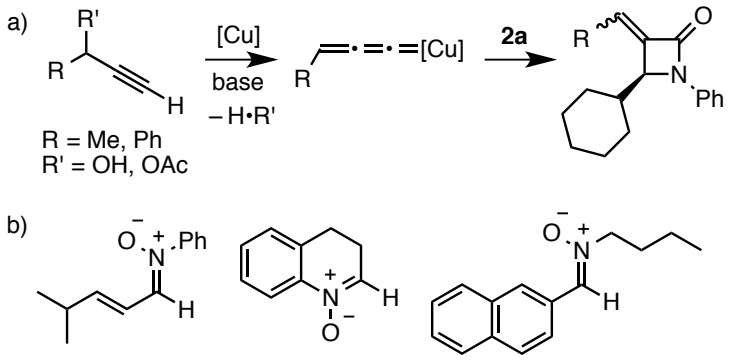

Figure 4. a) Generation of 3-methylene azetidinone from substituted propargyl alcohols, b) nitrone substrates that do not furnish the product in Kinugasa reaction.

Most cases of lower product yields were due to the consumption of substrates. As shown in scheme 5, the formation of four compounds other than **3kj** (28% yield) was observed when the reaction between **1k** and **2j** was conducted. Amide **4** was generated from alkyne **1k**. The presence of a Cu(II) species and an oxygen atom source was known to allow a terminal alkyne to react with a secondary amine and produce amide product.[14] In addition, the oxygen atom transfer from nitrone **2j** was mediated by copper species and afforded the corresponding imine **5**, followed by partially hydrolysis to form an aldehyde **6** and an aniline **7**.[5] Thus the observations were resulted from

competing nitrone deoxygenation and alkyne-amine coupling reaction.

Scheme 5. Byproducts formation pathways.

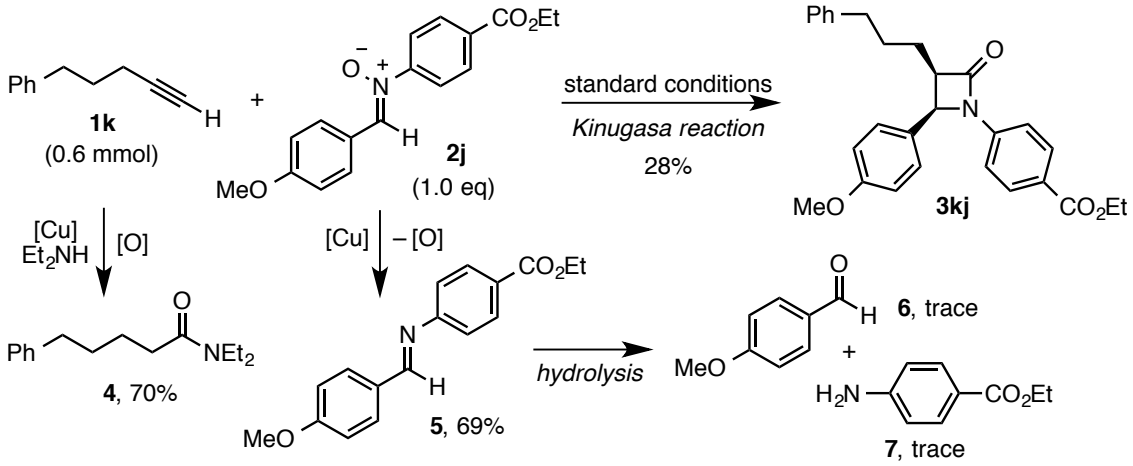

Determination of absolute configuration

Some β-lactam products, which mainly have more than two aryl substituents, were capable of being recrystallized and obtained predominantly as *cis*-isomeric pure. The single crystal of the bromo-substituted *cis*-**3ea** (98% ee) was obtained by recrystallization from CH_2Cl_2/hexane. According to X-ray analysis, the absolute configuration was determined as 3*R*,4*S* (Figure 5).

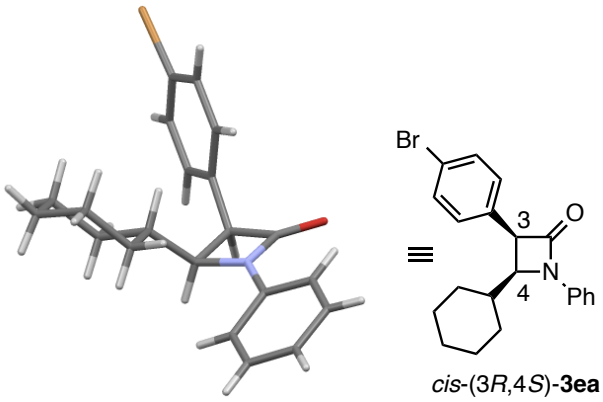

Figure 5. Crystal structure for *cis*-(3*R*,4*S*)-**3ea**.

Furthermore, an optically rotation of the β-lactam product was agreement with the observed absolute configuration by comparison with the reported data. The

cis-(3*R*,4*S*)-**3aa** generated in this reaction was $[\alpha]_D = -66.5$ (c 0.84, $CHCl_3$), while Feng reported *cis*-(3*S*,4*R*)-**3aa** product with the opposite rotation, $[\alpha]_D = +66.0$ (c 0.57, $CHCl_3$).[7a]

For *trans*-β-lactams, vibrational circular dichroism (VCD) and IR spectra was used to determine absolute configuration.[15] The comparison with computational results confirmed that *trans*-**3ba** and **3ja** have 3*S*,4*S* configurations.

Synthetic Applications

Most drugs containing β-lactam scaffold display *trans* manner. Although this protocol afforded the isomeric mixture of β-lactams, the products can kinetically converge at *trans* side via the epimerization at the carbonyl α position under the basic condition. For **3ba**, the treatment with potassium alkoxide at room temperature is allowed to isolate pure *trans* isomer in high enantiomeric purity (Scheme 6).

Scheme 6. *Cis*-to-*trans* isomerization of **3ba** under the basic condition.

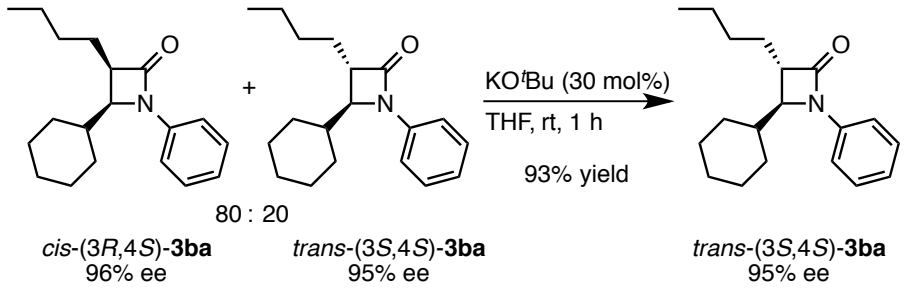

Since the alkylation of the β-lactam nitrogen can build up the precursors for bicyclic β-lactams, unsubstituted β-lactam at *N*-1 are required.[2c] The oxidative deprotection of *N*-aryl moiety of the β-lactam **3bb** with ammonium cerium nitrate (CAN) was demonstrated (Scheme 7). This conversion provided only the *cis*-substituted 2-azetidinone **8** in 66% yield.

Scheme 7. Deprotection of *N*-*p*-methoxyphenyl moiety.

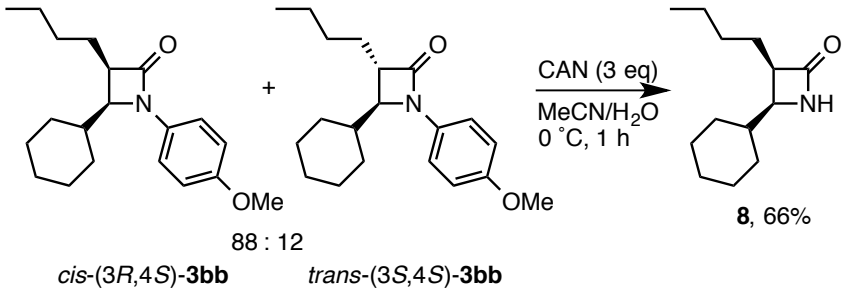

Possible Reaction Pathway

According to the generally proposed mechanism of Kinugasa reaction, DFT calculations in this system was performed and summerized in Figure 6. Copper(II) species was reduced in situ into copper(I)[16], and the P,N-chelation of the ligand to copper occurred. The hydroxy group provide a hydrogen-bond-donor site by coordinating to the copper. Consequently, a P,N,O-bound copper(I)–alkyne complex forms a hydrogen-bonded complex (**A**) with Et_2NH. Proton relay through Et_2NH in **A** leads to C(sp)–H activation of terminal alkyne **1** to generate copper acetylide **B** with a Cu-bound hydroxy group. Complex **B** formed O–H···O and C(sp^3)–H···O hydrogen bonding with the nitrone, shown as complex **C**. The oxyanion of the nitrone is hydrogen-bonded with the ligand hydroxyl group. A non-classical C(sp^3)–H···O hydrogen bond is consistent with the previous report.[11] In the next step, the possibility of a typical [3+2] cycloaddition pathway forming both C–C and C–O bond has to be considered. However, since the nitrone is captured through two-point-hydrogen-bonding, subsequent C–C bond formation may occur in a stepwise manner rather than a [3+2] cycloaddition manner.[17] Thus the copper acetylide reacted at the carbon β to the copper atom to develop a new C–C bond with the nitrone imino carbon. In the transition state [**TS (C-D)**] the steric repulsion between the substituent of the alkyne (R^1) and the aryl group on N atom (R^3) should be minimized. This stereochemical model can be proposed on the basis of the observation that more sterically demanding *N*-substituents such as *o*-tolyl and 1-naphthyl groups afforded better enantioselectivities (Table 6, entries 7–10). The C–C bond forms first (**D**), and

then ring closure occurs upon C–O bond formation (**E**). After the formation of the five membered ring, the last step is the stereoselective protonation and dissociation of the β-lactam product from the catalyst, allowing regeneration of complex **A**.

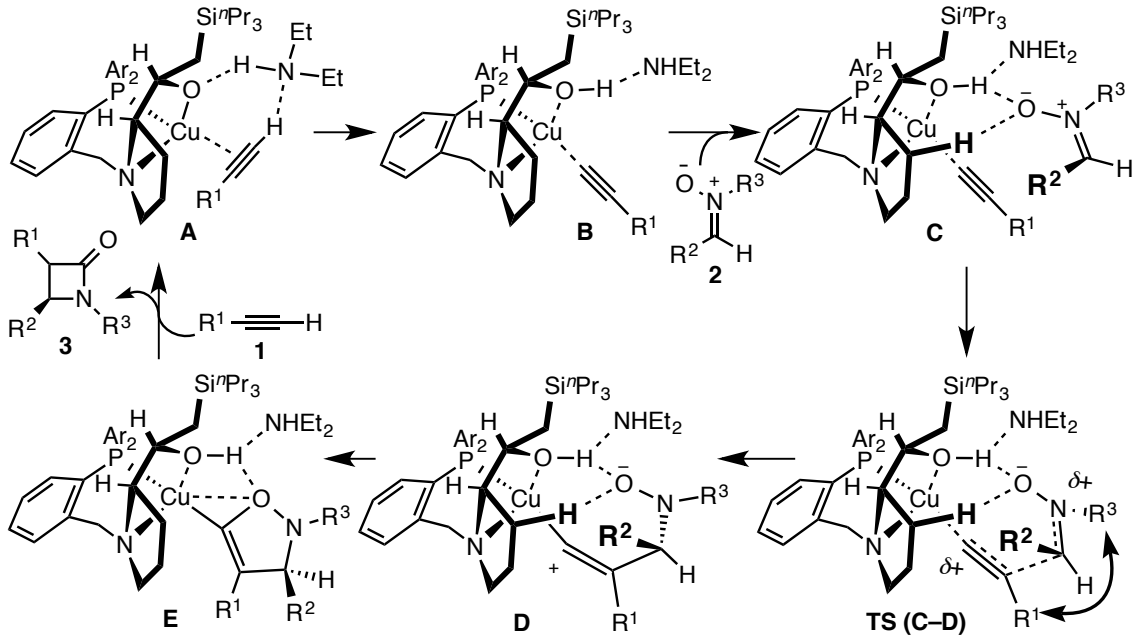

Figure 6. Proposed mechanistic cycle.

The atomic distances by DFT calculations also suggested two-point hydrogen bonding interactions between the catalyst and the nitrone as shown in Figure 7: the relatively short hydroxyl hydrogen···oxygen interaction (1.48 Å) and the secondary interaction of one hydrogen of the pyrrolidine moiety with the same oxygen (2.33 Å).

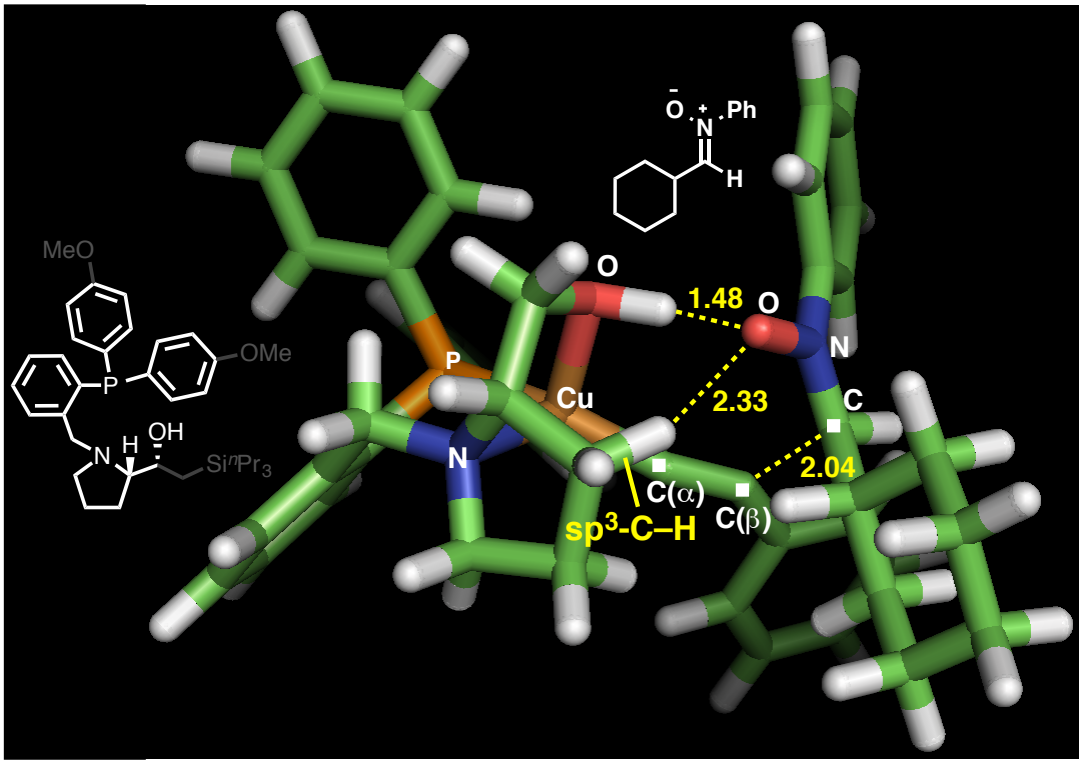

Figure 7. A transition state **TS (C–D)**. The alkyl moiety at α position of the hydroxy group and the OMe groups on the *P*-Aryl substituents of the ligand was omitted.

Conclusion

The author developed copper-catalyzed asymmetric Kinugasa reaction using a new silyl-induced hydroxy amino phosphine ligand. This system showed broad substrate scope and tolerated diverse functionalities on both terminal alkynes and nitrones, including halides, esters, ethers, amines and an unprotected hydroxy group. In particular, the C-3 introduction of an aliphatic side chain of β-lactams using alkylacetylenes can provide a practice approach for the synthesis of bioactive and pharmatheutical compounds. The catalytic reaction mechanism was also proposed by DFT calculations, which revealed that the hydrogen-bonding interactions between the ligand and the nitrone involved the first C–C bond formation step.

Experimental Section

Instrumentation and chemicals

NMR spectra were recorded on a Varian Gemini 2000 spectrometer, operating at 300 MHz for ^{1}H NMR and 75.4 MHz for ^{13}C NMR, and a JEOL ECX-400, operating at 400 MHz for ^{1}H NMR, 100.5 MHz for ^{13}C NMR and 161.8 MHz for ^{31}P NMR. Chemical shift values for ^{1}H and ^{13}C and ^{31}P NMR are referenced to Me_4Si, the residual solvent resonances and external aqueous 85% H_3PO_4, respectively. Chemical shifts are reported in δ ppm. Mass spectra were obtained with Thermo Fisher Scientific Exactive, JEOL JMS-T100LP or JEOL JMS-700TZ at the Instrumental Analysis Division, Equipment Management Center, Creative Research Institution, Hokkaido University. Melting points were measured on a Yanaco MP-500D apparatus. HPLC analyses were conducted on a HITACHI ELITE LaChrom system with a HITACHI L-2455 diode array detector. IR spectra were measured with a Perkin-Elmer Spectrum One. TLC analyses were performed on commercial glass plates bearing 0.25 mm layer of Merck Silica gel $60F_{254}$. Silica gel (Kanto Chemical Co., Silica gel 60 N, spherical, neutral) was used for column chromatography.

All reactions were carried out under nitrogen or argon atmosphere. Unless otherwise noted, materials obtained from commercial suppliers were used without further purification. $Cu(OTf)_2$ was purchased from Tokyo Chemical Industry Co., Ltd. and stored under nitrogen. Diethylamine was purchased from Junsei Chemical Co., Ltd. and stored under argon. *The Kinugasa reactions were conducted with freshly distilled amine within 1 month, which was crucial for the reproducibility*. All solvents for catalytic reactions were degassed and stored over 4Å molecular sieves in a glove box.

Preparation of hydroxy amino phosphine derivatives

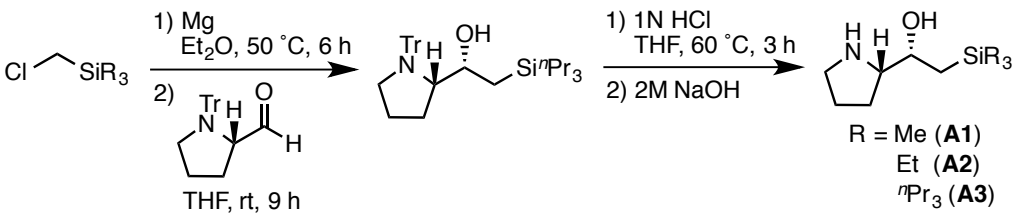

(α*R*,2*S*)-α-tripropylsilylmethyl-2-pyrrolidinemethanol (A3)

The stereocontrolled Grignard addition with *N*-tritylprolinal invoked by an acyclic Felkin-Anh model was applied to the reaction with tripropylsilylmethylmagnesium chloride. Tripropylsilylmethyl chloride (6.2 g, 30.0 mmol) was mixed with magnesium (730.0 mg, 30 mmol) in Et_2O (20 mL) and allowed at 50 ˚C for 6 h. The Grignard reagent was added to a solution of *N*-tritylprolinal (5.1 g, 15.0 mmol) in THF (30 mL) in water bath to prevent temperature increasing. After being stirred for 9 h at room temperature, the mixture was quenched with a saturated aqueous NH_4Cl at 0 °C. The mixture was filtered through a pad of Celite® and the solvent was removed under reduced pressure. The crude product was diluted with THF (30 mL) and 1M HCl (22.5 mL, 1.5 mmol) was added to the solution. After 3 h of vigorous stirring at 60 ˚C, the mixuture was eluted with $CHCl_3$ and 2M NaOH (20 mL) was added. The mixture was extracted with $CHCl_3$, dried and concentrated *in vacuo* to afford **A3** (4.3 g, 15.9 mmol) in 53% yield.

Determination of the relative configuration

The amino alcohol was converted to the cyclic carbamate according to the Chemla's method.[18] The 1,2-*cis* relative configuration of was confirmed by coupling constant and NOESY measurements.

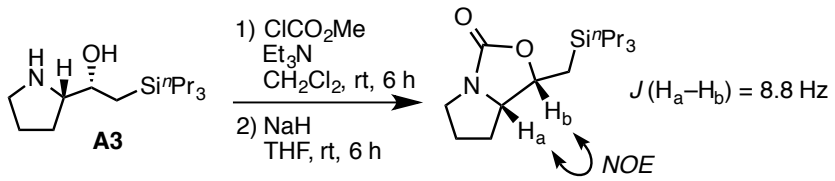

Colorless oil. **^{1}H NMR** δ 0.53–0.65 (m, 6H), 0.86 (dd, *J* = 6.6, 14.7 Hz, 1H), 0.97 (t, *J* = 6.9 Hz, 9H), 1.12 (dd, *J* = 9.0, 14.7 Hz, 1H), 1.23–1.40 (m, 6H), 1.49 (m, 1H), 1.68 (m, 1H), 1.85 (m, 1H), 2.06 (m, 1H), 3.18 (ddd, *J* = 3.6, 9.6, 11.4 Hz, 1H), 3.62–3.76 (m, 2H), 4.80 (td, *J* = 6.6, 9.0 Hz, 1H). **^{13}C NMR** δ 14.49, 15.44, 17.32, 18.54, 24.78, 25.13, 46.18, 65.00, 74.77, 162.13. **HRMS–ESI** (*m/z*): $[M+Na]^+$ calcd for $C_{16}H_{31}NO_2NaSi$, 320.2016; found, 320.2016.

(α*R*,2*S*)-(–)-1-(2-Diphenylphosphinobenzyl)-α-(trimethylsilylmethyl)-2-pyrrolidinemethanol (L3)

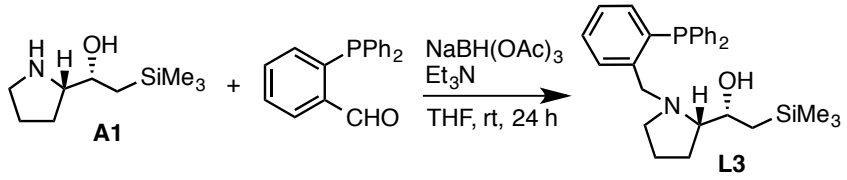

To a solution of **A1** (2.5 g, 14.6 mmol) in THF (50 mL) was added 2-diphenylphosphinobenzaldehyde (3.9 g, 14.6 mmol), Et_3N (10 mL, 73.0 mmol) and $NaBH(OAc)_3$ (6.2 g, 29.2 mmol) at room temperature. The mixture was stirred at room temperature for 12 h. The mixture was quenched with H_2O. The aqueous layer was extracted with Et_2O several times, and the combined organic layer was dried over $MgSO_4$ and concentrated. The residue was purified by silica gel chromatography (hexane/EtOAc 93:7) to give **L3** (4.7 g, 10.5 mmol) in 72% yield.

Off-white solid. **Mp** 67.0–69.1 °C. **^{1}H NMR** δ 0.04 (s, 9H), 0.59 (dd, *J* = 6.9, 14.7 Hz, 1H), 0.81–0.96 (m, 2H), 1.31–1.79 (m, 3H), 1.99 (q, *J* = 9.6 Hz, 1H), 2.26 (m, 2H), 2.51 (t, *J* = 7.8 Hz, 1H), 3.25 (d, *J* = 12.9 Hz, 1H), 3.38 (s, 1H), 4.05 (dt, *J* = 1.9, 7.5 Hz, 1H), 4.42 (d, *J* = 12.3 Hz, 1H), 6.96 (m, 1H), 7.15–7.38 (m, 13H). **^{13}C NMR** δ –0.71, 21.34, 22.21, 22.95, 54.49, 58.02 (d, *J* = 14.4 Hz), 65.85, 70.36, 127.34, 127.91 (d, *J* = 1.8 Hz), 128.35 (d, *J* = 6.6 Hz), 128.43 (d, *J* = 8.7 Hz), 128.44 (d, *J* = 20.1 Hz), 128.88, 129.59 (d, *J* = 5.7 Hz), 133.48 (d, *J* = 19.2 Hz), 133.62 (d, *J* = 19.2 Hz), 134.88, 135.73 (d, *J* = 13.5 Hz), 136.33 (d, *J* = 7.5 Hz), 136.33 (d, *J* = 7.5 Hz), 138.03 (d, *J* = 10.5 Hz), 144.22 (d, *J* = 24.0 Hz). **^{31}P NMR** δ –17.04. **HRMS–ESI** (*m*/*z*): $[M+H]^+$ calcd for $C_{28}H_{37}NOSiP$, 462.2377; found, 462.2371. **$[\alpha]_D^{20}$** –78.0 (*c* 0.93, $CHCl_3$).

(α*R*,2*S*)-(–)-1-(2-Diphenylphosphinobenzyl)-α-(triethylsilylmethyl)-2-pyrrolidinemethanol (L4)

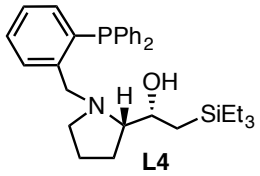

L4

Off-white solid. **Mp** 82.4–83.5 °C. **^{1}H NMR** δ 0.48–0.66 (m, 6H), 0.82–1.03 (m, 9H), 1.20–1.64 (m, 4H), 1.74 (m, 1H), 2.00 (m, 1H), 2.27 (t, *J* = 7.8 Hz, 1H), 2.52 (t, *J* = 7.8 Hz, 1H), 3.27 (d, *J* = 12.6 Hz, 1H), 3.34 (d, *J* = 5.4 Hz, 1H), 4.05 (m, 1H), 4.39 (d, *J* = 12.6 Hz, 1H), 6.95 (m, 1H), 7.03–7.40 (m, 13H). **^{13}C NMR** δ 3.89, 7.47, 16.22, 22.21, 22.99, 54.43, 57.98, 65.57, 70.53, 127.26, 128.25 (d, *J* = 6.3 Hz), 128.26, 128.32 (d, *J* = 5.2 Hz), 128.35 (d, *J* = 12.9 Hz), 128.77, 129.51 (d, *J* = 6.3 Hz), 133.39 (d, *J* = 19.5 Hz), 133.53 (d, *J* = 19.2 Hz), 134.74 (d, *J* = 1.2 Hz), 135.67 (d, *J* = 13.5 Hz), 136.31 (d, *J* = 7.5 Hz), 137.90 (d, *J* = 10.5 Hz), 144.10 (d, *J* = 24.0 Hz). **^{31}P NMR** δ –16.88. **HRMS–ESI** (*m*/*z*): $[M+H]^+$ calcd for $C_{31}H_{42}NOSiP$, 504.2846; found, 504.2844. **$[\alpha]_D^{24}$** –57.7 (*c* 1.17, $CHCl_3$).

(α*R*,2*S*)-(–)-1-(2-Diphenylphosphinobenzyl)-α-(tripropylsilylmethyl)-2-pyrrolidinemethanol (L5)

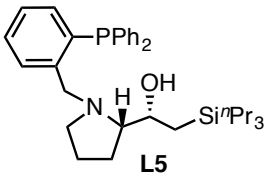

L5

Colorless oil. **^{1}H NMR** δ 0.48–0.65 (m, 7H), 0.82–0.92 (m, 1H), 0.95 (t, *J* = 7.5 Hz, 9H), 1.22–1.60 (m, 9H), 1.72 (m, 1H), 2.00 (m, 1H), 2.26 (m, 1H), 2.52 (t, *J* = 7.5 Hz, 1H), 3.28 (d, *J* = 12.9 Hz, 1H), 3.31 (s, 1H), 4.04 (dt, *J* = 1.8, 7.5 Hz, 1H), 4.40 (d, *J* = 12.3 Hz, 1H), 6.96 (m, 1H), 7.15–7.40 (m, 13H). **^{13}C NMR** δ 15.95, 17.42, 17.48, 18.70, 22.40, 23.12, 54.52, 58.03 (d, *J* = 14.4 Hz), 65.78, 70.57, 127.36, 127.91, 128.36 (d, *J* = 6.3 Hz), 128.42 (d, *J* = 6.0 Hz), 128.44 (d, *J* = 11.4 Hz), 128.86, 129.64 (d, *J* = 6.3 Hz),

133.47 (d, *J* = 19.6 Hz), 133.68 (d, *J* = 19.6 Hz), 134.83 (d, *J* = 1.5 Hz), 135.81 (d, *J* = 13.8 Hz), 136.49 (d, *J* = 7.5 Hz), 137.99 (d, *J* = 10.8 Hz), 144.29 (d, *J* = 24.0 Hz). **^{31}P NMR** δ –17.01. **HRMS–ESI** (*m*/*z*): $[M+H]^+$ calcd for $C_{34}H_{49}NOSiP$, 546.3316; found, 546.3324. **$[\alpha]_D^{25}$** –46.1 (*c* 1.18, $CHCl_3$).

(α*R*,2*S*)-(–)-1-(2-Di(4-methoxyphenyl)phosphinobenzyl)-α-(2,2-dimethylpropyl) -2-pyrrolidinemethanol (L6)

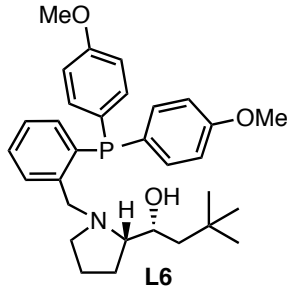

L6

Pale yellow oil. **^{1}H NMR** δ 0.95 (s, 9H), 1.04–1.63 (m, 5H), 1.74 (m, 1H), 2.00 (m, 1H), 2.21 (m, 1H), 2.59 (t, *J* = 7.8 Hz, 1H), 3.28 (d, *J* = 12.9 Hz, 1H), 3.43 (s, 1H), 3.795 (s, 3H), 3.798 (s, 3H), 3.89 (d, *J* = 7.8 Hz, 1H), 4.29 (d, *J* = 12.9 Hz, 1H), 6.82–6.89 (m, 4H), 6.93 (m, 1H), 7.10–7.31 (m, 6H), 7.35 (m, 1H). **^{13}C NMR** δ 22.46, 23.15, 29.99, 30.23, 46.90, 54.21, 55.07, 55.08, 57.54 (d, *J* = 14.4 Hz), 65.43, 70.35, 114.10, 114.21, 127.22, 127.54 (d, *J* = 5.1 Hz), 128.61, 128.87 (d, *J* = 8.1 Hz), 129.46 (d, *J* = 5.7 Hz), 134.08, 135.20 (d, *J* = 20.7 Hz), 135.23 (*J* = 21.3 Hz), 137.01 (d, *J* = 14.4 Hz), 143.69 (d, *J* = 22.2 Hz), 160.13, 160.20. **^{31}P NMR** δ –19.50. **HRMS–ESI** (*m*/*z*): $[M+H]^+$ calcd for $C_{31}H_{41}NO_3P$, 506.2819; found, 506.2817. **$[\alpha]_D^{23}$** –49.3 (*c* 1.23, $CHCl_3$).

(α*R*,2*S*)-(–)-1-(2-Di(4-fluorophenyl)phosphinobenzyl)-α-(2,2-dimethylpropyl)-2-pyrrolidinemethanol (L7)

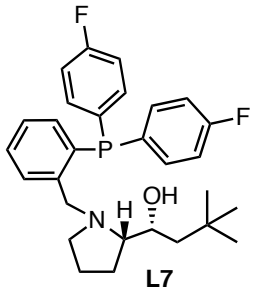

L7

Off-white solid. **Mp** 114.1–115.1 °C. **^{1}H NMR** δ 0.83–1.45 (m, 4H), 0.96 (s, 9H), 1.56 (m, 1H), 1.71 (m, 1H), 1.95 (q, J = 9.6 Hz, 1H), 2.18 (m, 1H), 2.43 (t, J = 8.1 Hz, 1H), 3.21 (d, J = 12.3 Hz, 1H), 3.38 (s, 1H), 3.98 (d, J = 8.4 Hz, 1H), 4.41 (d, J = 12.3 Hz, 1H), 6.93 (dd, J = 4.8, 7.5 Hz, 1H), 7.02 (q, J = 9.3 Hz, 4H), 7.10–7.38 (m, 7H). **^{13}C NMR** δ 22.10, 23.06, 30.04, 30.27, 46.89, 54.09, 57.88 (d, J_p = 12.9 Hz), 65.34, 70.56, 115.49 (dd, J_P = 7.5, J_F = 21.0 Hz), 115.77 (dd, J_P = 7.5, J_F = 21.0 Hz), 127.47, 129.10, 129.78 (d, J_P = 6.3 Hz), 131.69 (dd, J_F = 3.3, J_P = 7.5 Hz), 133.28 (dd, J_F = 3.3, J_P = 10.2 Hz), 134.40, 135.21 (dd, J_F = 8.1, J_P = 9.6 Hz), 135.46 (d, J_P = 14.4 Hz), 135.49 (dd, J_F = 8.1, J_P = 9.9 Hz), 143.98 (d, J_P = 23.7 Hz), 163.11 (d, J_F = 248.7 Hz), 163.22 (d, J_F = 248.7 Hz). **^{31}P NMR** δ –19.21. **HRMS–ESI** (*m/z*): $[M+H]^+$ calcd for $C_{29}H_{35}NOF_2P$, 482.2419; found, 482.2416. **$[\alpha]_D^{24}$** –64.0 (*c* 1.02, $CHCl_3$).

(α*R*,2*S*)-(–)-1-(2-Di(3,5-bis(*tert*-butyl)-4-methoxyphenyl)phosphinobenzyl)-α-(2,2-dimethylpropyl)-2-pyrrolidinemethanol (L8)

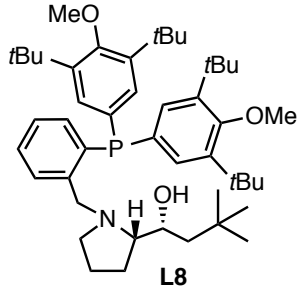

L8

White solid. **Mp** 142.1–144.2 °C. **^{1}H NMR** δ 0.95 (s, 9H), 1.08–1.60 (m, 5H), 1.29 (s, 18H), 1.30 (s, 18H), 1.71 (m, 1H), 1.89 (m, 1H), 2.21 (m, 1H), 2.50 (t, J = 7.5 Hz, 1H), 3.31–3.41 (m, 2H), 3.64 (s, 3H), 3.66 (s, 3H), 3.96 (d, J = 7.5 Hz, 1H), 4.38 (d, J = 12.9

Hz, 1H), 6.92 (m, 1H), 6.97 (d, *J* = 7.5 Hz, 2H), 7.07 (d, *J* = 8.4 Hz, 2H), 7.16–7.42 (m, 3H). **^{13}C NMR** δ 22.15, 23.19, 30.17, 30.33, 31.99, 35.74, 35.80, 47.01, 54.12, 57.44 (d, *J* = 15.3 Hz), 64.22, 64.27, 65.32, 70.35, 126.84, 128.47, 129.06 (d, *J* = 5.7 Hz), 130.04 (d, *J* = 3.9 Hz), 131.30 (d, *J* = 7.8 Hz), 132.03 (d, *J* = 20.1 Hz), 132.17 (d, *J* = 20.1 Hz), 134.20, 137.13 (d, *J* = 15.3 Hz), 143.18 (d, *J* = 9.6 Hz), 143.25 (d, *J* = 9.6 Hz), 143.81 (d, *J* = 21.9 Hz), 159.67, 159.85. **^{31}P NMR** δ –16.31. **HRMS–ESI** (*m/z*): $[M+H]^+$ calcd for $C_{47}H_{73}NO_3P$, 730.5323; found, 730.5319. **$[\alpha]_D^{21}$** –29.1 (*c* 0.73, $CHCl_3$).

(α*R*,2*S*)-(–)-1-(2-Di(4-methoxyphenyl)phosphinobenzyl)-α-(tripropylsilylmethyl)-2-pyrrolidinemethanol (L10)

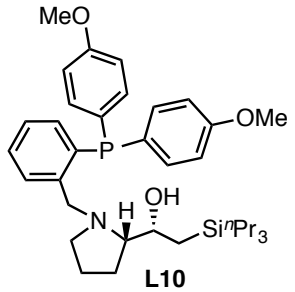

L10

Oil. **^{1}H NMR** δ 0.47–0.64 (m, 7H), 0.82–1.13 (m, 2H), 0.95 (t, *J* = 7.2 Hz, 9H), 1.22–1.62 (m, 8H), 1.76 (m, 1H), 2.02 (m, 1H), 2.27 (m, 1H), 2.56 (t, *J* = 7.8 Hz, 1H), 3.28 (d, *J* = 12.6 Hz, 1H), 3.41 (s, 1H), 3.80 (s, 6H), 4.00 (dt, *J* = 1.5, 7.5 Hz, 1H), 4.32 (d, *J* = 12.6 Hz, 1H), 6.81–6.89 (m, 4H), 6.94 (ddd, *J* = 1.5, 4.8, 7.8 Hz, 1H), 7.10–7.21 (m, 5H), 7.28 (m, 1H), 7.35 (m, 1H). **^{13}C NMR** δ 15.90, 17.34, 17.45, 22.53, 23.17, 54.54, 55.08, 57.82 (d, *J* = 13.2 Hz), 65.78, 70.40, 113.99, 114.07, 127.18, 127.62 (d, *J* = 5.7 Hz), 128.52, 128.88 (d, *J* = 8.4 Hz), 129.50 (d, *J* = 5.7 Hz), 134.18, 134.88 (d, *J* = 21.0 Hz), 135.11 (d, *J* = 21.0 Hz), 136.83 (d, *J* = 14.4 Hz), 143.73 (d, *J* = 22.8 Hz), 159.94. **^{31}P NMR** δ –19.90. **HRMS–ESI** (*m/z*): $[M+H]^+$ calcd for $C_{36}H_{53}NO_3SiP$, 606.3527; found, 606.3528. **$[\alpha]_D^{25}$** –49.5 (*c* 1.05, $CHCl_3$).

(α*R*,2*S*)-(–)-1-(2-Di(4-fluorophenyl)phosphinobenzyl)-α-(tripropylsilylmethyl)-2-pyrrolidinemethanol (L11)

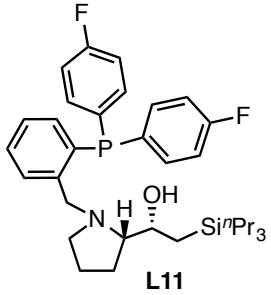

L11

Oil. **^{1}H NMR** δ 0.48–0.68 (m, 7H), 0.80–1.15 (m, 2H), 0.96 (t, *J* = 7.2 Hz, 9H), 1.21–1.60 (m, 8H), 1.79 (m, 1H), 2.05 (m, 1H), 2.30 (m, 1H), 2.60 (t, *J* = 7.5 Hz, 1H), 3.25 (d, *J* = 12.0 Hz, 1H), 3.38 (s, 1H), 4.04 (dt, *J* = 1.8, 7.8 Hz, 1H), 4.35 (d, *J* = 12.0 Hz, 1H), 6.88–7.06 (m, 5H), 7.12–7.38 (m, 7H). **^{13}C NMR** δ 15.89, 17.33, 17.43, 18.66, 22.24, 23.02, 54.44, 58.06 (d, J_P = 13.2 Hz), 65.71, 70.57, 115.54 (dd, J_P = 7.8, J_F = 21.0 Hz), 115.74 (dd, J_P = 7.8, J_F = 21.0 Hz), 127.51, 129.09, 129.84 (d, J_P = 6.6 Hz), 131.88 (dd, J_F = 3.3, J_P = 7.2 Hz), 133.26 (dd, J_F = 3.0, J_F = 10.5 Hz), 134.47, 135.19 (dd, J_F = 7.8, J_P = 15.0 Hz), 135.41 (dd, J_F = 7.5, J_P = 14.4 Hz), 135.45 (d, J_P = 14.4 Hz), 144.10 (d, J_P = 24.0 Hz), 163.15 (d, J_F = 247.8 Hz), 163.18 (d, J_F = 247.8 Hz). **^{31}P NMR** δ –19.45. **HRMS–ESI** (*m*/*z*): $[M+H]^+$ calcd for $C_{34}H_{47}NOF_2SiP$, 582.3127; found, 582.3119. **$[\alpha]_D^{24}$** –58.1 (*c* 0.99, $CHCl_3$).

Preparation of alkynes and nitrones

Alkynes **1a**, **1b**, **1c**, **1d**, **1e**, **1h**, **1i**, **1j**, **1k**, **1l** and **1s** were obtained from commercial suppliers and distilled before use. Alkynes **1f**, **1m**, **1n**, **1o**, **1p**, **1q** and **1r** were synthesized by simple derivatization from commercial available alkynes. Alkyne **1g**[19] was prepared according to the reported procedures.

Preparation of nitrones

Method A: To a solution of the nitro compound (1.0 eq), aldehyde (1.0 eq), NH_4Cl (1.3 eq) in EtOH/H_2O (3:1) at 0 ˚C was added zinc powder (2.0 eq) portionwise over 1 h and the reaction mixture was allowd to warm to rt and stirred for 9 h. The mixture was

filtered through a Celite pad and the filtrate was extracted with CH_2Cl_2 (x3). The combined organic phases were dried over Na_2SO_4, filtered and concentrated *in vacuo*. The crude mixture was purified with column chromatography on silica gel (EtOAc/*n*-hexane = 10 to 50%, then MeOH/CH_2Cl_2 = 5%). Following by recrystallization from CH_2Cl_2/*n*-hexane or wash with Et_2O, the nitrone was obtained as a white or off-white solid.

Method B: To a solution of the hydroxyamine (1.0 eq) and $MgSO_4$ (1.2 eq) in CH_2Cl_2 was added the aldehyde and the reaction mixture was stirred at rt until complete by TLC. The reaction mixture was then filtered and concentrated in vacuo to afford the crude product, then which was purified via silica gel column chromatography (EtOAc/*n*-hexane = 10 to 50%, then MeOH/CH_2Cl_2 = 5%) to give the nitrone.

(*Z*)-1-Cyclohexyl-*N*-(4-fluorophenyl)methanimine Oxide (2c)

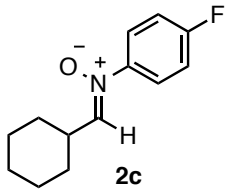

2c

White solid. **Mp** 128.2–129.0 ˚C. **^{1}H NMR** δ 1.22–1.35 (m, 3H), 1.38–1.52 (m, 2H), 1.67–1.81 (m, 3H), 1.96–2.05 (m, 2H), 3.19 (m, 1H), 7.00 (d, *J* = 7.5 Hz, 1H), 7.06–7.14 (m, 2H), 7.62–7.70 (m, 2H). **^{13}C NMR** δ 25.23, 25.91, 28.82, 35.70, 115.82 (d, *J* = 22.8 Hz), 123.60 (d, *J* = 8.7 Hz), 143.45, 144.03, 162.95 (d, *J* = 247.8 Hz). **HRMS–ESI** (*m*/*z*): $[M+H]^+$ calcd for $C_{13}H_{17}NOF$, 222.1289; found, 222.1289.

(*Z*)-1-Cyclohexyl-*N*-(2-methylphenyl)methanimine Oxide (2d)

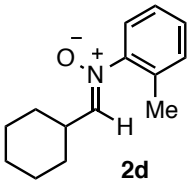

2d

White solid. **Mp** 58.4–60.4 °C. **^{1}H NMR** δ 1.22–1.35 (m, 3H), 1.40–1.53 (m, 2H), 1.66–1.81 (m, 3H), 1.97–2.07 (m, 2H), 2.37 (s, 3H), 3.24 (m, 1H), 6.68 (d, *J* = 8.1 Hz, 1H), 7.18–7.34 (m, 4H). **^{13}C NMR** δ 16.73, 25.15, 25.88, 28.84, 34.98, 123.38, 126.58, 129.16, 131.24, 131.50, 146.85, 147.56. **HRMS–ESI** (*m*/*z*): $[M+Na]^+$ calcd for $C_{14}H_{19}NONa$, 240.1359; found, 240.1361.

(*Z*)-1-Cyclohexyl-*N*-(1-naphthyl)methanimine Oxide (2e)

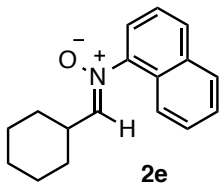

2e

White solid. **Mp** 142.2–143.3 °C. **^{1}H NMR** δ 1.24–1.58 (m, 5H), 1.70–1.85 (m, 3H), 2.08–2.17 (m, 2H), 3.39 (m, 1H), 6.93 (d, *J* = 7.5 Hz, 1H), 7.40–7.62 (m, 4H), 7.84–7.92 (m, 2H), 8.06 (d, *J* = 8.1 Hz, 1H). **^{13}C NMR** δ 25.19, 25.89, 28.92, 35.27, 120.23, 122.55, 124.78, 126.84, 126.93, 127.68, 127.94, 129.71, 134.07, 144.85, 148.21. **HRMS–ESI** (*m*/*z*): $[M+Na]^+$ calcd for $C_{17}H_{19}NONa$, 276.1359; found, 276.1359.

(*Z*)-1-((*N*-*tert*-Butoxycarbonyl)-4-piperidyl)-*N*-phenylmethanimine Oxide (2h)

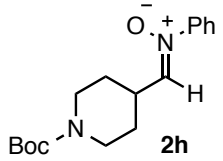

2h

White solid. **Mp** 98.8–99.2 °C. **^{1}H NMR** δ 1.39–1.53 (m, 2H), 1.49 (s, 9H), 1.97–2.07 (m, 2H), 2.85–3.01 (m, 2H), 3.34 (m, 1H), 3.98–4.25 (m, 2H), 7.07 (d, *J* = 7.2 Hz, 1H), 7.41–7.47 (m, 3H), 7.62–7.68 (m, 2H). **^{13}C NMR** δ 27.77, 28.42, 34.23, 43.25, 79.59, 121.61, 129.08, 130.05, 141.07, 147.59, 154.75. **HRMS–ESI** (*m*/*z*): $[M+Na]^+$ calcd for $C_{17}H_{24}N_2O_3Na$, 327.1679; found, 327.1680.

(*Z*)-1-(4-Trifluoromethylphenyl)-*N*-(4-carboethoxyphenyl)methanimine Oxide (2k)

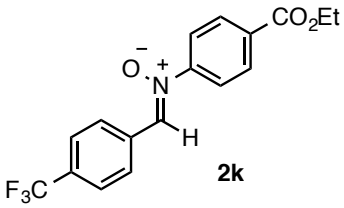

2k

White solid. **Mp** 167.9–168.2 ˚C. **^{1}H NMR** δ 1.43 (t, *J* = 7.2 Hz, 3H), 4.43 (q, *J* = 7.2 Hz, 2H), 7.74 (d, *J* = 8.1 Hz, 2 H), 7.83–7.91 (m, 2H), 8.06 (s, 1H), 8.15–8.22 (m, 2H), 8.52 (d, *J* = 8.4 Hz, 2H). **^{13}C NMR** δ 14.24, 61.56, 121.74, 123.63 (q, *J* = 270.9 Hz), 125.60 (d, *J* = 3.9 Hz), 129.09, 130.72, 132.18 (q, *J* = 32.4 Hz), 132.24, 133.34, 133.64, 151.62, 165.19. **HRMS–ESI** (*m/z*): $[M+H]^+$ calcd for $C_{17}H_{15}NO_3F_3$, 338.0999; found, 338.1003.

General procedures for the copper-catalyzed alkyne-nitrone coupling reaction between 1a and 2a (Table 1, entry 14).

A mixture of **L10** (12.1 mg, 0.02 mmol) and $Cu(OTf)_2$ (7.2 mg, 0.02 mmol) in toluene (1.0 mL) was stirred under N_2 at room temperature. After 5 min, Et_2NH (20.7 μL, 0.2 mmol) was added to the colorless solution. When the color of the resulting mixture turned yellow orange, nitrone **2a** (40.6 mg, 0.2 mmol) was added. Cooling to –40 ˚C immediately, alkyne **1a** (22.0 μL, 0.2 mmol) was added portionwise. After 24 h stirring at –40 ˚C, the reaction mixture was diluted with Et_2O. The mixture was filtered through a short plug of Celite with Et_2O as an eluent. After volatiles were removed under reduced pressure, flash column chromatography on silica gel (EtOAc/*n*-hexane = 1 to 10%) gave **3aa** (59.0 mg, 0.19 mmol) in 97% yield.

Characterization data

1,3-Diphenyl-4-pentyl-2-azetidinone (3aa)

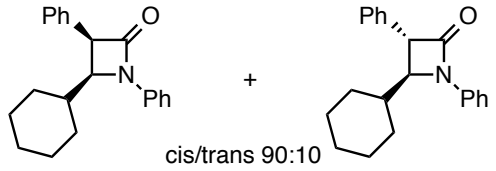

cis-(3*R*,4*S*)-**3aa** (92% ee) *trans*-(3*S*,4*S*)-**3aa** (51% ee)

3aa was reported in the literature.[7a] The cis and trans isomers were separated by silica-gel column chromatography. Absolute configurations of *cis*- and *trans*-**3aa** were determined by optical rotations {*cis*-**3aa**: $[\alpha]_D^{23}$ –43.4 (*c* 0.87, $CHCl_3$); *trans*-**3aa**: $[\alpha]_D^{23}$ +15.54 (*c* 0.59, $CHCl_3$)}.[7a] The ee values were determined by chiral HPLC analysis of **3aa** [CHIRALCEL® AD-H (4.6 mm × 250 mm), hexane/2-propanol 90:10, 0.5 mL/min, 40 ˚C, 250 nm UV detector, retention time = 17.2 min (cis-minor), 54.3 min (cis-major), 21.5 min (trans-major), and 27.2 min (trans-minor)].

1-Phenyl-3-butyl-4-cyclohexyl-2-azetidinone (3ba)

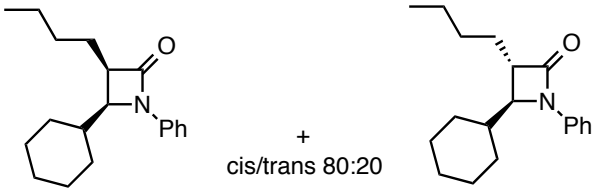

cis-(3*R*,4*S*)-**3ba** (98% ee) *trans*-(3*S*,4*S*)-**3ba** (97% ee)

Yellow oil. **^{1}H NMR** (for *cis*-**3ba**) δ 0.87–1.90 (m, 20H), 3.28 (m, 1H), 3.99 (dd, *J* = 5.6, 7.2 Hz, 1H), 7.08 (m, 1H), 7.28–7.42 (m, 4H). **^{13}C NMR** (for *cis*-**3ba**) δ 13.95, 22.86, 25.03, 26.10, 26.17, 30.54, 31.05, 31.31, 39.52, 51.86, 59.42, 118.69, 123.86, 128.74, 138.47, 169.65. **HRMS–ESI** (*m*/*z*): $[M+Na]^+$ calcd for $C_{19}H_{27}NONa$, 308.1985; found, 308.1987. $[\alpha]_D^{26}$ +108.2 (*c* 0.52, $CHCl_3$, cis/trans 80:20). The ee values were determined by chiral HPLC analysis of **3ba**. HPLC analysis [CHIRALCEL® OD-3 column (4.6 mm × 250 mm), hexane/2-propanol = 99:1, 0.5 mL/min, 40 ˚C, 250 nm UV detector, retention time = 16.8 min (cis-minor), 47.4 min (cis-major), 15.1 min (trans-minor), and 32.7 min (trans-major)].

1-(4-Methoxyphenyl)-3-phenyl-4-cyclohexyl-2-azetidinone (3ab)

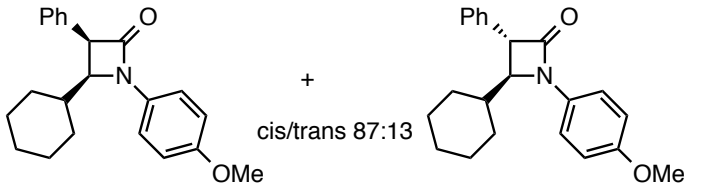

cis-(3*R*,4*S*)-**3ab** (80% ee) *trans*-(3*S*,4*S*)-**3ab** (37% ee)

3ab was reported in the literature.[7a] $[\alpha]_D^{24}$ –64.1 (*c* 0.71, $CHCl_3$, cis/trans 87:13). The ee values were determined by chiral HPLC analysis of **3ab**. HPLC analysis [CHIRALCEL® AD-3 column (4.6 mm × 250 mm), hexane/2-propanol = 90:10, 0.5 mL/min, 40 ˚C, 250 nm UV detector, retention time = 33.4 min (cis-minor), 57.4 min (cis-major), 38.0 min (trans-minor), and 53.6 min (trans-major)].

1-(4-Methoxyphenyl)-3-butyl-4-cyclohexyl-2-azetidinone (3bb)

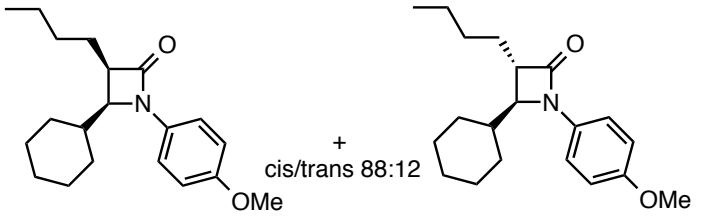

cis-(3*R*,4*S*)-**3bb** (>99% ee) *trans*-(3*S*,4*S*)-**3bb** (99% ee)

Pale yellow solid. **Mp** 83.2–84.3 ˚C. **^{1}H NMR** (for *cis*-**3bb**) δ 0.87–1.88 (m, 20H), 3.25 (dt, *J* = 5.4, 9.9 Hz, 1H), 3.79 (s, 3H), 3.93 (dd, *J* = 5.4, 7.5 Hz, 1H), 6.83–6.88 (m, 2H), 7.22–7.27 (m, 2H). **^{13}C NMR** (for *cis*-**3bb**) δ 13.94, 22.87, 25.08, 26.05, 26.11, 26.16, 30.54, 31.03, 31.25, 39.44, 51.76, 55.42, 59.70, 113.98, 120.38, 131.83, 156.12, 169.35. **HRMS–ESI** (*m/z*): $[M+Na]^+$ calcd for $C_{20}H_{29}NO_2Na$, 338.2091; found, 338.2095. $[\alpha]_D^{21}$ +100.9 (*c* 0.72, $CHCl_3$, cis/trans 88:12). The ee values were determined by chiral HPLC analysis of **3bb**. HPLC analysis [CHIRALCEL® OD-3 column (4.6 mm × 250 mm), hexane/2-propanol = 97:3, 0.5 mL/min, 40 ˚C, 250 nm UV detector, retention time = 17.8 min (cis-minor), 76.1 min (cis-major), 13.6 min (trans-minor), and 22.8 min (trans-major)].

1-(4-Fluorophenyl)-3-phenyl-4-cyclohexyl-2-azetidinone (3ac)

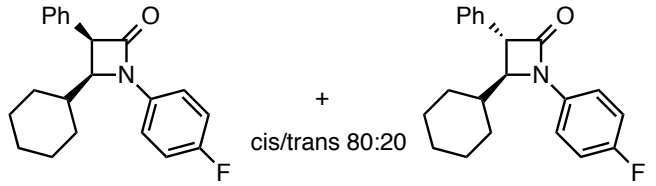

cis-(3*R*,4*S*)-**3ac** (90% ee) *trans*-(3*S*,4*S*)-**3ac** (54% ee)

White solid. **Mp** 126.6–128.1 ˚C. **^{1}H NMR** (for cis-**3ac**) δ 0.63–1.97 (m, 11H), 4.16 (dd, *J* = 6.0, 8.7 Hz, 1H), 4.68 (d, *J* = 6.0 Hz, 1H), 7.02–7.10 (m, 2H), 7.28–7.45 (m, 7H). **^{13}C NMR** (for cis-**3ac**) δ 25.35, 25.76, 25.86, 29.43, 31.03, 39.46, 57.66, 61.73, 115.58 (d, *J* = 22.8 Hz), 120.60 (d, *J* = 7.8 Hz), 127.78, 128.36, 129.92, 132.70, 134.39, 159.36 (d, *J* = 243.3 Hz), 167.20. **HRMS–ESI** (*m/z*): [M+Na]$^+$ calcd for $C_{21}H_{22}NOFNa$, 346.1578; found, 346.1581. **[α]$_D^{21}$** –40.4 (*c* 0.84, $CHCl_3$, cis/trans 80:20). The ee values were determined by chiral HPLC analysis of **3ac**. HPLC analysis [CHIRALCEL® AD-3 column (4.6 mm × 250 mm), hexane/2-propanol = 97:3, 0.5 mL/min, 40 ˚C, 250 nm UV detector, retention time = 32.7 min (cis-minor), 76.6 min (cis-major), 45.8 min (trans-major), and 57.3 min (trans-minor)].

1-(4-Fluorophenyl)-3-butyl-4-cyclohexyl-2-azetidinone (3bc)

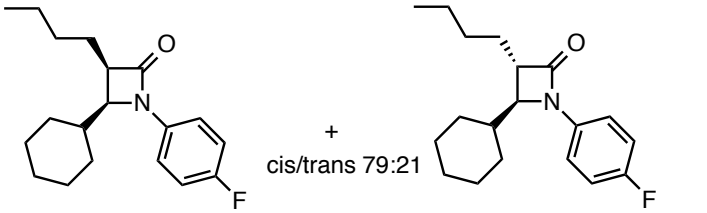

cis-(3*R*,4*S*)-**3bc** (98% ee) *trans*-(3*S*,4*S*)-**3bc** (97% ee)

White solid. **Mp** 56.3–58.2 ˚C. **^{1}H NMR** (for *cis*-**3bc**) δ 0.88–2.04 (m, 20H), 3.29 (m, 1H), 3.94 (dd, *J* = 6.0, 7.2 Hz, 1H), 6.97–7.06 (m, 2H), 7.23–7.33 (m, 2H). **^{13}C NMR** (for *cis*-**3bc**) δ 13.94, 22.85, 25.02, 26.03, 26.10, 26.14, 30.50, 31.12, 31.27, 39.49, 51.97, 59.81, 115.52 (d, *J* = 21.9 Hz), 120.29 (d, *J* = 7.5 Hz), 134.59, 159.14 (d, *J* = 241.2 Hz), 169.49. **HRMS–ESI** (*m/z*): [M+Na]$^+$ calcd for $C_{19}H_{26}NOFNa$, 326.1891; found, 326.1894. **[α]$_D^{22}$** +115.0 (*c* 0.62, $CHCl_3$, cis/trans 79:21). The ee values were determined by chiral HPLC analysis of **3bc**. HPLC analysis [CHIRALCEL® OD-3 column (4.6 mm × 250 mm), hexane/2-propanol = 99:1, 0.5 mL/min, 40 ˚C, 250 nm UV

detector, retention time = 15.9 min (cis-minor), 25.9 min (cis-major), 14.4 min (trans-minor), and 17.8 min (trans-major)].

1-(2-Methylphenyl)-3-phenyl-4-cyclohexyl-2-azetidinone (3ad)

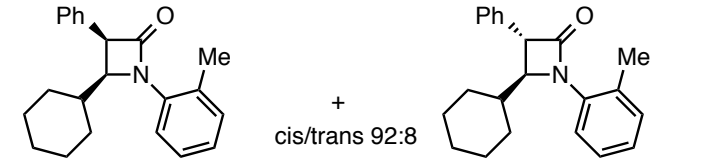

cis-(3*R*,4*S*)-**3ad** (92% ee) *trans*-(3*S*,4*S*)-**3ad** (80% ee)

White solid. **Mp** 114.0–115.3 °C. **^{1}H NMR** (for cis-**3ad**) δ 0.63–1.01 (m, 5H), 1.10–1.53 (m, 6H), 2.51 (s, 3H), 4.18 (dd, *J* = 5.7, 9.9 Hz, 1H), 4.63 (d, *J* = 5.7 Hz, 1H), 7.13–7.42 (m, 9H). **^{13}C NMR** (for cis-**3ad**) δ 19.31, 25.11, 25.56, 25.90, 29.02, 30.41, 39.17, 57.21, 63.49, 123.26, 126.23, 126.86, 127.67, 128.43, 129.84, 131.18, 133.16, 133.69, 136.79, 166.93. **HRMS–ESI** (*m*/*z*): $[M+Na]^+$ calcd for $C_{22}H_{25}NONa$, 342.1828; found, 342.1830. **$[\alpha]_D^{22}$** –33.4 (*c* 0.55, $CHCl_3$, cis/trans 92:8). The ee values were determined by chiral HPLC analysis of **3ad**. HPLC analysis [CHIRALCEL® AD-H column (4.6 mm × 250 mm), hexane/2-propanol = 95:5, 0.5 mL/min, 40 °C, 250 nm UV detector, retention time = 32.4 min (cis-minor), 170.8 min (cis-major), 38.1 min (trans-major), and 53.1 min (trans-minor)].

1-(2-Methylphenyl)-3-butyl-4-cyclohexyl-2-azetidinone (3bd)

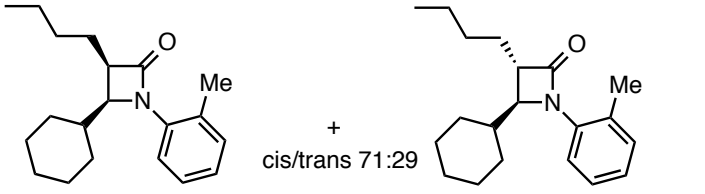

cis-(3*R*,4*S*)-**3bd** (99% ee) *trans*-(3*S*,4*S*)-**3bd** (98% ee)

Yellow oil. **^{1}H NMR** (for *cis*-**3bd**) δ 0.72–1.92 (m, 20H), 2.35 (s, 3H), 3.24 (m, 1H), 3.96 (dd, *J* = 5.7, 9.3 Hz, 1H), 7.05–7.24 (m, 4H). **^{13}C NMR** (for *cis*-**3bd**) δ 13.92, 18.89, 22.93, 25.46, 25.58, 25.84, 26.07, 30.38, 30.74, 39.49, 50.92, 61.25, 123.21, 126.02, 126.36, 131.04, 133.56, 136.76, 169.48. **HRMS–ESI** (*m*/*z*): $[M+Na]^+$ calcd for $C_{20}H_{29}NONa$, 322.2141; found, 322.2149. **$[\alpha]_D^{26}$** +96.6 (*c* 0.96, $CHCl_3$, cis/trans 71:29).

The ee values were determined by chiral HPLC analysis of **3bd**. HPLC analysis [CHIRALCEL® AD-3 column (4.6 mm × 250 mm), hexane/2-propanol = 97:3, 0.5 mL/min, 40 ˚C, 250 nm UV detector, retention time = 17.9 min (cis-minor), 45.3 min (cis-major), 23.7 min (trans-major), and 28.9 min (trans-minor)].

1-(1-Naphthyl)-3-phenyl-4-cyclohexyl-2-azetidinone (3ae)

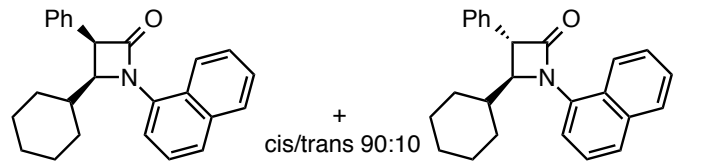

cis-(3*R*,4*S*)-**3ae** (99% ee) *trans*-(3*S*,4*S*)-**3ae** (90% ee)

Brown solid. **Mp** 213.3–213.9 ˚C. **^{1}H NMR** (for cis-**3ae**) δ 0.63–1.65 (m, 11H), 4.40 (dd, *J* = 6.0, 9.6 Hz, 1H), 4.76 (d, *J* = 6.0 Hz, 1H), 7.28–7.51 (m, 7H), 7.56 (ddd, *J* = 1.5, 6.9, 8.4 Hz, 1H), 7.65 (ddd, *J* = 1.5, 6.9, 8.4 Hz, 1H), 7.79 (d, *J* = 7.5 Hz, 1H), 7.88 (d, *J* = 8.4 Hz, 1H), 8.19 (d, *J* = 8.7 Hz, 1H). **^{13}C NMR** (for cis-**3ae**) δ 25.14, 25.49, 25.86, 29.10, 30.37, 39.17, 57.26, 64.06, 120.15, 124.15, 125.11, 126.55, 126.58, 127.26, 127.80, 128.20, 128.52, 128.55, 129.93, 133.11, 134.45, 134.74, 167.90. **HRMS–ESI** (*m/z*): $[M+H]^+$ calcd for $C_{25}H_{26}NO$, 356.2009; found, 356.2013. **$[\alpha]_D^{21}$** +31.1 (*c* 0.59, $CHCl_3$, cis/trans 90:10). The ee values were determined by chiral HPLC analysis of **3ae**. HPLC analysis [CHIRALCEL® OD-3 column (4.6 mm × 250 mm), hexane/2-propanol = 90:10, 0.5 mL/min, 40 ˚C, 250 nm UV detector, retention time = 21.2 min (cis-minor), 91.1 min (cis-major), 18.5 min (trans-minor), and 54.1 min (trans-isomer)].

1-(1-Naphthyl)-3-butyl-4-cyclohexyl-2-azetidinone (3be)

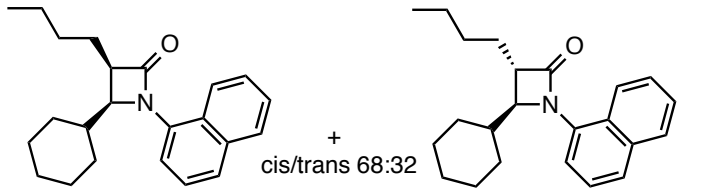

cis-(3*R*,4*S*)-**3be** (99% ee) *trans*-(3*S*,4*S*)-**3be** (98% ee)

Orange oil. **^{1}H NMR** (for *cis*-**3be**) δ 0.72–2.01 (m, 20H), 3.37 (m, 1H), 4.18 (dd, *J* = 5.4, 8.7 Hz, 1H), 7.26 (m, 1H), 7.39–7.59 (m, 3H), 7.74 (m, 1H), 7.85 (m, 1H), 8.04 (d,

J = 8.4 Hz, 1H) . **^{13}C NMR** (for *cis*-**3be**) δ 13.97, 22.98, 25.59, 25.76, 26.00, 30.42, 30.72, 30.82, 39.45, 50.99, 61.82, 119.87, 124.21, 125.05, 126.22, 126.35, 126.76, 127.99, 128.60, 134.33, 134.73, 170.36. **HRMS–ESI** (*m*/*z*): $[M+Na]^+$ calcd for $C_{23}H_{29}NONa$, 358.2141; found, 358.2145. **$[\alpha]_D^{26}$** +219.7 (*c* 1.02, $CHCl_3$, cis/trans 68:32). The ee values were determined by chiral HPLC analysis of **3be**. HPLC analysis [CHIRALCEL® OD-3 column (4.6 mm × 250 mm), hexane/2-propanol = 90:10, 0.5 mL/min, 40 ˚C, 250 nm UV detector, retention time = 12.4 min (cis-minor), 84.4 min (cis-major), 11.2 min (trans-minor), and 76.5 min (trans-major)].

1,3-Diphenyl-4-isopropyl-2-azetidinone (3af)

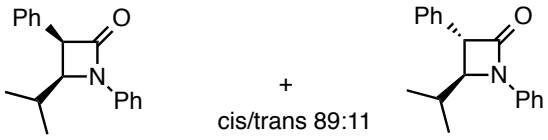

cis-(3*R*,4*S*)-**3af** (91% ee) *trans*-(3*S*,4*S*)-**3af** (54% ee)

3af were reported in the literature.[5] **$[\alpha]_D^{24}$** –98.2 (*c* 0.84, $CHCl_3$, cis/trans 89:11). The ee values were determined by chiral HPLC analysis of **3af**. HPLC analysis [CHIRALCEL® AD-3 column (4.6 mm × 250 mm), hexane/2-propanol = 97:3, 0.5 mL/min, 40 ˚C, 250 nm UV detector, retention time = 37.7 min (cis-minor), 144.7 min (cis-major), 48.5 min (trans-major), and 51.5 min (trans-minor)].

1-Phenyl-3-butyl-4-isopropyl-2-azetidinone (3bf)

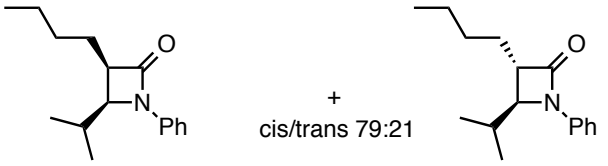

cis-(3*R*,4*S*)-**3bf** (99% ee) *trans*-(3*S*,4*S*)-**3bf** (98% ee)

Yellow oil. **^{1}H NMR** (for *cis*-**3bf**) δ 0.85–1.07 (m, 9H), 1.32–1.90 (m, 6H), 2.16 (m, 1H), 3.30 (m, 1H), 4.02 (dd, *J* = 6.0, 7.5 Hz, 1H), 7.08 (m, 1H), 7.28–7.42 (m, 4H). **^{13}C NMR** (for *cis*-**3bf**) δ 13.92, 20.37, 22.87, 25.11, 29.18, 30.65, 52.02, 60.44, 118.77, 123.94, 128.80, 138.18, 169.49. **HRMS–ESI** (*m*/*z*): $[M+Na]^+$ calcd for $C_{16}H_{23}NONa$, 268.1672; found, 268.1674. **$[\alpha]_D^{20}$** +106.1 (*c* 0.37, $CHCl_3$, cis/trans 72:28). The ee

values were determined by chiral HPLC analysis of **3bf**. HPLC analysis [CHIRALCEL® AD-3 column (4.6 mm × 250 mm), hexane/2-propanol = 99:1, 0.5 mL/min, 40 ˚C, 250 nm UV detector, retention time = 34.8 min (trans-minor), 40.4 min (trans-major), 37.8 min (cis-minor), and 76.9 min (cis-major)].

1,3-Diphenyl-4-pentyl-2-azetidinone (3ag)

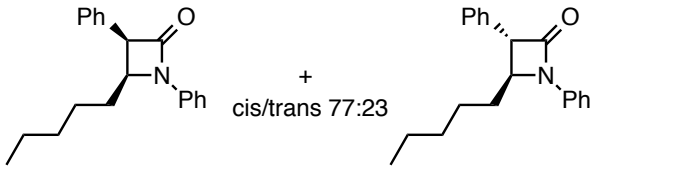

cis-(3*R*,4*S*)-**3ag** (82% ee) *trans*-(3*S*,4*S*)-**3ag** (7% ee)

Yellow oil. **^{1}H NMR** (for *cis*-**3ag**) δ 0.68 (t, *J* = 6.9 Hz, 3H), 0.81–1.14 (m, 5H), 1.23–1.53 (m, 2H), 1.87 (m, 1H), 4.31 (ddd, *J* = 3.3, 6.0, 9.9 Hz, 1H), 4.69 (d, *J* = 6.0 Hz, 1H), 7.12 (m, 1H), 7.22–7.51 (m, 9H). **^{13}C NMR** (for *cis*-**3ag**) δ 13.70, 21.97, 24.58, 27.73, 31.35, 56.62, 57.76, 117.37, 124.00, 127.77, 128.46, 129.15, 129.71, 132.45, 137.34, 165.91. **HRMS–ESI** (*m/z*): $[M+Na]^+$ calcd for $C_{20}H_{23}NONa$, 316.1672; found, 316.1676. **$[\alpha]_D^{26}$** –35.8 (*c* 0.61, $CHCl_3$, cis/trans 77:23). The ee values were determined by chiral HPLC analysis of **3ag**. HPLC analysis [CHIRALCEL® AD-3 column (4.6 mm × 250 mm), hexane/2-propanol = 99:1, 0.5 mL/min, 40 ˚C, 250 nm UV detector, retention time = 59.5 min (cis-minor), 124.8 min (cis-major), 80.4 min (trans-major), and 96.2 min (trans-minor)].

1-Phenyl-3-butyl-4-pentyl-2-azetidinone (3bg)

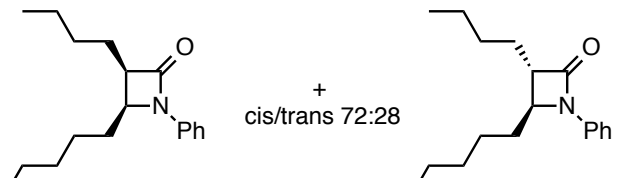

cis-(3*R*,4*S*)-**3bg** (98% ee) *trans*-(3*S*,4*S*)-**3bg** (96% ee)

Yellow oil. **^{1}H NMR** (for *cis* -**3bg**) δ 0.83–1.00 (m, 6H), 1.22–2.01 (m, 14H), 3.29 (m, 1H), 4.08 (m, 1H), 7.08 (m, 1H), 7.28–7.42 (m, 4H). **^{13}C NMR** (for *cis*-**3bg**) δ 13.93, 13.97, 22.48, 22.84, 24.50, 26.22, 27.92, 30.25, 31.90, 51.94, 54.86, 117.36,

123.59, 129.05, 137.52, 168.53. **HRMS–ESI** (*m/z*): $[M+Na]^+$ calcd for $C_{18}H_{27}NONa$, 296.1985; found, 296.1991. $[\alpha]_D^{20}$ +99.8 (*c* 0.47, $CHCl_3$, cis/trans 72:28). The ee values were determined by chiral HPLC analysis of **3bg**. HPLC analysis [CHIRALCEL® AD-3 column (4.6 mm × 250 mm), hexane/2-propanol = 99:1, 0.5 mL/min, 40 ˚C, 250 nm UV detector, retention time = 30.1 min (cis-minor), 51.7 min (cis-major), 32.7 min (trans-minor), and 35.7 min (trans-major)].

1,3-Diphenyl-4-(*N*-tert-butoxycarbonyl-4-piperidyl))-2-azetidinone (3ah)

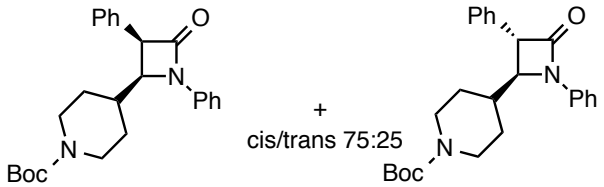

cis-(3*R*,4*S*)-**3ah** (92% ee) *trans*-(3*S*,4*S*)-**3ah** (46% ee)

White solid. **Mp** 71.1–72.3 ˚C. **^{1}H NMR** (for *cis*-**3ah**) δ 0.94–1.75 (m, 5H), 1.38 (m, 9H), 2.12 (m, 1H), 2.38 (m, 1H), 3.72–4.10 (m, 2H), 4.23 (dd, *J* = 6.0, 9.3 Hz, 1H), 4.72 (d, *J* = 6.0 Hz, 1H), 7.15 (m, 1H), 7.28–7.48 (m, 9H). **^{13}C NMR** (for *cis*-**3ah**) δ 28.35, 30.27, 38.42, 43.54, 57.62, 60.42, 79.39, 119.03, 124.71, 128.10, 128.60, 128.99, 129.94, 132.45, 137.91, 154.55, 166.96. **HRMS–ESI** (*m/z*): $[M+Na]^+$ calcd for $C_{25}H_{30}N_2O_3Na$, 429.2147; found, 429.2148. $[\alpha]_D^{26}$ –52.6 (*c* 0.87, $CHCl_3$, cis/trans 75:25). The ee values were determined by chiral HPLC analysis of **3ah**. HPLC analysis [CHIRALCEL® OD-3 column (4.6 mm × 250 mm), hexane/2-propanol = 90:10, 0.5 mL/min, 40 ˚C, 250 nm UV detector, retention time = 17.1 min (cis-minor), 33.1 min (cis-major), 23.0 min (trans-minor), and 27.5 min (trans-major)].

1-(4-Carboethoxyphenyl)-3-phenyl-4-(4-methoxyphenyl)-2-azetidinone (3aj)

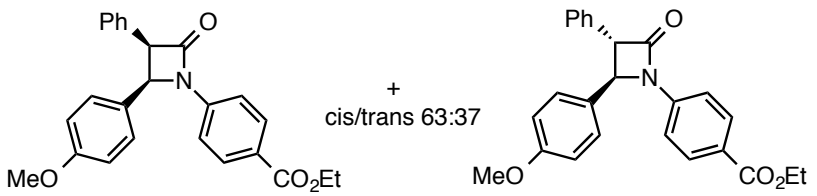

cis-(3*R*,4*S*)-**3aj** (60% ee) *trans*-(3*S*,4*S*)-**3aj** (59% ee)

Yellow oil. **^{1}H NMR** (for *cis*-**3aj**) δ 0.90 (t, *J* = 7.8 Hz, 3H), 3.78 (s, 3H), 4.20 (q, *J* =

9.6 Hz, 2H), 5.04 (d, *J* = 5.7 Hz, 1H), 5.45 (d, *J* = 5.7 Hz, 1H), 6.90–7.38 (m, 11H), 7.91 (d, *J* = 8.1 Hz, 2H). **^{13}C NMR** (for *cis*-**3aj**) δ 14.31, 30.06, 30.85, 35.80, 43.24, 53.49, 59.40, 63.12, 114.21, 123.26, 124.59, 125.71, 127.83, 128.10, 128.73, 130.42, 142.67, 143.70, 156.28, 163.08, 164.78. **HRMS–ESI** (*m*/*z*): $[M+Na]^+$ calcd for $C_{25}H_{23}NO_4Na$, 424.1519; found, 424.1526. **$[\alpha]_D^{26}$** –2.3 (*c* 0.50, $CHCl_3$). The ee value was determined by chiral HPLC analysis of **3aj**. HPLC analysis [CHIRALCEL® OD-3 column, 4.6 mm × 250 mm, Daicel Chemical Industries, hexane/2-propanol = 90:10, 0.5 mL/min, 40 ˚C, 250 nm UV detector, retention time = 27.7 min (cis-minor), 34.4 min (cis-major), 21.7 min (trans-minor), and 19.2 min (trans-major)].

1-(4-Carboethoxyphenyl)-3-phenyl-4-(4-trifluoromethylphenyl)-2-azetidinone (3ak)

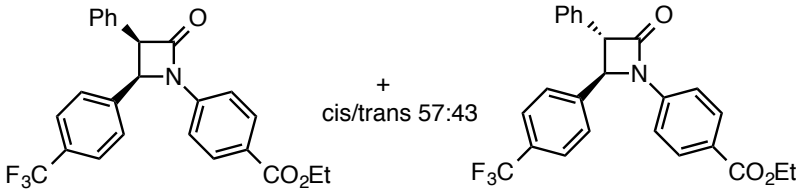

cis-(3*R*,4*S*)-**3ak** (73% ee) *trans*-(3*S*,4*S*)-**3ak** (67% ee)

Yellow oil. **^{1}H NMR** (for *cis*-**3ak**) δ1.37 (t, *J* = 6.9 Hz, 3H), 4.35 (q, *J* = 6.9 Hz, 2H), 5.12 (d, *J* = 6.0 Hz, 1H), 5.56 (d, *J* = 6.0 Hz, 1H), 6.94–7.23 (m, 7H), 7.38 (d, *J* = 8.7 Hz, 2H), 7.41 (d, *J* = 8.4 Hz, 2H), 8.00 (d, *J* = 8.7 Hz, 2H). **^{13}C NMR** (for *cis*-**3ak**) δ 14.31, 59.96, 60.77, 60.96, 116.61, 123.67 (q, *J* = 270.9 Hz), 125.34 (q, *J* = 3.9 Hz), 126.19, 127.42, 127.73, 128.42, 128.68, 130.29 (q, *J* = 32.4 Hz), 130.99, 131.05, 138.14, 140.79, 165.46, 165.86. **HRMS–ESI** (*m*/*z*): $[M+Na]^+$ calcd for $C_{25}H_{20}NO_3F_3Na$, 462.1288; found, 462.1295. **$[\alpha]_D^{26}$** –1.7 (*c* 0.66, $CHCl_3$). The ee value was determined by chiral HPLC analysis of **3ak**. HPLC analysis [CHIRALCEL® AD-3 column, 4.6 mm × 250 mm, Daicel Chemical Industries, hexane/2-propanol = 95:5, 0.5 mL/min, 40 ˚C, 250 nm UV detector, retention time = 40.8 min (cis-minor), 45.8 min (cis-major), 63.9 min (trans-minor), and 59.0 min (trans-major)].

1-Phenyl-3-(4-methoxyphenyl)-4-cyclohexyl-2-azetidinone (3ca)

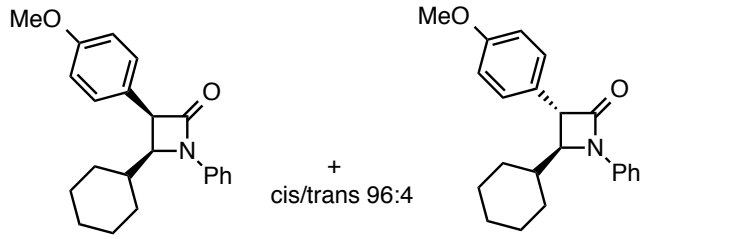

cis-(3*R*,4*S*)-**3ca** (92% ee) *trans*-(3*S*,4*S*)-**3ca** (36% ee)

White solid. **Mp** 97.2–98.0 ˚C. **^{1}H NMR** (for *cis*-**3ca**) δ 0.68–1.65 (m, 11H), 3.83 (s, 3H), 4.15 (dd, *J* = 6.0, 8.7 Hz, 1H), 4.62 (d, *J* = 6.0 Hz, 1H), 6.87–6.92 (m, 2H), 7.13 (m, 1H), 7.23–7.29 (m, 2H), 7.32–7.39 (m, 2H), 7.41–7.46 (m, 2H). **^{13}C NMR** (for *cis*-**3ca**) δ 25.49, 25.89, 25.95, 29.44, 31.11, 39.56, 55.21, 56.93, 61.49, 113.75, 118.92, 124.26, 124.88, 128.76, 131.08, 138.37, 159.02, 167.77. **HRMS–ESI** (*m*/*z*): $[M+Na]^+$ calcd for $C_{22}H_{25}NO_2Na$, 358.1778; found, 358.1777. **$[\alpha]_D^{26}$** –67.4 (*c* 0.94, $CHCl_3$, cis/trans 96:4). The ee values were determined by chiral HPLC analysis of **3ca**. HPLC analysis [CHIRALCEL® OD-3 column, 4.6 mm × 250 mm, Daicel Chemical Industries, hexane/2-propanol = 97:3, 0.5 mL/min, 40 ˚C, 250 nm UV detector, retention time = 41.8 min (cis-minor), 56.5 min (cis-major), 25.9 min (trans-minor), and 37.8 min (trans-major)].

1-Phenyl-3-(4-fluorophenyl)-4-cyclohexyl-2-azetidinone (3da)

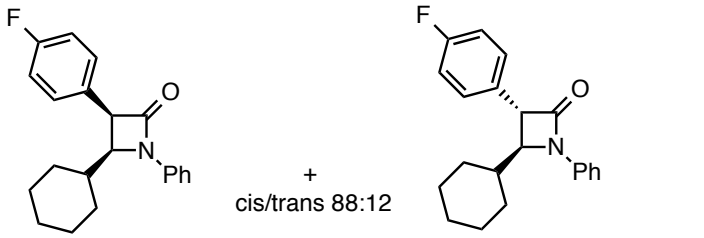

cis-(3*R*,4*S*)-**3da** (91% ee) *trans*-(3*S*,4*S*)-**3da** (44% ee)

White solid. **Mp** 151.9–152.5 ˚C. **^{1}H NMR** (for *cis*-**3da**) δ 0.67–1.65 (m, 11H), 4.19 (dd, *J* = 6.0, 8.4 Hz, 1H), 4.65 (d, *J* = 6.0 Hz, 1H), 6.99–7.18 (m, 3H), 7.23–7.48 (m, 6H). **^{13}C NMR** (for *cis*-**3da**) δ 25.49, 25.88, 25.92, 29.54, 31.03, 39.62, 56.79, 61.34, 115.41 (d, *J* = 22.2 Hz), 119.00, 124.50, 128.79 (d, *J* = 3.9 Hz), 128.86, 131.62 (d, *J* = 8.7 Hz), 138.21, 162.30 (d, *J* = 246.3 Hz), 167.11. **HRMS–ESI** (*m*/*z*): $[M+Na]^+$ calcd

for $C_{21}H_{22}NOFNa$, 346.1578; found, 346.1577. $[\alpha]_D^{22}$ –69.8 (*c* 0.44, $CHCl_3$, cis/trans 88:12). The ee values were determined by chiral HPLC analysis of **3da**. HPLC analysis [CHIRALCEL® OJ-3 column (4.6 mm × 250 mm), hexane/2-propanol = 97:3, 0.5 mL/min, 40 ˚C, 250 nm UV detector, retention time = 25.2 min (cis-minor), 31.0 min (cis-major), 17.4 min (trans-major), and 20.8 min (trans-minor)].

1-Phenyl-3-(4-bromophenyl)-4-cyclohexyl-2-azetidinone (3ea)

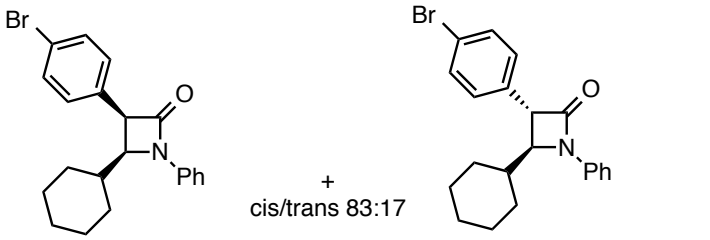

cis-(3*R*,4*S*)-**3ea** (92% ee) *trans*-(3*S*,4*S*)-**3ea** (41% ee)

White solid. **Mp** 179.4–179.8 ˚C. **^{1}H NMR** (for *cis*-**3ea**) δ 0.70–1.88 (m, 11H), 4.20 (d, *J* = 6.0, 8.4 Hz, 1H), 4.62 (d, *J* = 6.0Hz, 1H), 7.11–7.54 (m, 9H). **^{13}C NMR** (for *cis*-**3ea**) δ 25.48, 25.83, 25.89, 29.59, 30.99, 39.57, 56.90, 61.23, 119.01, 121.84, 124.56, 128.87, 131.58, 131.63, 132.03, 138.12, 166.69. **HRMS–ESI** (*m*/*z*): $[M+Na]^+$ calcd for $C_{21}H_{22}NONaBr$, 406.0777; found, 406.0783. $[\alpha]_D^{22}$ –39.9 (*c* 0.95, $CHCl_3$, cis/trans 83:17). The ee values were determined by chiral HPLC analysis of **3ea**. HPLC analysis [CHIRALCEL® AD-3 column, 4.6 mm × 250 mm, Daicel Chemical Industries, hexane/2-propanol = 90:10, 0.5 mL/min, 40 ˚C, 250 nm UV detector, retention time = 18.5 min (cis-minor), 83.8 min (cis-major), 28.5 min (trans-major), and 48.3 min (trans-minor)]. Absolute configuration of *cis*-**3ea** was determined by single crystal X-ray diffraction. Configurations of other β-lactams were assigned on the basis of stereochemistry of the reaction.

1-Phenyl-3-(4-carbomethoxyphenyl)-4-cyclohexyl-2-azetidinone (3fa)

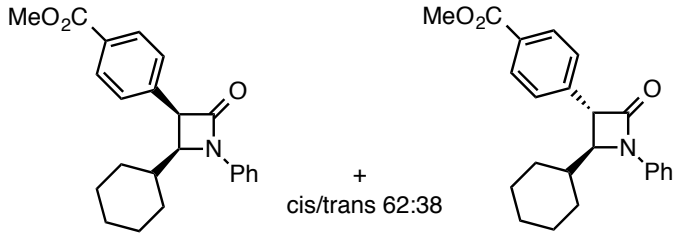

cis-(3*R*,4*S*)-**3fa** (83% ee) *trans*-(3*S*,4*S*)-**3fa** (78% ee)

White solid. **Mp** 136.0–138.2 °C. **^{1}H NMR** (for *cis*-**3fa**) δ 0.62–1.87 (m, 11H), 3.94 (s, 3H), 4.25 (dd, *J* = 6.0, 8.7 Hz, 1H), 4.72 (d, *J* = 6.0 Hz, 1H), 7.15 (m, 1H), 7.32–7.49 (m, 6H), 7.98–8.08 (m, 2H). **^{13}C NMR** (for *cis*-**3fa**) δ 25.46, 25.82, 25.86, 29.62, 30.94, 39.62, 52.20, 57.30, 61.35, 119.07, 124.63, 128.90, 129.53, 129.64, 130.06, 138.09, 138.32, 166.46, 166.81. **HRMS–ESI** (*m/z*): $[M+Na]^+$ calcd for $C_{23}H_{25}NO_3Na$, 386.1727; found, 386.1731. **$[\alpha]_D^{22}$** –45.4 (*c* 0.47, $CHCl_3$, cis/trans 62:38). The ee values were determined by chiral HPLC analysis of **3fa**. HPLC analysis [CHIRALCEL® AD-3 column (4.6 mm × 250 mm), hexane/2-propanol = 90:10, 0.5 mL/min, 40 °C, 250 nm UV detector, retention time = 25.0 min (cis-minor), 87.5 min (cis-major), 60.8 min (trans-major), and 108.3 min (trans-minor)].

1-Phenyl-3-(5-methyl-2-thienyl)-4-cyclohexyl-2-azetidinone (3ga)

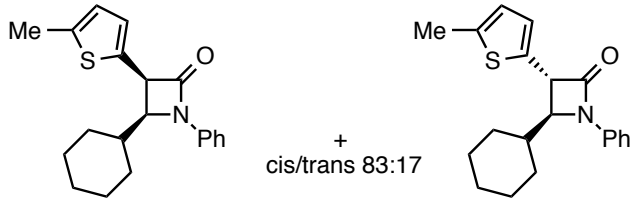

cis-(3*R*,4*S*)-**3ga** (99% ee) *trans*-(3*S*,4*S*)-**3ga** (98% ee)

Yellow oil. **^{1}H NMR** (for *cis*-**3ga**) δ 0.82–1.87 (m, 11H), 2.48 (d, *J* = 0.9 Hz, 3H), 4.15 (dd, *J* = 6.0, 8.7 Hz, 1H), 4.79 (d, *J* = 6.0 Hz, 1H), 6.67 (m, 1H), 6.89 (d, *J* = 3.6 Hz, 1H), 7.13 (m, 1H), 7.30–7.45 (m, 4H). **^{13}C NMR** (for *cis*-**3ga**) δ 15.37, 25.62, 25.92, 26.00, 30.01, 31.12, 39.95, 52.57, 61.71, 118.93, 124.39, 125.07, 128.46, 128.79, 131.64, 138.21, 140.27, 166.60. **HRMS–ESI** (*m/z*): $[M+Na]^+$ calcd for $C_{20}H_{23}NONaS$, 348.1393; found, 348.1393. **$[\alpha]_D^{26}$** –53.7 (*c* 0.68, $CHCl_3$, cis/trans 83:17). The ee values were determined by chiral HPLC analysis of **3ga**. HPLC analysis [CHIRALCEL® AD-3

column (4.6 mm × 250 mm), hexane/2-propanol = 97:3, 0.5 mL/min, 40 °C, 250 nm UV detector, retention time = 32.9 min (cis-minor), 99.7 min (cis-major), 51.3 min (trans-minor), and 54.4 min (trans-major)].

1-Phenyl-3-(1-cyclohexenyl)-4-cyclohexyl-2-azetidinone (3ha)

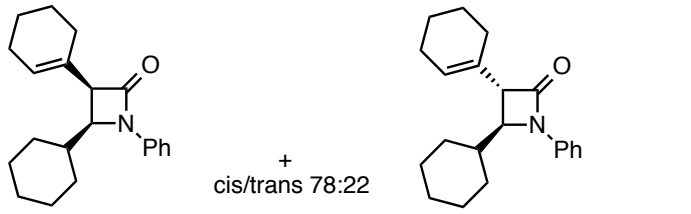

cis-(3*R*,4*S*)-**3ha** (98% ee) *trans*-(3*S*,4*S*)-**3ha** (73% ee)

White solid. **Mp** 99.3–100.9 °C. **^{1}H NMR** (for *cis*-**3ha**) δ 0.97–1.34 (m, 5H), 1.53–1.81 (m, 9H), 1.98–2.23 (m, 4H), 3.89 (d, *J* = 6.0 Hz, 1H), 4.04 (dd, *J* = 6.0, 8.4 Hz, 1H), 5.85 (m, 1H), 7.09 (m, 1H), 7.28–7.39 (m, 4 H). **^{13}C NMR** (for *cis*-**3ha**) δ 21.96, 22.78, 25.38, 26.08, 26.13, 26.19, 29.75, 30.75, 31.25, 39.89, 58.81, 61.13, 118.83, 124.09, 128.74, 129.37, 129.68, 138.43, 167.82. **HRMS–ESI** (*m*/*z*): $[M+Na]^+$ calcd for $C_{21}H_{27}NONa$, 332.1985; found, 332.1988. **$[\alpha]_D^{22}$** –17.5 (*c* 0.90, $CHCl_3$, cis/trans 78:22). The ee values were determined by chiral HPLC analysis of **3ha**. HPLC analysis [CHIRALCEL® AD-3 column (4.6 mm × 250 mm), hexane/2-propanol = 99:1, 0.5 mL/min, 40 °C, 250 nm UV detector, retention time = 48.8 min (cis-minor), 175.9 min (cis-major), 61.8 min (trans-major), and 68.6 min (trans-minor)].

1-Phenyl-3-isobutyl-4-cyclohexyl-2-azetidinone (3ia)

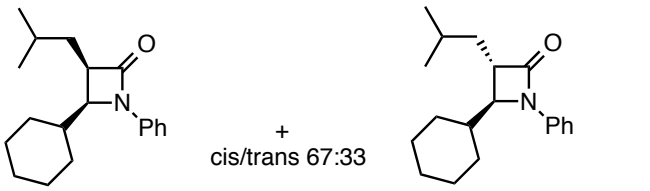

cis-(3*R*,4*S*)-**3ia** (99% ee) *trans*-(3*S*,4*S*)-**3ia** (98% ee)

White solid. **Mp** 63.3–63.8 °C. **^{1}H NMR** (for *cis*-**3ia**) δ 0.97 (d, *J* = 6.6 Hz, 3H), 1.00 (d, *J* = 6.6 Hz, 3H), 1.02–1.33 (m, 5H), 1.43 (m, 1H), 1.57–1.85 (m, 7H), 1.98 (m, 1H), 3.39 (td, *J* = 5.7, 11.1 Hz, 1H), 3.99 (m 1H), 7.07 (m, 1H), 7.26–7.40 (m, 4H). **^{13}C**

NMR (for *cis*-**3ia**) δ 22.02, 23.46, 26.17, 26.75, 30.89, 31.44, 33.91, 39.48, 49.91, 59.42, 118.67, 123.85, 128.74, 138.51, 169.62. **HRMS–ESI** (*m/z*): $[M+Na]^+$ calcd for $C_{19}H_{27}NONa$, 308.1985; found, 308.1988. $[\alpha]_D^{26}$ +75.8 (*c* 0.50, $CHCl_3$, cis/trans 67:33). The ee values were determined by chiral HPLC analysis of **3ia**. HPLC analysis [CHIRALCEL® OD-3 column (4.6 mm × 250 mm), hexane/2-propanol = 99:1, 0.5 mL/min, 40 ˚C, 250 nm UV detector, retention time = 16.6 min (cis-minor), 40.8 min (cis-major), 13.4 min (trans-minor), and 25.0 min (trans-major)].

1-Phenyl-3,4-dicyclohexyl-2-azetidinone (3ja)

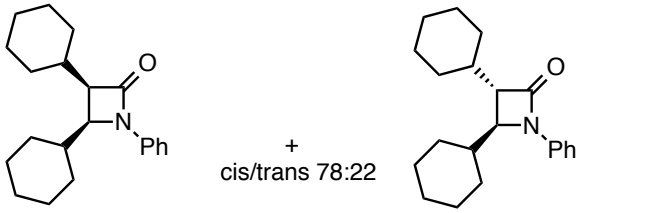

cis-(3*R*,4*S*)-**3ja** (97% ee) *trans*-(3*S*,4*S*)-**3ja** (92% ee)

White solid. **Mp** 169.5–169.9 ˚C. **^{1}H NMR** (for *cis*-**3ja**) δ 0.95–1.40 (m, 11H), 1.60–1.85 (m, 10H), 2.24 (m, 1H), 3.10 (dd, *J* = 6.0, 8.4 Hz, 1H), 4.04 (dd, *J* = 4.5, 6.0 Hz, 1H), 7.07 (m, 1H), 7.27–7.42 (m, 4H). **^{13}C NMR** (for *cis*-**3ja**) δ 25.95, 26.04, 26.15, 26.17, 26.23, 26.72, 30.20, 31.03, 33.30, 33.83, 34.89, 38.86, 57.60, 59.42, 118.57, 123.79, 128.79, 138.59, 168.32. **HRMS–ESI** (*m/z*): $[M+Na]^+$ calcd for $C_{21}H_{29}NONa$, 334.2141; found, 334.2140. $[\alpha]_D^{26}$ +33.3 (*c* 0.81, $CHCl_3$, cis/trans 78:22). The ee values were determined by chiral HPLC analysis of **3ja**. HPLC analysis [CHIRALCEL® OD-3 column (4.6 mm × 250 mm), hexane/2-propanol = 99.5:0.5, 0.5 mL/min, 40 ˚C, 250 nm UV detector, retention time = 30.2 min (cis-minor), 104.6 min (cis-major), 19.6 min (trans-minor), and 36.5 min (trans-major)].

1-Phenyl-3-(3-phenylpropyl)-4-cyclohexyl-2-azetidinone (3ka)

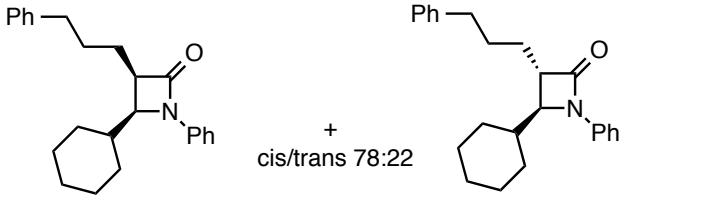

cis-(3*R*,4*S*)-**3ka** (97% ee) *trans*-(3*S*,4*S*)-**3ka** (91% ee)

Yellow oil. **^{1}H NMR** (for *cis*-**3ka**) δ 0.93–1.35 (m, 5H), 1.53–2.15 (m, 10H), 2.61–2.79 (m, 2H), 3.30 (td, *J* = 5.7, 9.9 Hz, 1H), 3.98 (dd, *J* = 5.7, 7.5 Hz, 1H), 7.08 (m, 1H), 7.15–7.40 (m, 9H). **^{13}C NMR** (for *cis*-**3ka**) δ 24.81, 26.06, 26.09, 26.11, 26.14, 30.06, 30.99, 31.31, 35.91, 39.50, 51.69, 59.42, 118.68, 123.93, 125.79, 128.32, 128.46, 128.76, 138.43, 141.94, 169.35. **HRMS–ESI** (*m*/*z*): $[M+Na]^+$ calcd for $C_{24}H_{29}NONa$, 370.2141; found, 370.2141. **$[\alpha]_D^{26}$** +83.6 (*c* 0.98, $CHCl_3$, cis/trans 78:22). The ee values were determined by chiral HPLC analysis of **3ka**. HPLC analysis [CHIRALCEL® OD-3 column (4.6 mm × 250 mm), hexane/2-propanol = 95:5, 0.5 mL/min, 40 °C, 250 nm UV detector, retention time = 16.8 min (cis-minor), 32.3 min (cis-major isomer), 18.9 min (trans-minor), and 22.8 min (trans-major)].

1-Phenyl-3-(4-chlorobutyl)-4-cyclohexyl-2-azetidinone (3la)

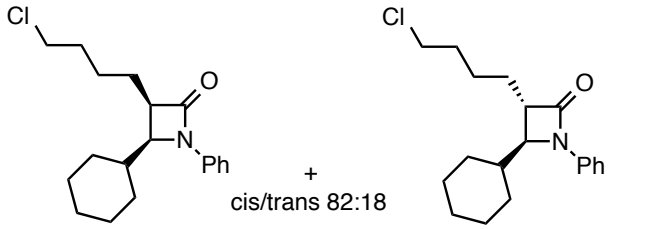

cis-(3*R*,4*S*)-**3la** (98% ee) *trans*-(3*S*,4*S*)-**3la** (95% ee)

Pale yellow solid. **Mp** 65.6–70.7 °C. **^{1}H NMR** (for *cis*-**3la**) δ 0.97–1.95 (m, 17H), 3.29 (m, 1H), 3.52–3.65 (m, 2H), 4.01 (dd, *J* = 5.7, 7.2 Hz, 1H), 7.09 (m, 1H), 7.28–7.44 (m, 1H). **^{13}C NMR** (for *cis*-**3la**) δ 24.67, 25.66, 26.07, 26.12, 31.04, 31.26, 32.65, 39.54, 44.68, 51.56, 59.36, 118.71, 124.02, 128.76, 138.32, 169.20. **HRMS–ESI** (*m*/*z*): $[M+Na]^+$ calcd for $C_{19}H_{26}NONaCl$, 342.1595; found, 342.1598. **$[\alpha]_D^{26}$** +93.7 (*c* 1.08, $CHCl_3$, cis/trans 82:18). The ee values were determined by chiral HPLC analysis of **3la**. HPLC analysis [CHIRALCEL® OD-3 column (4.6 mm × 250 mm), hexane/2-propanol

= 97:3, 0.5 mL/min, 40 ˚C, 250 nm UV detector, retention time = 18.8 min (cis-minor), 45.0 min (cis-major), 20.5 min for (trans-minor), and 35.8 min (trans-major)].

1-Phenyl-3-(3-(*tert*-butylcarbonyloxy)propyl)-4-cyclohexyl-2-azetidinone (3ma)

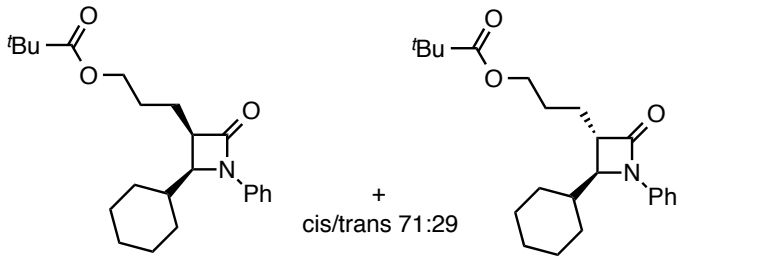

cis-(3*R*,4*S*)-**3ma** (99% ee) *trans*-(3*S*,4*S*)-**3ma** (99% ee)

Yellow oil. **^{1}H NMR** (for *cis*-**3ma**) δ 0.92–1.96 (m, 15H), 1.21 (s, 9H), 3.32 (m, 1H), 4.01 (dd, *J* = 6.0, 7.5 Hz, 1H), 4.02–4.22 (m, 2H), 7.09 (m, 1H), 7.27–7.42 (m, 4H). **^{13}C NMR** (for *cis*-**3ma**) δ 21.91, 26.02, 26.11, 27.19, 27.32, 31.08, 31.20, 38.78, 39.62, 51.13, 59.30, 63.94, 118.74, 124.05, 128.78, 138.29, 169.07, 178.56. **HRMS–ESI** (*m/z*): $[M+Na]^+$ calcd for $C_{23}H_{33}NO_3Na$, 394.2353; found, 394.2354. **$[\alpha]_D^{26}$** +74.8 (*c* 0.69, $CHCl_3$, cis/trans 71:29). The ee values were determined by chiral HPLC analysis of **3ma**. HPLC analysis [CHIRALCEL® OD-3 column (4.6 mm × 250 mm)/OJ-3 column (4.6 mm × 250 mm), hexane/2-propanol = 97:3, 0.5 mL/min, 40 ˚C, 250 nm UV detector, retention time = 34.6 min (cis-minor), 44.9 min (cis-major), 31.2 min (trans-minor), and 38.2 min (trans-major)].

1-Phenyl-3-(3-phthalimidepropyl)-4-cyclohexyl-2-azetidinone (3na)

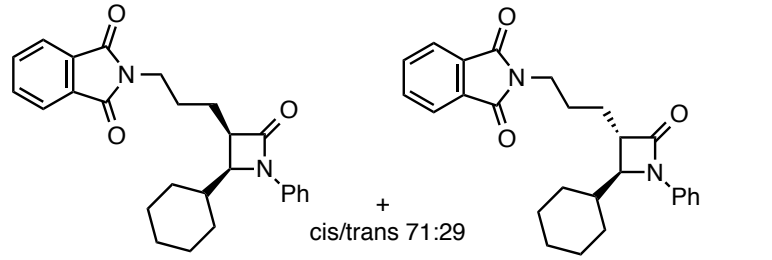

cis-(3*R*,4*S*)-**3na** (96% ee) *trans*-(3*S*,4*S*)-**3na** (94% ee)

Yellow solid. **Mp** 65.6–70.7 ˚C. **^{1}H NMR** (for *cis*-**3na**) δ 0.97–2.18 (m, 15H), 3.36 (m, 1H), 3.68–3.87 (m, 2H), 4.01 (dd, *J* = 6.0, 7.5 Hz, 1H), 7.08 (m, 1H), 7.22–7.38 (m, 4H), 7.72 (dd, *J* = 3.3, 5.4 Hz, 2H), 7.86 (dd, *J* = 3.3, 5.4 Hz, 2H). **^{13}C NMR** (for

cis-**3na**) δ 22.57, 26.00, 26.07, 26.10, 27.28, 31.02, 31.22, 37.65, 39.55, 51.05, 59.29, 118.71, 123.21, 124.00, 128.75, 132.08, 133.91, 138.32, 168.35, 168.85. **HRMS–ESI** (*m*/*z*): $[M+Na]^+$ calcd for $C_{26}H_{28}N_2O_3Na$, 439.1992; found, 439.1994. $[\alpha]_D^{21}$ +71.7 (*c* 0.50, $CHCl_3$). The ee value was determined by chiral HPLC analysis of **3na**. HPLC analysis [CHIRALCEL® OD-3 column, 4.6 mm × 250 mm, Daicel Chemical Industries, hexane/2-propanol = 90:10, 0.5 mL/min, 40 ˚C, 250 nm UV detector, retention time = 26.2 min (cis-minor), 41.0 min (cis-major), 22.7 min (trans-minor), and 31.6 min (trans-major)].

1-Phenyl-3-(3-(*tert*-butyldimethylsilyloxy)propyl)-4-cyclohexyl-2-azetidinone (3oa)

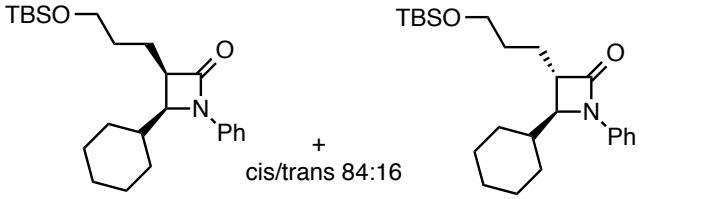

cis-(3*R*,4*S*)-**3oa** (98% ee) *trans*-(3*S*,4*S*)-**3oa** (97% ee)

Yellow oil. **^{1}H NMR** (for *cis*-**3oa**) δ 0.068 (s, 3H), 0.071 (s, 3H), 0.91 (s, 9H), 1.00–1.33 (m, 5H), 1.61–2.08 (m, 10H), 3.31 (dt, *J* = 6.0, 9.6 Hz, 1H), 3.60–3.78 (m, 2H), 4.00 (dd, *J* = 6.0, 7.5 Hz, 1H), 7.08 (m, 1H), 7.28–7.42 (m, 4H). **^{13}C NMR** (for *cis*-**3oa**) δ –5.30, –5.26, 18.34, 21.86, 25.94, 26.08, 26.17, 31.09, 31.24, 39.58, 51.51, 59.41, 62.73, 118.71, 123.92, 128.75, 138.44, 169.53. **HRMS–ESI** (*m*/*z*): $[M+Na]^+$ calcd for $C_{24}H_{39}NO_2NaSi$, 424.2642; found, 424.2644. $[\alpha]_D^{26}$ +73.2 (*c* 0.98, $CHCl_3$, cis/trans 84:16). The ee values were determined by chiral HPLC analysis of **3oa**. HPLC analysis [CHIRALCEL® OD-3 column (4.6 mm × 250 mm)/ OD-H column (4.6 mm × 250 mm), hexane/2-propanol = 99:1, 0.5 mL/min, 40 ˚C, 250 nm UV detector, retention time = 38.5 min (cis-minor), 61.2 min (cis-major), 35.6 min (trans-minor), and 46.6 min (trans-major)].

1-Phenyl-3-(2-(1,3-dioxan-2-yl)ethyl)-4-cyclohexyl-2-azetidinone (3pa)

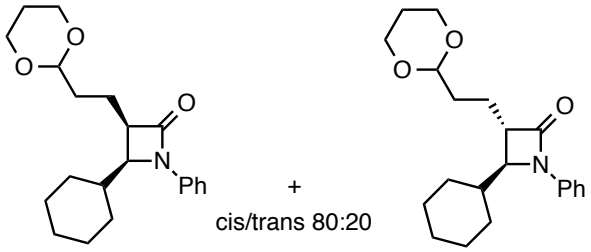

cis-(3*R*,4*S*)-**3pa** (97% ee) *trans*-(3*S*,4*S*)-**3pa** (94% ee)

White solid. **Mp** 113.3–115.4 °C. **^{1}H NMR** (for *cis*-**3pa**) δ 0.79–2.17 (m, 17H), 3.31 (dt, *J* = 6.0, 9.9 Hz, 1H), 3.74–3.85 (m, 2H), 3.99 (dd, *J* = 6.0, 7.2 Hz, 1H), 4.04–4.18 (m, 2H), 4.65 (t, *J* = 5.1 Hz, 1H), 7.09 (m, 1H), 7.21–7.42 (m, 4H). **^{13}C NMR** (for *cis*-**3pa**) δ 19.50, 25.78, 26.07, 26.11, 26.13, 31.02, 31.33, 33.49, 39.33, 51.49, 59.45, 66.86, 101.60, 118.69, 123.88, 128.72, 138.41, 169.20. **HRMS–ESI** (*m*/*z*): $[M+Na]^+$ calcd for $C_{21}H_{29}NO_3Na$, 366.2040; found, 366.2041. **$[\alpha]_D^{26}$** +68.9 (*c* 0.90, $CHCl_3$, cis/trans 80:20). The ee values were determined by chiral HPLC analysis of **3pa**. HPLC analysis [CHIRALCEL® OD-3 column, 4.6 mm × 250 mm, Daicel Chemical Industries, hexane/2-propanol = 97:3, 0.5 mL/min, 40 °C, 250 nm UV detector, retention time = 35.1 min (cis-minor), 46.9 min (cis-major), 23.4 min (trans-minor), and 38.1 min (trans-major)].

1-Phenyl-3-((dibenzylamino)methyl)-4-cyclohexyl-2-azetidinone (3qa)

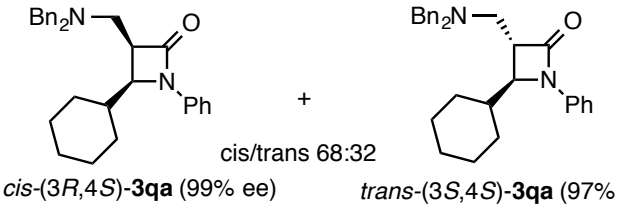

cis-(3*R*,4*S*)-**3qa** (99% ee) *trans*-(3*S*,4*S*)-**3qa** (97% ee)

White solid. **Mp** 93.9–96.9 °C. **^{1}H NMR** (for *cis*-**3qa**) (400 MHz, $CDCl_3$) δ 0.82–1.77 (m, 11H), 2.83 (m, 1H), 3.00 (dd, *J* = 6.3, 13.2 Hz, 1H), 3.49 (d, *J* = 13.5 Hz, 2H), 3.58 (m, 1H), 3.85 (d, *J* = 13.5 Hz, 2H), 3.93 (t, *J* = 6.3 Hz, 1H), 7.07 (m, 1H), 7.18–7.45 (m, 14H). **^{13}C NMR** (for *cis*-**3qa**) (100 MHz, $CDCl_3$) δ 25.85, 26.04, 26.11, 30.29, 31.45, 38.85, 48.92, 50.61, 58.70, 59.59, 118.47, 123.94, 126.99, 128.27, 128.77, 128.97, 138.34, 139.23, 168.28. **HRMS–ESI** (*m*/*z*): $[M+H]^+$ calcd for $C_{30}H_{35}N_2O$, 439.2744; found, 439.2745. **$[\alpha]_D^{26}$** +31.5 (*c* 0.92, $CHCl_3$, cis/trans 68:32). The ee values

were determined by chiral HPLC analysis of **3qa**. HPLC analysis [CHIRALCEL® OD-3 column (4.6 mm × 250 mm), hexane/2-propanol = 97:3, 0.5 mL/min, 40 ˚C, 250 nm UV detector, retention time = 21.9 min (cis-minor), 40.2 min (cis-major), 13.8 min (trans-minor), and 17.5 min (trans-major)].

1-Phenyl -3-(methoxymethoxymethyl)-4-cyclohexyl-2-azetidinone (3ra)

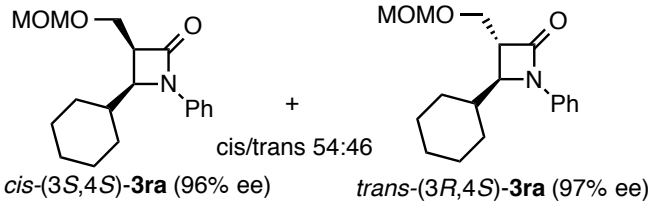

cis-(3*S*,4*S*)-**3ra** (96% ee) *trans*-(3*R*,4*S*)-**3ra** (97% ee)

Yellow oil. **^{1}H NMR** (for *cis*-**3ra**) δ 0.98–1.36 (m, 6H), 1.59–2.13 (m, 5H), 3.42 (s, 3H), 3.66 (m, 1H), 3.89 (dd, *J* = 5.4, 9.9 Hz, 1H), 4.02 (dd, *J* = 2.7, 5.4 Hz, 1H), 4.09 (dd, *J* = 5.4, 8.1 Hz, 1H), 4.69 (d, *J* = 3.9 Hz, 2H), 7.10 (m, 1H), 7.29–7.44 (m, 4H). **^{13}C NMR** (for *cis*-**3ra**) δ 25.67, 25.99, 26.10, 26.27, 30.67, 39.47, 52.58, 55.60, 59.78, 62.55, 96.78, 118.91, 124.25, 128.77, 138.17, 166.56. **HRMS–ESI** (*m*/*z*): $[M+Na]^+$ calcd for $C_{18}H_{25}NO_3Na$, 326.1727; found, 326.1728. **$[\alpha]_D^{26}$** +72.6 (*c* 0.71, $CHCl_3$, cis/trans 54:46). The ee values were determined by chiral HPLC analysis of **3ra**. HPLC analysis [CHIRALCEL® OD-3 column (4.6 mm × 250 mm), hexane/2-propanol = 98:2, 0.5 mL/min, 40 ˚C, 250 nm UV detector, retention time = 21.8 min (cis-minor), 35.4 min (cis-major), 18.7 min (trans-minor), and 25.5 min (trans-major)].

1-Phenyl-3-hydroxymethyl-4-cyclohexyl-2-azetidinone (3sa)

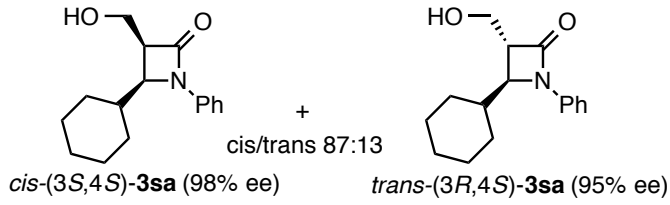

cis-(3*S*,4*S*)-**3sa** (98% ee) *trans*-(3*R*,4*S*)-**3sa** (95% ee)

White solid. **Mp** 90.4–93.4 ˚C. **^{1}H NMR** (for *cis*-**3sa**) δ 0.98–1.35 (m, 5H), 1.58–1.84 (m, 5H), 1.92 (m, 1H), 2.22 (m, 1H), 3.57 (q, *J* = 6.0 Hz, 1H), 3.99–4.17 (m, 2H), 4.09 (dd, *J* = 6.0, 8.1 Hz, 1H), 7.10 (m, 1H), 7.28–7.41 (m, 4H). **^{13}C NMR** (for *cis*-**3sa**)

δ 25.89, 26.03, 26.10, 30.59, 31.43, 39.51, 54.08, 58.05, 59.90, 118.99, 124.40, 128.80, 138.00, 167.72. **HRMS–ESI** (*m/z*): $[M+Na]^+$ calcd for $C_{16}H_{21}NO_2Na$, 282.1465; found, 282.1466. $\mathbf{[\alpha]_D^{21}}$ +108.4 (*c* 0.80, $CHCl_3$, cis/trans 87:13). The ee values were determined by chiral HPLC analysis of **3sa**. HPLC analysis [CHIRALCEL® OD-3 column, 4.6 mm × 250 mm, Daicel Chemical Industries, hexane/2-propanol = 98:2, 0.5 mL/min, 40 ˚C, 250 nm UV detector, retention time = 53.2 min (cis-minor), 86.9 min (cis-major), 55.8 min (trans-minor), and 70.0 min (trans-major)].

1-(1-Naphthyl)-3-(4-chlorobutyl)-4-cyclohexyl-2-azetidinone (3le)

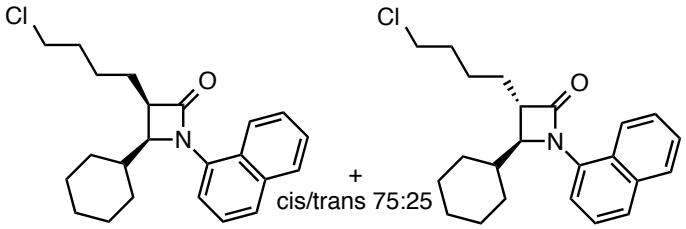

cis-(3*R*,4*S*)-**3le** (99% ee) *trans*-(3*S*,4*S*)-**3le** (98% ee)

Orange oil. **^{1}H NMR** (for *cis*-**3le**) δ 0.72–2.05 (m, 17H), 3.39 (q, *J* = 5.1 Hz, 1H), 3.55–3.68 (m, 2H), 4.20 (dd, *J* = 5.1, 8.4 Hz, 1H), 7.26 (m, 1H), 7.40–7.59 (m, 3H), 7.74 (m, 1H), 7.85 (m, 1H), 8.02 (d, *J* = 8.7 Hz, 1H). **^{13}C NMR** (for *cis*-**3le**) δ 25.22, 25.59, 25.73, 25.96, 30.69, 30.81, 32.78, 39.48, 44.71, 50.71, 61.78, 119.93, 124.09, 125.05, 126.28, 126.40, 126.89, 128.04, 128.56, 134.33, 134.57, 169.93. **HRMS–ESI** (*m/z*): $[M+Na]^+$ calcd for $C_{23}H_{28}NONaCl$, 392.1752; found, 392.1760. $\mathbf{[\alpha]_D^{26}}$ +174.2 (*c* 1.11, $CHCl_3$, cis/trans 75:25). The ee values were determined by chiral HPLC analysis of **3le**. HPLC analysis [CHIRALCEL® AD-3 column (4.6 mm × 250 mm), hexane/2-propanol = 90:10, 0.5 mL/min, 40 ˚C, 250 nm UV detector, retention time = 19.1 min (cis-minor), 77.2 min (cis-major), 28.2 min (trans-minor), and 34.8 min (trans-major)].

1-(4-Carboethoxyphenyl)-3-(4-chlorobutyl)-4-phenyl-2-azetidinone (3li)

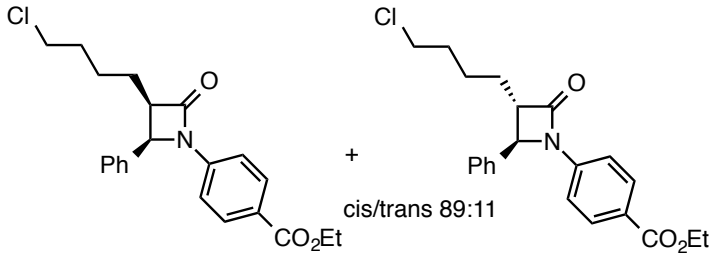

cis-(3*R*,4*R*)-**3li** (94% ee) *trans*-(3*S*,4*R*)-**3li** (78% ee)

White solid. **Mp** 77.3–78.9 °C. **^{1}H NMR** (for *cis*-**3li**) δ 1.12–1.73 (m, 6H), 1.35 (t, *J* = 6.9 Hz, 3H), 3.29–3.42 (m, 2H), 3.61 (m, 1H), 4.33 (q, *J* = 6.9 Hz, 2H), 5.25 (d, *J* = 6.0 Hz, 1H), 7.20–7.42 (m, 7H), 7.91–7.97 (m, 2H). **^{13}C NMR** (for *cis*-**3li**) δ 14.31, 24.51, 24.65, 32.20, 44.44, 54.71, 58.43, 60.84, 116.61, 125.55, 127.02, 128.58, 128.85, 130.81, 134.14, 141.03, 166.01, 168.01. **HRMS–ESI** (*m/z*): $[M+Na]^+$ calcd for $C_{22}H_{24}NO_3NaCl$, 408.1337; found, 408.1338. **$[\alpha]_D^{22}$** +56.3 (*c* 0.93, $CHCl_3$, cis/trans 89:11). The ee values were determined by chiral HPLC analysis of **3li**. HPLC analysis [CHIRALCEL® AD-3 column (4.6 mm × 250 mm), hexane/2-propanol = 95:5, 0.5 mL/min, 40 °C, 250 nm UV detector, retention time = 50.1 min (cis-major), 77.6 min (cis-minor), 47.1 min (trans-major), and 100.1 min (trans-minor)].

1-(4-Carboethoxyphenyl)-3-(3-phenylpropyl)-4-(4-methoxyphenyl)-2-azetidinone (3kj)

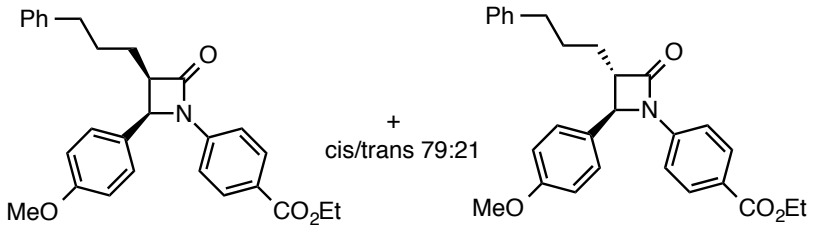

cis-(3*R*,4*S*)-**3kj** (87% ee) *trans*-(3*S*,4*S*)-**3kj** (84% ee)

Oil. **^{1}H NMR** (for *cis*-**3kj**) δ 0.94–1.38 (m, 7H), 2.71 (m, 2H), 3.31 (m, 1H), 3.80 (s, 3H), 4.23 (q, *J* = 9.3 Hz, 2H), 5.16 (d, *J* = 6.0 Hz, 1H), 6.86 (d, *J* = 8.1 Hz, 2H), 6.98 (d, *J* = 8.1 Hz, 2H), 7.30 (d, *J* = 8.4 Hz, 2H), 7.92 (d, *J* = 8.4 Hz, 2H). **^{13}C NMR** (for *cis*-**3kj**) δ 14.31, 30.06, 30.85, 35.80, 43.24, 53.49, 59.40, 63.12, 114.21, 123.26, 124.59, 125.71, 127.83, 128.10, 128.73, 130.42, 142.67, 143.70, 156.28, 163.08, 164.78.

HRMS–ESI (*m/z*): $[M+Na]^+$ calcd for $C_{28}H_{29}NO_4Na$, 466.1989; found, 466.2000. $[\alpha]_D^{22}$ –94.7 (*c* 0.56, $CHCl_3$). The ee value was determined by chiral HPLC analysis of **3kj**. HPLC analysis [CHIRALCEL® OD-3 column, 4.6 mm × 250 mm, Daicel Chemical Industries, hexane/2-propanol = 90:10, 0.5 mL/min, 40 ˚C, 250 nm UV detector, retention time = 24.1 min (cis-major), 29.6 min (cis-minor), 18.1 min (trans-major), and 19.9 min (trans-minor)].

Cis-to-Trans Isometization of 3-Alkyl-β-lactams

3ba (28.3 mg, 0.1 mmol) and potassium *tert*-butoxide (1.7 mg, 0.015 mmol) were placed in a vial. Under argon atmosphere, 1 mL of THF was added, and the mixture was stirred at room temperature. After 1 h, the end of the reaction was checked by TLC. Water was added to the reaction mixture, and the mixture was extracted with Et_2O and brine. The combined organic layers were evaporated and purified by flash column chromatography (5% EtOAc/hexane) to give *trans*-**3ba** (26.5 mg, 0.09 mmol) in 93% yield.

(3*S*,4*S*)-1-Phenyl-3-butyl-4-cyclohexyl-2-azetidinone (*trans*-3ba)

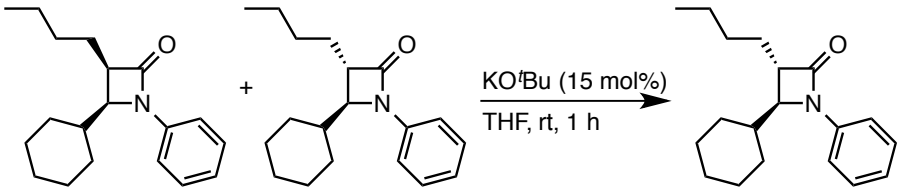

		ee (%)	
	cis/trans	cis	trans (calc.)
reaction product	80:20	96	95
epimerized	1:>99	–	95 (96)

White solid. **Mp** 79.5–81.0 ˚C. **^{1}H NMR** δ 0.92 (t, *J* = 7.2 Hz, 3H), 0.98–1.88 (m, 16H), 2.01 (m, 1H), 3.01 (m, 1H), 3.70 (dd, *J* = 2.1, 4.5 Hz, 1H), 7.08 (m, 1H), 7.29–7.41 (m, 4H). **^{13}C NMR** δ 13.89, 22.72, 25.69, 25.83, 26.15, 26.32, 29.08, 29.54, 29.85, 38.22, 51.00, 62.64, 117.40, 123.64, 129.06, 138.16, 168.33. $[\alpha]_D^{27}$ +66.1 (*c* 1.34,

$CHCl_3$). The ee value was determined by chiral HPLC analysis of *trans*-**3ba** [CHIRALCEL® OD-3 (4.6 mm × 250 mm), hexane/2-propanol 99:1, 0.5 mL/min, 40 ˚C, 250 nm UV detector, retention time = 16.0 min (minor) and 30.8 min (major)].

(3*S*,4*S*)-1-Phenyl-3,4-dicyclohexyl-2-azetidinone (*trans*-3ja)

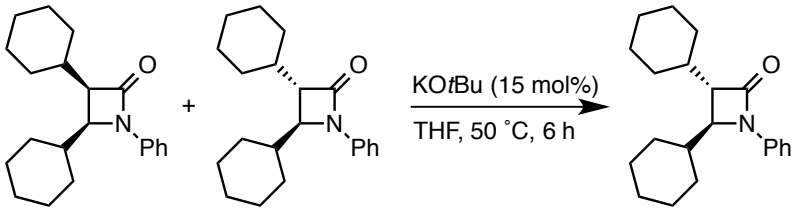

		ee (%)	
	cis/trans	cis	trans (calc.)
reaction product	78:22	97	92
epimerized	1:>99	–	98 (97)

White solid. **Mp** 96.0–98.4 ˚C. **^{1}H NMR** δ 0.97–1.34 (m, 10H), 1.56–1.83 (m, 10H), 1.94–2.09 (m, 2H), 2.85 (dd, *J* = 2.4, 7.5 Hz, 1H), 3.80 (dd, *J* = 2.4, 4.5 Hz, 1H), 7.07 (t, *J* = 7.2 Hz, 1H), 7.29–7.42 (m, 4H). **^{13}C NMR** δ 25.73, 25.83, 25.95, 26.11, 26.20, 26.25, 26.31, 30.14, 30.94, 31.26, 38.05, 38.12, 56.69, 59.90, 117.33, 123.56, 129.02, 137.99, 167.67. **$[\alpha]_D^{26}$** +59.9 (*c* 0.76, $CHCl_3$). The ee value was determined by chiral HPLC analysis of *trans*-**3ja** [CHIRALCEL® OD-3 column (4.6 mm × 250 mm), hexane/2-propanol 99.5:0.5, 0.5 mL/min, 40 ˚C, 250 nm UV detector, retention time = 19.4 min (minor) and 34.9 min (major)].

(3*S*,4*S*)-1-Phenyl-3-(2-(1,3-dioxan-2-yl)ethyl)-4-cyclohexyl-2-azetidinone (*trans*-3pa)

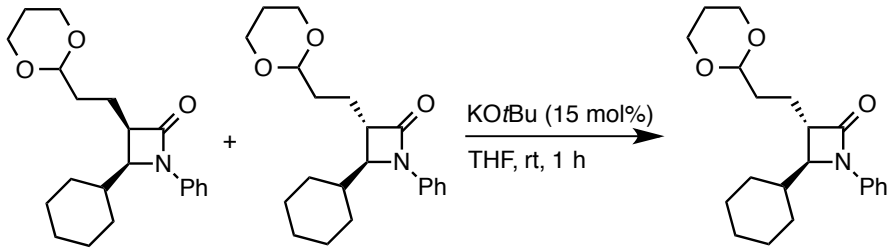

		ee (%)	
	cis/trans	cis	trans (calc.)
reaction product	80:20	97	94
epimerized	1:>99	–	97 (96)

Colorless oil. **^{1}H NMR** δ 0.95–1.38 (m, 6H), 1.56–1.82 (m, 8H), 1.88–2.05 (m, 3H), 3.02 (m, 1H), 3.71 (dd, *J* = 2.4, 4.8 Hz, 1H), 3.72–3.81 (m, 2H), 4.05–4.13 (m, 2H), 4.57 (t, *J* = 4.8 Hz, 1H), 7.07 (m, 1H), 7.29–7.39 (m, 4H). **^{13}C NMR** δ 23.71, 25.66, 25.76, 25.83, 26.10, 26.31, 29.90, 32.99, 38.14, 50.65, 62.58, 66.87, 101.67, 117.44, 123.68, 129.03, 138.04, 167.80. **$[\alpha]_D^{24}$** +36.3 (*c* 0.70, $CHCl_3$). The ee value was determined by chiral HPLC analysis of *trans*-**3pa** [CHIRALCEL® OD-3 (4.6 mm × 250 mm), hexane/2-propanol 97:3, 0.5 mL/min, 40 ˚C, 250 nm UV detector, retention time = 23.7 min (minor) and 38.7 min (major)].

3-Butyl-4-cyclohexyl-2-azetidinone (8)

Deprotection of *N*-PMP moiety: A solution of **3bb** (31.0 mg, 0.1 mmol) in MeCN (1 mL) was stirred. CAN (164.0 mg, 0.3 mmol) in H_2O (2 mL) was added portionwise to the mixture at 0 ˚C. After monitored by TLC, the reaction mixture was diluted with EtOAc. The mixture was extracted with EtOAc and brine. The combined organic layers was evaporated and purified by flash column chromatography (*n*-hexane/EtOAc = 20%) to give the title compound **8** (13.9 mg, 0.06 mmol) in 66% yield.

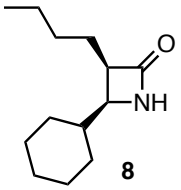

8

Orange solid. **Mp** 56.7–57.7 °C. **^{1}H NMR** δ 0.92 (t, *J* = 7.2 Hz, 3H), 1.10–1.82 (m, 17H), 3.15 (m, 1H), 3.28 (dd, *J* = 5.4, 10.2 Hz, 1H), 5.79 (s, 1H). **^{13}C NMR** δ 13.92, 22.87, 25.06, 25.32, 25.59, 26.18, 29.99, 30.02, 30.05, 37.99, 52.73, 56.95, 172.16. **HRMS–ESI** (*m/z*): $[M+Na]^+$ calcd for $C_{13}H_{23}NONa$, 232.1672; found, 232.1672. **$[\alpha]_D^{20}$** +81.0 (*c* 0.77, $CHCl_3$).

X-ray crystallographic Analysis

A colorless prism crystal of $C_{21}H_{22}NOBr$ having approximate dimensions of 0.200 x 0.150 x 0.100 mm was mounted on a glass fiber. All measurements were made on a Rigaku Mercury70 diffractometer using graphite monochromated Mo-Kα radiation. The crystal-to-detector distance was 44.89 mm. Readout was performed in the 0.137 mm pixel mode. Of the 15236 reflections were collected, where 7657 were unique (R_{int} = 0.0345); equivalent reflections were merged. The linear absorption coefficient, μ, for Mo-Kα radiation is 22.903 cm^{-1}. An empirical absorption correction was applied which resulted in transmission factors ranging from 0.514 to 0.795. The data were corrected for Lorentz and polarization effects. The cell constants, data collection conditions, and refinement results is summarized in Table 9.

The structure was solved by direct methods[20] and expanded using Fourier techniques. The non-hydrogen atoms were refined anisotropically. Hydrogen atoms were refined using the riding model. The final cycle of full-matrix least-squares refinement[21] on F[22] was based on 6755 observed reflections and 433 variable parameters and converged (largest parameter shift was 0.00 times its esd) with unweighted and weighted agreement factors of:

$$R1 = \Sigma \, ||Fo| - |Fc|| \, / \, \Sigma \, |Fo| = 0.0397$$

$$wR2 = [\ \Sigma\ (w(Fo^2 - Fc^2)^2\ )/\ \Sigma w(Fo^2)^2\ ]^{1/2} = 0.0791$$

The goodness of fit[23] was 0.84. Unit weights were used. The maximum and minimum peaks on the final difference Fourier map corresponded to 0.42 and –0.57 $e^-/Å^3$, respectively. The final Flack parameter[24] was 0.009(7), indicating that the present absolute structure is correct.[25] Neutral atom scattering factors were taken from International Tables for Crystallography (IT), Vol. C, Table 6.1.1.4.[26] Anomalous dispersion effects were included in Fcalc[27]; the values for Df' and Df" were those of Creagh and McAuley.[28] The values for the mass attenuation coefficients are those of Creagh and Hubbell.[29] All calculations were performed using the CrystalStructure[30] crystallographic software package except for refinement, which was performed using SHELXL Version 2014/7[31].

Table 9. Crystal data and details of data collection and refinement parameters for **3ea**.

Formula	$C_{21}H_{22}NOBr$
Formula weight	384.31
Crystal Dimensions	0.20 × 0.15 × 0.15 mm^3
Crystal system	monoclinic
Lattice parameters	a = 11.7360(0) Å
	b = 9.5370(0) Å
	c = 16.4850(0) Å
	β = 101.9080(0) °
Volume	1805.3976(2) Å
Space group	$P2_1$ (#4)
Z Value	4
Temperature	–103.0 °C
Density, calculated	1.414 g/cm^3
μ (Mo-Kα)	22.903 cm^{-1}

$2\theta_{max}$	52.0 °
No. of reflections measured	Total: 13989
	Unique: 6755 (R_{int} = 0.0345)
No. observations	6755
No. variables	433
R (I>2.00σ(I))	0.0397
w*R*2	0.0791
Goodness of fit indicater	0.844
Flack parameter	0.009(7)
Max shift/error in final cycle	0.000

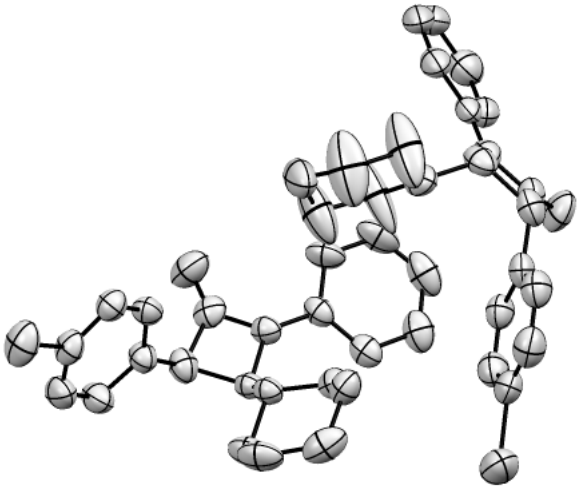

Figure 8. The ORTEP figure. A pair of molecules is different in amounts of electron density on the cyclohexane ring.

VCD Spectrum for Determination of Absolute Configuration of *trans*-β-Lactams

VCD and IR spectra were recorded on a BioTools Chiral*ir-2X* spectrometer at a resolution of 8 cm^{-1} under ambient temperature for 4000 and 16 scans, respectively. Samples were measured in $CDCl_3$ (*c* = 0.15 M) using an 85 μm BaF_2 cell. All spectral data were corrected by a solvent spectrum obtained under the identical experimental condition without correction based on the %ee of the sample, and presented as Δε and ε

(both in M^{-1} cm^{-1}).

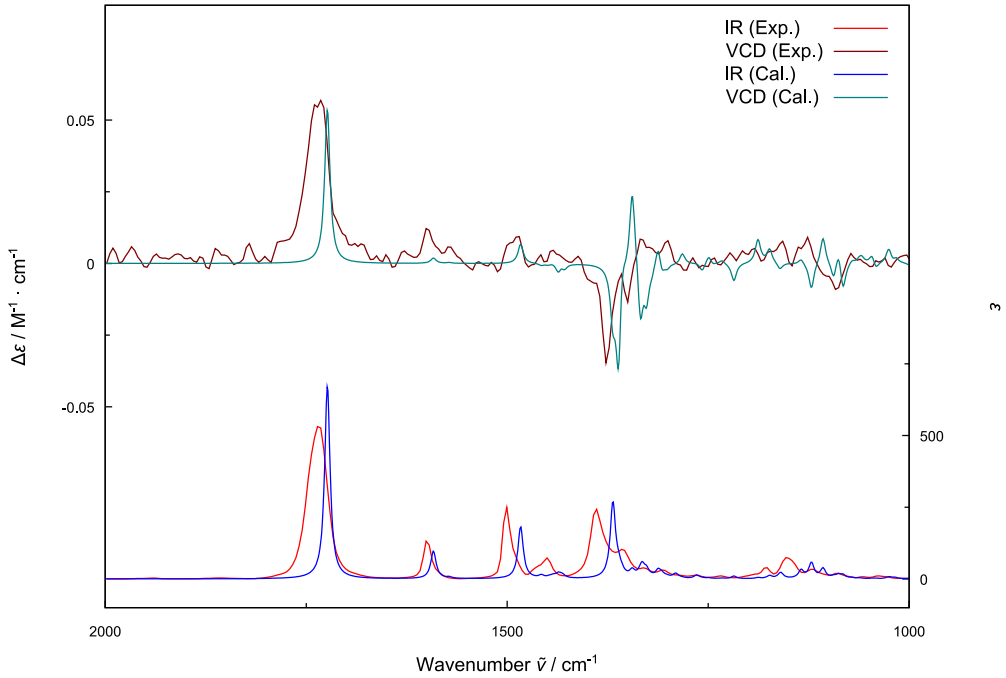

Figure 9. Comparison of the experimental and calculated VCD/IR spectra of *trans*-**3ba** (Gaussian 09 Rev D.01, BP86-D3^{BJ}(PCM)/def2-TZVPP, SpecDis 1.64, $\gamma = 4$ cm^{-1}).

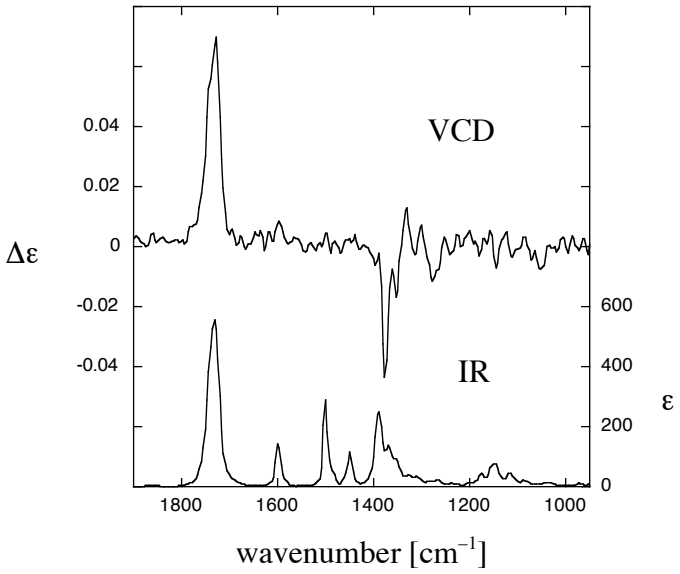

(b)

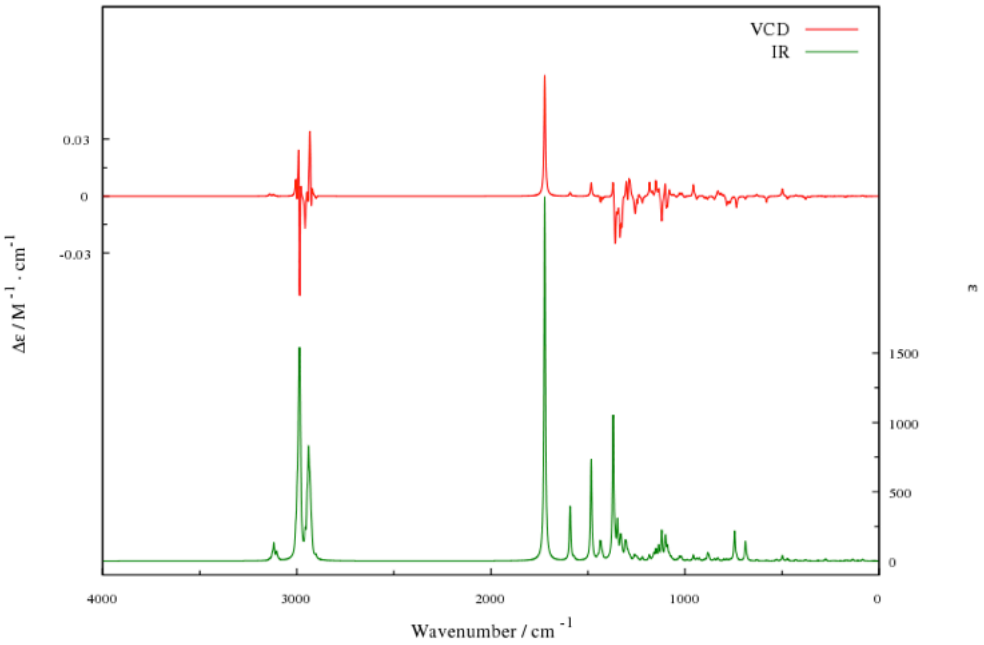

Figure 10. (a) Experimental and (b) calculated VCD/IR spectra of *trans*-**3ja** (Gaussian 09 Rev D.01, BP86-D3^{BJ}(PCM)/def2-TZVPP, SpecDis 1.64, $\gamma = 4\ cm^{-1}$).

Computational Details

Introduction

To elucidate details on the catalytic cycle and especially the effect of hydroxy amino phosphine ligand, the initial stereoselective carbon–carbon bond formation and the rearrangement pathway to β-lactam precursor have been investigated with density functional theory. All calculations were performed with Gaussian 09 program and BP86 DFT method. Therefore the system was truncated to generate a more suitable model and speed up the calculations. The alkyl moiety of the terminal alkyne and the *C*-substituent on the nitrone have been treated exclusively as a methyl group. The side chain at α position of the hydroxy group of the ligand has been replaced by a hydrogen atom, therefore removing various degrees of the system, significantly reducing the computational cost. The model system has later been extended to remove these approximations in order to confirm the validity of the initial model. Functional and basis set dependency has also been investigated.

Evaluating the model system

The model system proposed a total of 320 different configurations of the transition state geometry. There are ten configurations of the pyrrolidine moiety each for the twisted (T) and the envelope (E) type structure, and the copper can be bound to the top (t) or the bottom (b) of the nitrogen in respect to the five membered ring (Figure 11). There are two different possible conformations of the phosphine moiety for each of the previously noted (a or b). The environment of the central carbon in nitrone is planar, hence it is a prochiral center. For each of the previously mentioned conformations, there are two possible products, *R* and *S*, depending on the orientation of the nitrone. Last, the nitrone can coordinate via the hydroxyl site to the copper complex, or it can directly coordinate to the copper with the nitrone oxygen, putting the nitrone carbon in proximity to acetylene carbon. This coordination at the copper site is possible for all previously mentioned conformations.

Based on our previous work, only 80 states were treated to the full extent: These

are both stereo selective pathways (*R* and *S*) for all possible conformations of the pyrrolidine moiety with both phosphine arrangements where the copper is bound to the bottom of the ligand nitrogen. These 80 states converged after geometry optimization into six states for each stereo chemistry.

From the remaining 240 conformations, selected representative states for various pathways have been calculated as a comparison. These include the most stable transition states for each stereochemistry where the copper is bound to the top of the pyrrolidine nitrogen in both orientations of the phosphine moiety, i.e. E06tb and T06ta. A full treatment of these conformations would also have yielded 80 different transition states. The remaining 160 conformations refer to the reaction at the copper site, from which one transition state was considered for comparison. The lowest lying state (T05bbr) from the initial full treatment was chosen, which the converged into a conformation where the pyrrolidine moiety is of T04bb conformation.

In total nine different reaction pathways have been treated to determine the overall reaction mechanism. However, these calculations, employing methyl acetylene and the methyl substituted nitrone (R, R' = Me) have shown a stereo selectivity opposite to the experimentally observed (Table 9). Based on these results, all treated pathways of the model system have been extended to include the cyclohexyl moiety at the nitrone and the phenyl moiety at the acetylene.

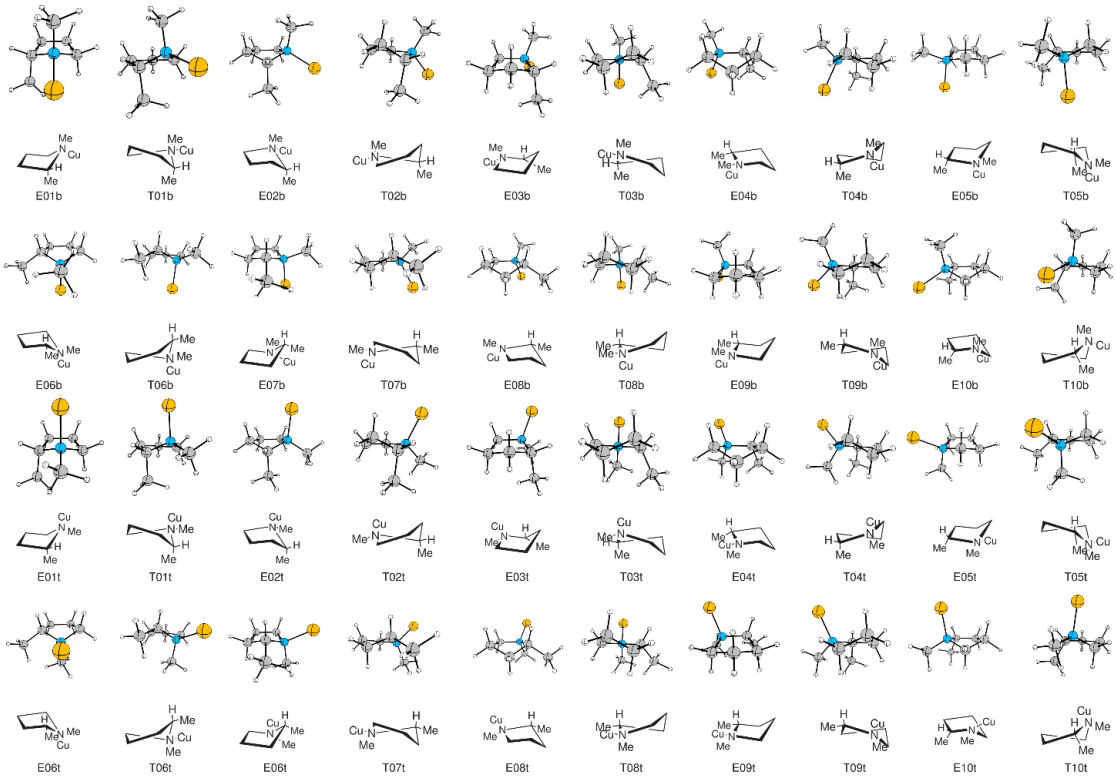

Figure 11. Conformational space of the pyrrolidine moiety.

Valuable insight into the reactivity could nevertheless be obtained. The interaction of the hydroxyl group is crucial in stabilizing the transition state. Only the first six entries in Table 9 have this interaction, the assumption on treating the remaining 240 states only exemplarily is justified. Of all calculated paths only one has been found significantly favored over all the others, by about 2 kcal/mol. In addition, no [3 + 2] cycloaddition could be observed, the carbon-carbon bond forms first, followed by the carbon-oxygen bond closing the five membered ring.

Table 9. Energy differences between the transition states of the methyl acetylene and methyl nitrone model system.[a]

entry		R-Type	S-Type
1	T03bb	–	6.6

1	T04bb	4.6	–
2	T05bb	0.7	0.0
3	T10bb	4.7	5.4
4	E01ba	4.6	5.3
5	T05ba	2.8	2.0
6	T08ba	4.0	2.8
7	E06tb	10.6	9.9
8	T06ta	17.0	18.4
9	T04bb'	8.0	5.8

[a] The denominator refer to the conformation of the pyrrolidine moiety (Figure 11), the last letter refers to the arrangement of the phosphine moiety. The prime indicates that this reaction takes place at the phosphine site.

Reaction paths of the extended model system

The reaction proceeds via a formally two-step process. First the initial carbon-carbon bond between the acetylene and the nitrone is formed. The carbon-carbon distance in the investigated transition states ranges from 1.970 Å to 2.065 Å, which is significantly shorter than the sum of the van der Waals radii (d_{vdW}(C–C) = 3.400 Å), but still considerably longer than a carbon-carbon single bond (d_{cov}(C–C)=1.500 Å). The carbon-carbon distances seemed to be independent of the energies in each path.

While the carbon-carbon distance is a primary criterion for the transition state, since it corresponds directly to the bond formation, the carbon–oxygen distance is only a secondary component. Most importantly the distance changes significantly depending on the chemical surrounding. When the reaction takes place at the hydroxyl site, the C–O distance ranges from 3.189 Å to 3.458 Å, which is about the same as the sum of the van der Waals radii (d_{vdW}(C–O) = 3.220 Å). These cases are somewhat special, since there is a hydrogen bond possible between the nitrone oxygen and the hydroxyl moiety of the ligand (Scheme 7, Table 10 and Table 11).

Scheme 7. Formation of the five membered ring intermediate.

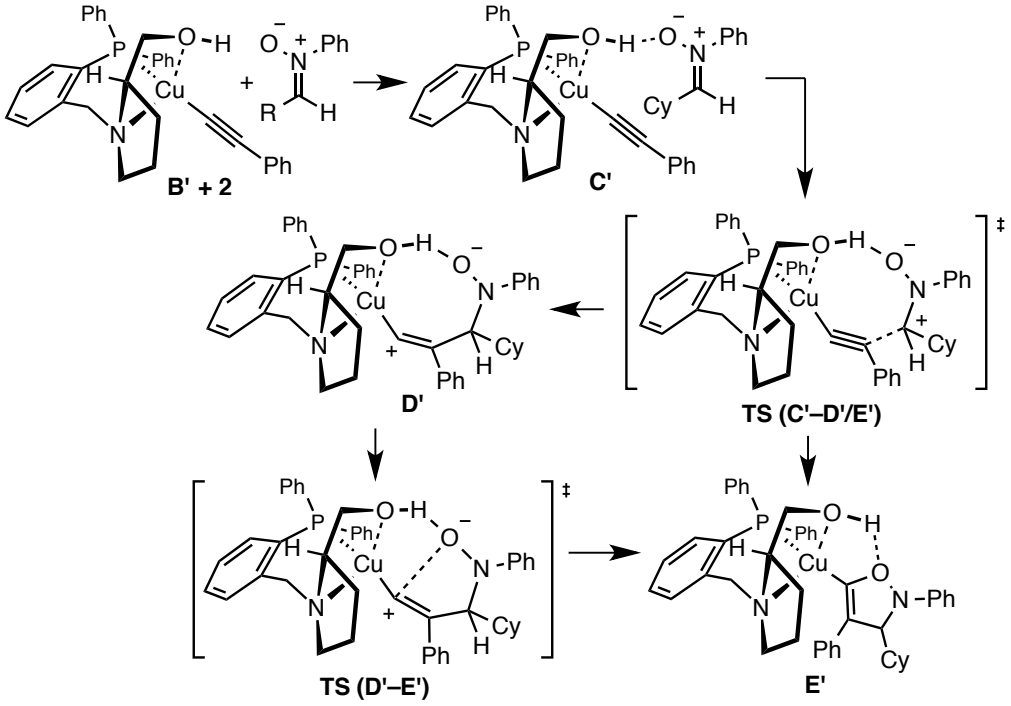

However, the molecular orbitals reveals that indicators for the formation of the C–O bond are already present. The highest occupied molecular orbital (HOMO) corresponds to a π-bond of the former acetylene in combination with a π*-orbital of the nitrone N–O bond. The lowest unoccupied molecular orbital (LUMO) corresponds to the formation of the carbon-carbon bond. Thus it is evident why the ring closing step is barrierless (Figure 12).

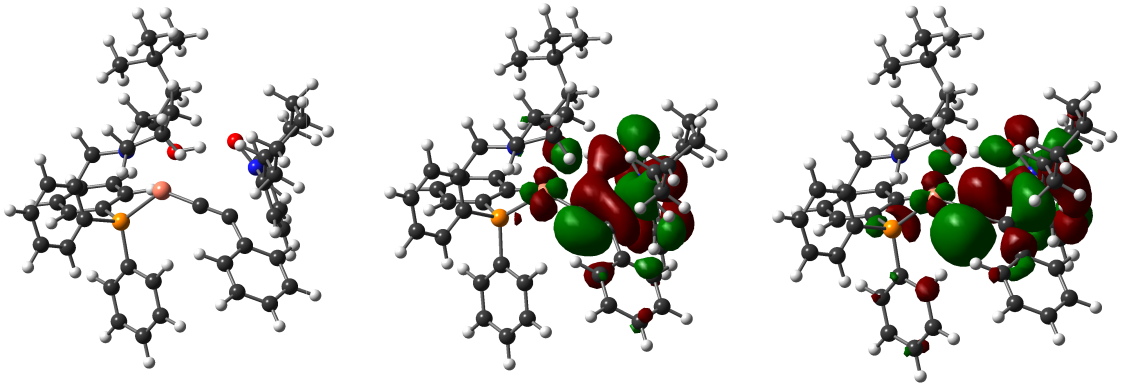

Figure 12. Orientation (left), HOMO (center) and LUMO (right) of the T05bbs transition state.

In the other pathways the C–O distance is significantly shorter, it ranges from 2.896 Å to 2.935 Å, which is due to the fact that the nitrone oxygen directly binds to the central copper (Table 10 and Table 11). The copper-oxygen distance ranges from 2.093 Å to 2.165 Å, which is just a little longer than what would be expected for a single bond (d_{cov}(Cu–O)=1.850 Å). The reaction therefore also proceeds via a different mechanism. Most notably it forms a different intermediate, which may best be described as a six membered metallacycle intermediate (Scheme 8, **G**).

Scheme 8. Alternative pathway for the formation of the five membered intermediate.

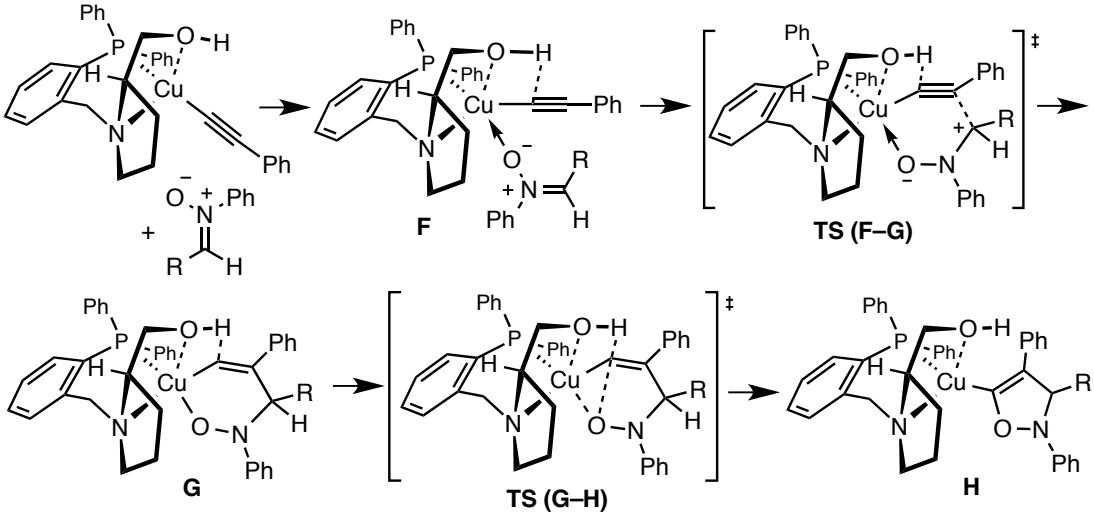

Table10. Energies for the reacion pathways of the extended model system.[a]

entry	path	**B' + 2**	**C'**	**TS (C'–D'/E')**	**E**
1	T05bbs	14.1 (-0.3)	0.8 (0.3)	16.2 (19.2)	-21.1 (-16.0)
2	T10bbr	15.7 (1.0)	4.8 (3.7)	19.6 (21.2)	-17.9 (-13.5)
3	T04bbr	17.5 (2.0)	4.4 (3.8)	19.3 (22.5)	-16.4 (-12.8)
4	T03bbs	17.5 (2.0)	4.9 (4.3)	25.0 (26.8)	-16.5 (-13.1)
5	E01bar	15.9 (1.7)	7.1 (6.6)	20.8 (23.2)	-20.2 (-15.7)
6	T05bas	16.2 (1.4)	3.2 (2.7)	17.3 (20.0)	-18.9 (-14.1)
7	T08bas	16.3 (1.1)	3.2 (2.4)	17.3 (20.1)	-18.9 (-14.4)

[a] Electronic energies (ΔE) and free energies at 298 K and 1 atm (ΔG^{298K} in parentheses) are given in kcal/mol (Gaussian 09, BP86/def2-SVP). Numbers refer to Scheme 7.

Table 11. Geometric parameters of the transition states of the investigated reaction paths.[a]

entry	path, **(C'–D'/E')**	d(C–C)	d(C–O)	d(CH–O)[b]	ΔG^{298K} (kcal/mol)
1	T05bbs	2.040	3.287	2.327	19.2
2	T10bbr	1.979	3.384		21.2
3	T04bbr	2.028	3.189	2.446[c]	22.5
4	T03bbs	1.970	3.334		26.8
5	E01bar	1.990	3.458	2.347	23.2
6	T05bas	2.065	3.316	2.326	20.0
7	T08bas	2.064	3.321	2.329	20.1

[a] Bond length in Å (Gaussian 09, BP86/def2-SVP). [b] This value is only shown if it is smaller than 2.5 Å. [c] Interaction of phenyl-hydrogen of the phosphine moiety.

Consequently in almost all pathways involving the interaction of the hydroxyl group with the nitrone, the carbon oxygen bond formation, i.e. the ring closing, is

barrierless. In all other cases, the carbon-carbon bond formation also leads to a shortening of the carbon–oxygen distance, which is evidently enough to also form this bond immediately and without a barrier. IRC calculations lead straight to the five membered ring intermediate.

The calculations indicate that the pathway T05bbs is the most efficient pathway. Notable features of this state are the relatively short hydroxyl hydrogen–oxygen interaction (1.476 Å), and the secondary interaction of one hydrogen of the pyrrolidine moiety with the same oxygen (2.327 Å) (Figure 13). The secondary interactions are only present in this state and are therefore very important to the selectivity of this reaction.

The analysis in terms of the Quantum Theory of Atoms in Molecules (QTAIM) confirms those findings as shown in Figure 14. The strong interaction between the hydroxyl hydrogen and the nitrone oxygen was observed. The minimum value of the electron density along the path connecting the two atoms is the bond critical point with a value of ϱ = 0.074 e/Å (BCP1). The same hydrogen is of course covalently bound to the oxygen of the ligand, so the value for electron density is much higher at this point (BCP3, ϱ = 0.269 e/Å). The before mentioned secondary interaction, i.e. the hydrogen bonding to the pyrrolidine moiety is also confirmed. Compared to the hydrogen bond it is a rather weak interaction, but certainly not negligible. The electron density is found to be ϱ = 0.013 e/Å (BCP2). In addition, the nitrone oxygen internally stabilizes with secondary interactions in the form of weak hydrogen bonds to the cyclohexyl and the phenyl moieties (Figure 13).

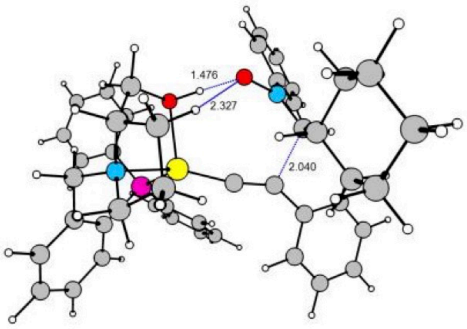

Figure 13. Molecular geometry of T05bbs. Bond lengths are given in Å. Gaussian 09 BP86/def2-SVP.

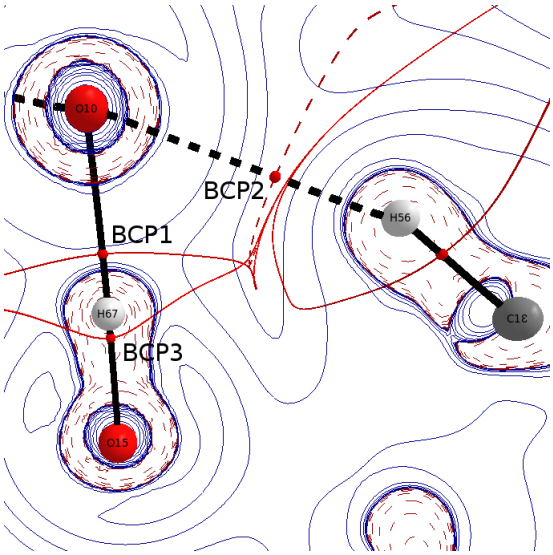

Figure 14. QTAIM Plot of the Laplacian distribution in the plane of the hydrogen bond interactions for the transition state **TS (C'–D'/E')**.

References and Notes

(1) For books on the biological activity of β-lactams, see: (a) *The Chemistry of β-Lactams*; Page, M. I., Ed.; Blackie Academic & Professional: New York, **1992**. (b) *Chemistry and Biology of β-Lactam Antibiotics*; Morin, R.B., Gorman, M., Eds.; Academic: New York, **1982**; Volumes 1–3.

(2) For books on the synthetic chemistry of β-lactams, see: (a) *Synthesis of β-Lactam Antibiotics: Chemistry, Biocatalysis and Process Integration*; Bruggink, A., Ed.; Kluwer: Dordrecht, Netherlands, **2001**. (b) *Enantioselective Synthesis of β-Amino Acids*; Juaristi, E., Ed.; VCH: New York, **1997**. (c) *The Organic Chemistry of β-Lactams*; Georg, G. I., Ed.; VCH: New York, **1993**.

(3) For reviews on the asymmetric Kinugasa reaction, see: (a) Chemler, S. R.; Fuller, P. H.; *Chem. Soc. Rev.* **2007**, *36*, 1153–1160. (b) Pal, R.; Ghosh, S. C.; Chandra, K.; Basak, A.; *Synlett* **2007**, 2321–2330. (c) Stanley, L. M.; Sibi, M. P. *Chem. Rev.* **2008**, *108*, 2887–2902. (d) Stecko, S.; Furman, B.; Chmielewski, M. *Tetrahedron*, **2014**, *70*, 7817–7844.

(4) Kinugasa, M.; Hashimoto, S. *J. Chem. Soc., Chem. Commun.* **1972**, 466–467.

(5) Miura, M.; Enna, M.; Okuro, K.; Nomura, M. *J. Org. Chem.* **1995**, *60*, 4999–5004.

(6) (a) Lo, M. M.-C.; Fu, G. C. *J. Am. Chem. Soc.* **2002**, *124*, 4572–4573. (b) Shintani, R.; Fu, G. C. *Angew. Chem. Int. Ed.* **2003**, *42*, 4082–4085.

(7) (a) Chen, Z.; Lin, L.; Wang, M.; Liu, X.; Feng, X. *Chem. Eur. J.* **2013**, *19*, 7561–7567. (b) Saito, T.; Kikuchi, T.; Tanabe, H.; Yahiro, J.; Otani, T. *Tetrahedron Lett.* **2009**, *50*, 4969–4972. (c) Coyne, A. G.; Müller-Bunz, H.; Guiry, P. J. *Tetrahedron: Asymm.* **2007**, *18*, 199–207. (d) Baeza, B.; Casarrubios, L.; Sierra, M. A.; *Chem. Eur. J.* **2013**, *19*, 11536–11540.

(8) (a) Wu, G.; Wong, Y.; Chen, X.; Ding, Z. *J. Org. Chem.* **1999**, *64*, 3714–3718. (b) Michalak, M.; Stodulski, M.; Stecko, S.; Mames, A.; Panfil, I.; Soluch, M.; Furman, B.; Chmielewski, M. *J. Org. Chem.* **2011**, *76*, 6931–6935.

(9) (a) Burnett, D. A.; Caplen, M. A.; Davis, J. H. R.; Burrier, R. E.; Clader, J. W. *J. Med. Chem.* **1994**, *37*, 1733–1736. (b) Braun, M.; Galle, D. *Synthesis* **1996**, 819–

820. (c) Burnett, D. A. *Tetrahedron Lett*. **1994**, *35*, 7339–7342.

(10) Chen, J.-H.; Liao, S.-H.; Sun, X.-L.; Shen, Q.; Tang, Y. *Tetrahedron*, **2012**, *68*, 5042–5045.

(11) Ishii, T.; Watanabe, R.; Moriya, T.; Ohmiya, H.; Mori, S.; Sawamura, M. *Chem. Eur. J*. **2013**, *19*, 13547–13553.

(12) (a) Harada, A.; Makida, Y.; Sato, T.; Ohmiya, H.; Sawamura, M. *J. Am. Chem. Soc*. **2014**, *136*, 13932–13939. (b) Ohmiya, H.; Zhang, H.; Shibata, S.; Harada, A.; Sawamura, M. *Angew. Chem. Int. Ed.,* **2016**, *55,* 4777–4780. (c) Yasuda, Y.; Ohmiya, H.; Sawamura, M. *Angew. Chem. Int. Ed.,* **2016**, *55,* 10816–10820.

(13) Another possibility on catalyst-driven formation of exomethylene β-lactams was discussed: Basak, A.; Ghosh, S. C. *Synlett*, **2004**, *9*, 1637–1639.

(14) Kim, J.; Stahl, S. S. *J. Org. Chem*. **2015**, *80*, 2448–2454.

(15) He, Y.; Wang, B.; Dukor, R. K.; Nafie, L. A. *Appl. Spectrosc*. **2011**, *65*, 699–723.

(16) It is possible that the cationic alkynyl-Cu(II) triflate complex is a key species to work as a Lewis acid catalyst: see ref. 7b.

(17) A theoretical suggestion of stepwise bonds formation: Santoro, S.; Liao, R.-Z.; Marcelli, T.; Hammar, P.; Himo, F. *J. Org. Chem*. **2015**, *80*, 2649–2660.

(18) Bejjani, J.; Chemla, F.; Audouin, M. *J. Org. Chem*. **2003**, *68*, 9747–9752.

(19) Pilzak, G. P.; van Gruijthuijsen, K.; van Doorn, R. H.; van Lagen, B.; Sudholter, E. J. R.; Zuilhof, H. *Chem. Eur. J*. **2009**, *15*, 9085–9096.

(20) CrystalClear: Data Collection and Processing Software, Rigaku Corporation (1998-2015). Tokyo 196-8666, Japan.

(21) SIR2011: Burla, M. C.; Caliandro, R.; Camalli, M.; Carrozzini, B.; Cascarano, G. L.; Giacovazzo, C.; Mallamo, M.; Mazzone, A.; Polidori, G.; Spagna, R. *J. Appl. Cryst*. **2012**, *45*, 357-361.

(22) Least Squares function minimized: (SHELXL Version 2014/7) $\Sigma w(Fo^2-Fc^2)^2$, where w = Least Squares weights.

(23) Goodness of fit is defined as: $[\Sigma w(Fo^2-Fc^2)^2/(No-Nv)]^{1/2}$, where: No = number of observations, Nv= number of variables.

(24) Parsons, S.; Flack, H. *Acta Cryst*. **2004**, A*60*, s61.

(25) Flack, H.D.; Bernardinelli, G. *J. Appl. Cryst*. **2000**, *33*, 1143–1148.

(26) International Tables for Crystallography, Vol.C (1992). Ed. A.J.C. Wilson, Kluwer Academic Publishers, Dordrecht, Netherlands, Table 6.1.1.4, pp. 572.

(27) Ibers, J. A.; Hamilton, W. C. *Acta Crystallogr*. **1964**, *17*, 781.

(28) Creagh, D. C.; McAuley, W.J. "International Tables for Crystallography", **1992**, Vol C, (Wilson, A.J.C. ed.), Kluwer Academic Publishers, Boston, Table 4.2.6.8, 219–222.

(29) Creagh, D. C.; Hubbell, J.H. "International Tables for Crystallography", **1992**, Vol C, (Wilson, A.J.C. ed.), Kluwer Academic Publishers, Boston, Table 4.2.4.3, 200–206.

(30) CrystalStructure 4.2: Crystal Structure Analysis Package, Rigaku Corporation (2000-2015). Tokyo 196-8666, Japan.

(31) SHELXL Version 2014/7: Sheldrick, G. M. *Acta Cryst*. **2008**, A*64*, 112–122.

Publication List

"Asymmetric Synthesis of β-Lactams through Copper-Catalyzed Alkyne-Nitrone Coupling with a Prolinol-Phosphine Chiral Ligand"

Yurie Takayama, Takaoki Ishii, Hirohisa Ohmiya, Tomohiro Iwai, Martin C. Schwarzer, Seiji Mori, Tohru Taniguchi, Kenji Monde, Masaya Sawamura

Chem. Eur. J. **2017**, *23*, 8400–8404.

"Copper-Catalyzed γ-Selective and Stereospecific Direct Allylic Alkylation of Terminal Alkynes: Synthesis of Skipped Enynes"

Yusuke Makida, Yurie Takayama, Hirohisa Ohmiya, Masaya Sawamura

Angew. Chem. Int. Ed. **2013**, *52*, 5350–5354.